

**YggB of *Corynebacterium glutamicum* -  
Dual function in osmotic stress response and  
glutamate production**

Inaugural-Dissertation  
**zur**  
**Erlangung des Doktorgrades**  
der Mathematisch-Naturwissenschaftlichen Fakultät  
der Universität zu Köln  
vorgelegt von

**Kirsten Börngen**  
aus Köln

**Köln, September 2009**

**Berichterstatter:**

Prof. Dr. Reinhard Krämer

Prof. Dr. Arnd Baumann

Tag der Disputation: 27.11.2009

„Phantasie ist wichtiger als Wissen, denn Wissen ist begrenzt“

Albert Einstein

## Abstract

The membrane protein YggB of *Corynebacterium glutamicum* was previously described to belong to the MscS-type family of mechanosensitive (MS) channels functioning as emergency valves upon osmotic downshift. Bacterial cells respond to rapid water influx by immediate activation of MS channels that allow efflux of compatible solutes to prevent cell lysis. Recently, YggB was also connected to the glutamate export in *C. glutamicum* under glutamate productive conditions. The mechanism of glutamate export is not fully understood so far although *C. glutamicum* has been used for the industrial production of amino acids for decades. Deletion of *yggB* led to a drastic decrease in glutamate excretion while truncation of 110 AA resulted in continuous export of glutamate. In this work YggB was characterized with respect to its dual function as MS channel on the one hand and in the excretion of glutamate on the other. Using the patch clamp technique and additional physiological approaches it was shown that YggB harbors the functions of a pressure-sensitive MS channel similar to the *E. coli* homolog MscS. However, for the first time also an involvement of a MS channel in bacterial response to hyperosmotic conditions was shown. A so called ‘pump and leak’ model including active betaine uptake (via BetP) and passive betaine efflux (via YggB) to accurately adjust the internal solute concentration, which are accumulated under hyperosmotic conditions to balance the osmotic gradient, is proposed. Concerning the second function of YggB in the glutamate production of *C. glutamicum* the integrity of the C-terminal domain was shown to have a strong effect on the inducibility of glutamate production. However, the exact function of the C-terminal domain cannot be unequivocally clarified. Additionally, this work provides strong evidence that glutamate excretion is triggered directly by the *C. glutamicum* MS channel YggB.

## Kurzzusammenfassung

Das Membranprotein YggB aus *Corynebacterium glutamicum* gehört zu der MscS-ähnlichen Familie von mechanosensitiven (MS) Kanälen, die im Fall eines osmotischen *downshifts* als Notfallventil dienen. Bakterielle Zellen antworten auf plötzlichen Wassereinstrom mit der direkten Aktivierung der MS Kanäle, die den Ausstrom von kompatiblen Soluten aus der Zelle erlauben und so die Zellyse verhindern. Vor kurzem wurde YggB auch mit dem Export von Glutamat aus *C. glutamicum* unter Glutamatproduzierenden Bedingungen in Verbindung gebracht. Der Mechanismus des Glutamatexports ist bisher nicht bekannt, obwohl *C. glutamicum* seit Jahrzehnten zur industriellen Produktion von Aminosäuren genutzt wird. Deletion von *yggB* hat eine drastische Verringerung der Glutamat Ausscheidung zur Folge während eine Verkürzung um 110 Aminosäuren zu kontinuierlich stattfindender Glutamatproduktion führt. In dieser Arbeit wurde YggB in Bezug auf seine duale Funktion charakterisiert, zum einen als MS Kanal und zum andern bei der Exkretion von Glutamat. Mit Hilfe der *Patch clamp* Technik und weiteren physiologischen Ansätzen konnte gezeigt werden, dass YggB die Funktionen eines Druck-sensitiven MS Kanals ähnlich wie das *E. coli* Homolog MscS besitzt. Allerdings konnte in dieser Arbeit auch zum ersten Mal eine Beteiligung eines MS Kanals in der bakteriellen Antwort auf hyperosmotische Bedingungen gezeigt werden. Ein sogenanntes ‚pump and leak‘ Modell wird vorgeschlagen, welches die aktive Aufnahme (via BetP) und den passiven Ausstrom von Betain (via YggB) beinhaltet, um die interne Solutkonzentration, welche unter hyperosmotischen Bedingungen akkumuliert werden um den osmotischen Gradienten auszugleichen, sehr genau einzustellen. Bezogen auf die zweite Funktion von YggB in der Glutamatproduktion von *C. glutamicum*, konnte gezeigt werden, dass die Integrität der C-terminalen Domäne einen starken Effekt auf die Induzierbarkeit der Glutamatproduktion hat. Allerdings bleibt die genaue Funktion der C-terminalen Domäne von YggB unklar. Zusätzlich liefert diese Arbeit starke Anhaltspunkte dafür, dass der Export von Glutamat direkt durch den MS Kanal YggB aus *C. glutamicum* vermittelt wird.

## Contents

<b>1</b>	<b>Introduction</b>	<b>1</b>
1.1	YggB of <i>Corynebacterium glutamicum</i>	1
1.2	<i>C. glutamicum</i> in general	2
1.3	Osmotic stress response in <i>C. glutamicum</i>	3
1.3.1	Response to <b>hyper</b> osmotic stress conditions	3
1.3.2	Response to <b>hypo</b> osmotic stress conditions	5
1.4	Glutamate production by <i>C. glutamicum</i>	9
1.5	Glutamate export	14
1.6	Thesis objective	16
<b>2</b>	<b>Materials and Methods</b>	<b>17</b>
2.1	Bacterial strains and plasmids	17
2.2	Media and growth conditions	20
2.3	Molecular biological approaches	21
2.3.1	Preparation of competent <i>E. coli</i> cells and transformation	21
2.3.2	Preparation of competent <i>C. glutamicum</i> cells and transformation	22
2.3.3	DNA techniques	23
2.3.3.1	Isolation of plasmid DNA from <i>E. coli</i> and <i>C. glutamicum</i>	23
2.3.3.2	Isolation of genomic DNA from <i>E. coli</i> and <i>C. glutamicum</i>	23
2.3.3.3	Gel electrophoresis and extraction of DNA from agarose gels	23
2.3.3.4	Polymerase chain reaction (PCR)	24
2.3.3.5	Restriction, ligation, and sequencing of DNA	24
2.3.4	Construction of deletion strains and plasmids	25
2.3.5	Site-directed mutagenesis	26
2.4	General analytic methods	26
2.4.1	Cell disruption and membrane preparation	26
2.4.2	Determination of protein concentrations	27
2.4.3	SDS-Polyacrylamide Gel Electrophoresis (PAGE)	27
2.4.4	Staining of SDS-gels - Coomassie Brilliant Blue staining	28
2.4.5	Immunoblot analyses	28
2.4.6	Determination of osmolality	29
2.4.7	HPLC (high-performance liquid chromatography) – analysis	29

2.5	Biochemical approaches	30
2.5.1	Enzyme assays	30
2.5.2	Analysis of cell viability	31
2.5.3	Efflux of glutamate upon <b>hypo</b> osmotic shock	31
2.5.4	Efflux of glycine betaine upon <b>hypo</b> osmotic shock	32
2.5.5	Betaine uptake and efflux under <b>hyper</b> osmotic conditions	33
2.5.6	Betaine uptake rate during osmotic compensation	33
2.5.7	Determination of membrane potential	33
2.5.8	Determination of the internal pH and the pmf (proton motive force)	34
2.5.9	Test for pyruvate efflux	35
2.5.10	Test for K <sup>+</sup> permeability	35
2.5.11	Susceptibility of antibiotics	36
2.5.12	Glutamate production	36
2.5.13	Hypoosmotic stress response under glutamate productive conditions	37
2.6	Electrophysiological approaches	38
2.6.1	Preparation of giant spheroplasts	38
2.6.2	Electrical Recording	38
<b>3</b>	<b>Results</b>	<b>40</b>
3.1	Recombinant YggB proteins	40
3.2	Topology of <i>C. glutamicum</i> YggB	42
3.3	Electrophysiological characterization of YggB	43
3.4	Functionality of <i>C. glutamicum</i> YggB in <i>E. coli</i>	49
3.5	Function of YggB under osmotic stress conditions	50
3.5.1	Glutamate efflux upon osmotic downshift	50
3.5.2	Betaine efflux upon osmotic downshift	52
3.5.3	Betaine accumulation under hyperosmotic conditions	54
3.5.3.1	BetP activity during osmotic compensation	57
3.5.3.2	Energetics during betaine accumulation	59
3.5.4	Growth at different osmolalities	62
3.5.5	Characterization of leakiness mediated by YggB $\Delta$ 110-His	64
3.5.6	<i>E. coli</i> MscS and MscS/CtYggB in <i>C. glutamicum</i> $\Delta$ yggB	65
3.6	Glutamate production	66
3.6.1	Glutamate production upon different treatments	66

## Contents

---

3.6.2	Influence of external osmolality, media, and pH	69
3.6.3	Influence of on-going glutamate production on hypoosmotic stress	72
3.6.4	Alternative candidates for the glutamate exporter	73
3.6.5	<i>E. coli</i> MscS and MscS/CtYggB in <i>C. glutamicum</i> $\Delta$ yggB	76
3.6.6	LOF- and GOF mutants of <i>E. coli</i> MscS and MscS/CtYggB	78
<b>4</b>	<b>Discussion</b>	<b>82</b>
4.1	Topology of YggB	83
4.2	Electrophysiological characterization of YggB	83
4.3	Significance of YggB under osmotic stress conditions	85
4.4	Involvement of YggB in glutamate production	90
4.5	Function of YggB – current knowledge and future perspectives	96
<b>5</b>	<b>Summary</b>	<b>100</b>
<b>6</b>	<b>Literature</b>	<b>102</b>
<b>7</b>	<b>Supplement</b>	<b>116</b>

## Abbreviations

AA	amino acids
Am <sup>R</sup>	resistance towards ampicillin
ATP	adenosine triphosphate
BCIP	5-Bromo-4-chloro-3-indolyl phosphate
BHI	Brain heart infusion
bp	base pairs
BSA	bovine serum albumin
C	carbon
Cm <sup>R</sup>	resistance towards chloramphenicol
CTAB	cetyltrimethylammoniumbromide
cpm	counts per minute
dm	dry mass
DMSO	dimethyl sulfoxide
DNA	deoxyribonucleic acid
EDTA	ethylenediaminetetraacetic acid
<i>et al.</i>	<i>et alii</i> ("and others")
GOF	gain of function
HPLC	High-performance liquid chromatography
IPTG	isopropyl-1-thio- $\beta$ -D-galactosid
kDa	kilo Dalton
Km <sup>R</sup>	resistance towards kanamycin
LB	Luria-Bertani
LOF	loss of function
MM	minimal medium
MOPS	3-[N-morpholino]propanesulfonic acid
MS	mechanosensitive
OD <sub>600</sub>	optical density at 600 nm
OPNG	o – nitrophenyl $\beta$ -D-galactopyranoside
orf	open reading frame
o/n	over night
PAGE	polyacrylamide gel electrophoresis
PCR	polymerase chain reaction

## Abbreviations

---

pmf	proton motive force
Fmoc	fluorenylmethyloxycarbonyl chloride
PVDF	polyvinylidene difluoride
rpm	rounds per minute
RT	room temperature
SDS	sodium dodecylsulphate
TAE	Tris-Acetate-EDTA
TCA	trichloroacetic acid
TE	Tris-EDTA
TEMED	N,N,N',N'-tetramethyl-ethylendiamine
Tris	2-amino-hydroxymethylpropane-1,3-diol
TPP	tetraphenylphosphoniumbromid
(v/v)	volume per volume
(w/v)	weight per volume
wt	wild type
$\Delta\Psi$	membrane potential
$\Delta\text{pH}$	pH gradient

## 1 Introduction

### 1.1 YggB of *Corynebacterium glutamicum*

The membrane protein YggB of *Corynebacterium glutamicum* is proposed to harbor a dual function in the osmotic stress response and in the glutamate production by *C. glutamicum*. The combination of these two functions by one protein makes YggB a novel and quite interesting topic.

YggB is encoded by the gene *NCgl1221* (*yggB*) and harbors 533 amino acids (AA). Due to structural similarity the protein YggB belongs to the family of MscS-type (Mechanosensitive channel of small conductance) mechanosensitive (MS) channels (Ruffert *et al.*, 1999). These channels function as emergency valves preventing cell lysis under hypoosmotic conditions. Together with *yggB* another open reading frame (orf), *NCgl0843* (*mscL*), homologous to *mscL* of *E. coli* was identified by homology search for MS channel homologs within the genome of *C. glutamicum*. The related proteins were associated with the two different electrical conductances observed in patch clamp analysis of *C. glutamicum* membrane fragments fused into liposomes (Ruffert *et al.*, 1999). The MscL homolog (135 AA) has a high sequence similarity to MscL of *E. coli* (38 % identical and 57 % similar amino acids). On the contrary, YggB is more closely related to MS channel homologs from mycolic acid containing actinomycetes than to the *E. coli* MscS (only 26 % identical and 46 % similar amino acids) (Nottebrock *et al.*, 2003). The sequence similarity of YggB to MscS of *E. coli* is restricted to the three N-terminally located transmembrane domains. However, YggB contains 533 AA and is therefore almost double in length compared to the *E. coli* MscS (286 AA) (Fig. 1.1). The additional C-terminal elongation of *C. glutamicum* YggB, harboring 247 AA, includes a putative fourth transmembrane domain ([www.predictprotein.org](http://www.predictprotein.org)) and might therefore also harbor an additional function. However, the putative MS channels of *C. glutamicum* are barely characterized so far.

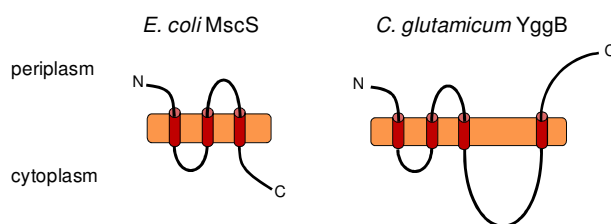


**Fig. 1.1: Schematic model of MscS and YggB.**

Topology of MscS of *E. coli* (286 AA) and predicted topology of YggB of *C. glutamicum* (533 AA).

Aside from its suggested function as MS channel, YggB was recently connected to the export of glutamate by *C. glutamicum*. A truncation mutant, missing 110 AA at the C-terminal end, led to permanent excretion of glutamate (Nakamura *et al.*, 2007). Additionally, an elevated expression level of the *yggB* gene was observed upon glutamate triggering treatments (Radmacher *et al.*, 2005, Schiekol, 2005). Since *C. glutamicum* is the most important organism used in industrial production of L-glutamate, understanding of the mechanisms leading to glutamate production and excretion are of major interest. Although *C. glutamicum* has been used in glutamate production for decades the mechanisms leading to glutamate production have not been completely resolved so far. The possible involvement of YggB in (a) osmotic stress situations functioning as MS channel and (b) glutamate production acting as excretion system makes the protein YggB of *C. glutamicum* a very interesting study object. For a better understanding, the two fields concerning YggB, osmotic stress and glutamate production, will be described in the following sections.

### **1.2 *C. glutamicum* in general**

*C. glutamicum*, a Gram-positive, biotin-auxotrophic bacterium, was isolated about 50 years ago in a screening program for L-glutamate-producing bacteria (Kinoshita *et al.*, 1957, Udeka, 1960). *C. glutamicum* is a nonmotile, aerobic, and nonsporulating bacterium inhabiting mainly the surface layers of the soil. In its natural environment *C. glutamicum* has to deal with several stress situations, e.g. osmotic stress caused by sudden changes of the external osmolarity. Like mycobacteria it belongs to the suborder *Corynebacterineae* which is characterized by very unique cell wall components and a high G+C content of the DNA (Stackebrandt *et al.*, 1997). In addition to a ubiquitous inner plasma membrane, the cell envelope has an outer lipid layer which contains mycolic acids and is probably also organized as a bilayer (Eggeling and Sahm, 2001). Importantly, this hydrophobic layer was shown in related genera to play an important role in drug and substrate transport due to its high impermeability (Jarlier and Nikaido, 1990; 1994). For *C. glutamicum* the mycolic acids were shown to be essential for the impermeability of the cell wall (Tropis *et al.*, 2005; Gebhardt *et al.*, 2007).

The 3.3 Mb genome of *C. glutamicum* was completely sequenced by three independent research groups in Europe and Japan (Kalinowski *et al.*, 2003; Ikeda and Nakagawa, 2003; Yukawa *et al.*, 2007). Due to many genes which are highly conserved within the *Corynebacterineae* species and its close relationship to pathogenic organisms, such as *C.*

*diphtheria*, *Mycobacterium tuberculosis*, and *M. leprae*, *C. glutamicum* is of high interest as non-pathogenic model organism. Furthermore, *C. glutamicum* is one of the biotechnologically most important bacterial species, because of its intense use for amino acid production. The annual production was more than two million tons of amino acids, mainly L-glutamate and L-lysine in 2005 (Leuchtenberger *et al.*, 2005). Up to now glutamate production alone has increased to an annual production of two million tons (Sano, 2009). Due to this immense industrial importance, glutamate production by *C. glutamicum* has been studied intensively.

### 1.3 Osmotic stress response in *C. glutamicum*

In the upper layer of the soil, the natural environment of *C. glutamicum*, changes in external osmolarity are very common as a result of environmental changes, like sunshine and rainfall, respectively. Compensation of these changes is essential for the cell to prevent dehydration or disrapture. Bacterial cells need to maintain an outwardly directed turgor, which pushes the cytoplasmic membrane against the cell wall and appears to be essential for the enlargement of the cell envelope and therefore for growth and cell division (Koch, 1983). To achieve this turgor, solutes are accumulated against their chemical gradient, leading to water flow into the cytoplasm (Epstein, 1986). In high osmolarity environments *C. glutamicum* actively accumulates these compatible solutes to ensure the continuous flow of water into the cytoplasm. After an osmotic downshift *C. glutamicum* releases solutes from the cytoplasm via so-called MS channels, thus counterbalancing excessive water influx to prevent cell lysis (Morbach and Krämer, 2002; 2008).

#### 1.3.1 Response to **hyperosmotic** stress conditions

As first consequence of environmental change to hyperosmotic conditions efflux of water occurs and cells impend to dehydrate. Thereupon, to maintain cell turgor, *C. glutamicum* as other bacteria responds with a fast influx of  $K^+$  followed by the accumulation of compatible solutes, such as glycine betaine, trehalose, and proline, at high concentrations (Wood, 1999; Morbach and Krämer, 2005a). These compatible solutes harbor two main characteristics. On the one hand they increase the internal osmolality in order to redirect water fluxes and maintain the necessary cell turgor. On the other hand compatible solutes are able to stabilize proteins and protect them against denaturation under hyperosmotic conditions (Bolen and Rose, 2008). Accumulation of compatible solutes can be accomplished either by *de novo* biosynthesis (mainly proline and trehalose) or by uptake

from the surrounding environment (Morbach and Krämer, 2005a). In general bacteria prefer uptake over biosynthesis due to lower energy costs. *C. glutamicum* harbors four osmoregulated uptake systems for compatible solutes, namely BetP, EctP, ProP, and LcoP (Peter *et al.*, 1998; Morbach and Krämer, 2005a). Among these BetP is the most intensively studied uptake system.

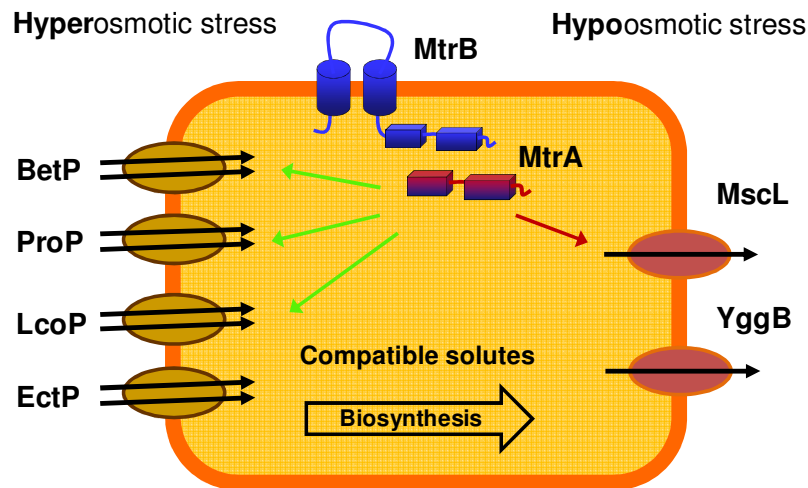


**Fig. 1.2: Systems involved in the osmotic stress response of *C. glutamicum*.**

Under hyperosmotic conditions compatible solutes are accumulated either via *de novo* synthesis or via the osmoregulated uptake systems BetP, ProP, EctP, and LcoP. The two-component system MtrBA senses these hyperosmotic conditions and regulates the transcription of several genes which are either up- (green arrow) or down-regulated (red arrow). To prevent cell lysis upon osmotic downshift the MS channels MscL and YggB open within milliseconds to allow the release of compatible solutes.

In order to adapt to osmolarity changes of the environment, bacterial cells have to sense these changes. Therefore, *C. glutamicum* harbors the osmosensory two-component system MtrAB consisting of a membrane-bound histidine kinase MtrB and the soluble response regulator MtrA (Möker *et al.*, 2004). MtrB is able to sense a so far unknown stimulus related to hyperosmotic stress via its cytoplasmatically located phosphorylation domain. The response regulator MtrA becomes phosphorylated by MtrB and binds to the DNA, regulating the transcription of several genes involved in osmoregulation, e.g. *betP*, *proP*, *lcoP*, and *mscL* (Krämer 2009).

One of these genes, *betP*, encodes the transporter BetP which is a specific uptake carrier for glycine betaine. BetP is a secondary transporter which belongs to the BCCT-type family of transporters (Krämer and Morbach, 2004). It consists of 594 AA forming 12 transmembrane segments. Both, the C- and N-terminal, domains of about 50-55 AA are exposed to the cytoplasm. Electron cryo-microscopy of 2D crystals revealed that three BetP proteins form a trimer (Ziegler *et al.*, 2004). Recently, the crystal structure of BetP

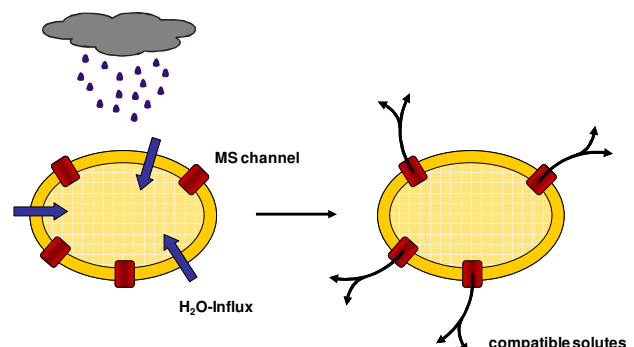
was also solved at a resolution of 3.3 Å (Ressl *et al.*, 2009). The uptake of glycine betaine is energetically coupled to the membrane potential dependent co-transport of two Na<sup>+</sup> ions (Peter *et al.*, 1996; Krämer and Morbach 2004; Morbach and Krämer, 2005b). Upon activation BetP transports betaine into the cell in a very specific manner reaching a K<sub>m</sub> value of 8.9 μM and so is able to build up extremely high betaine gradients of 4 x 10<sup>6</sup> (inside/out ratio) (Peter *et al.*, 1996). Besides its transport activity, BetP is also able to function as osmosensor. Three different stimuli are involved in the activation of BetP, (a) the C-terminal, regulatory domain, (b) the cytoplasmic K<sup>+</sup> concentration, and (c) negative membrane surface charges (Rübenhagen *et al.*, 2001; Ott *et al.*, 2008). Once the hyperosmotic stress is compensated the cell has to keep the internal betaine concentration at a constant level. Thus, an appropriate fine-tuning mechanism that regulates the internal betaine concentration by balancing uptake and efflux is necessary. In principle, two such mechanisms are possible. One is the gradual downregulation of the transport activity of BetP; the other is the presence of a counteracting efflux system compensating the ongoing betaine uptake. However, a combination of both mechanisms also seems possible. It was already shown that BetP activity is strongly decreased upon adaption to hyperosmotic stress (Botzenhardt *et al.*, 2004). Nevertheless, the knowledge of the exact fine-tuning process of internal betaine concentration is still very limited.

### 1.3.2 Response to **hyposmotic** stress conditions

Mechanosensitive (MS) channels are described as protection system against sudden osmotic downshifts. This rapid decrease of external osmolarity leads immediately to an excessive water influx and consequently to a dramatically increased turgor pressure. To avoid cell lysis, emergency release valves, the MS channels, are activated within milliseconds mediated by the increased membrane tension. As a result, cytoplasmic solutes are released into the environment and the driving force for water entry is reduced (Fig. 1.3) (Morbach and Krämer 2002; Booth *et al.*, 2007).

**Fig. 1.3: Response to hyposmotic stress conditions.**

Sudden decrease of the external osmolarity, e. g. caused by rainfall, leads to an excessive water influx. To prevent cell disruption mechanosensitive channels are activated immediately to allow the release of compatible solutes.



According to this function, MS channels have to sense lipid deforming forces within the membrane leading to structural rearrangements that lead to channel opening and allow immediate efflux of solutes. However, the way how MS channels respond to mechanical forces along the plane of the cell membrane is not completely clear. Changes in the lipid bilayer caused by increased membrane tension must somehow be sensed and transmitted to the channel (Martinac, 2004).

In contrast to *C. glutamicum*, the MS channels of *E. coli* have been intensively studied for many years. Using patch clamp techniques, three types of MS channels could be identified in *E. coli*. Dependent on their conductance the channels are named MscL, MscS and MscM for large, small or very small (*mini*) conductance (Fig. 1.4) (Berrier *et al.*, 1996; Perozo and Rees, 2003). Corresponding to their conductance the three channels open at different activation thresholds to allow a stepwise response to hypoosmotic conditions (Fig. 1.4) (Martinac *et al.*, 1987; Perozo and Rees, 2003).

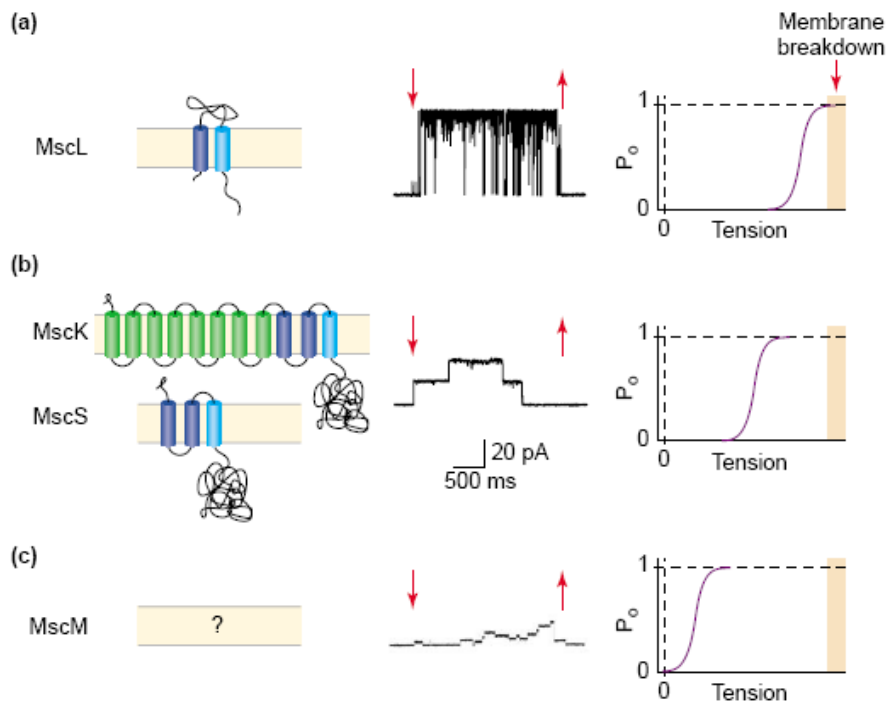


**Fig. 1.4: Mechanosensitive channels from *E. coli*.**

Shown are the channels responsible for (a) the MscL (large conductance), (b) two channels of small conductance, MscS (non specific) and MscK (potassium ions), and (c) MscM (*mini* conductance) mechanosensitive activity as topology model, their single channel activity, and activation threshold.

From: Perozo and Rees, 2003

While the associated genes of MscL (*mscL*) and MscS (*yggB*) have been identified, the gene encoding MscM is still unknown (Levina *et al.*, 1999). MscL and MscS have been

studied most extensively, resulting in the crystal structure of both proteins (Chang *et al.*, 1998; Bass *et al.*, 2002). These two channel proteins are generally not found in animals, but homologs are present in plants and in some fungi and oomycetes. Other structural classes of MS channels are known to exist in higher organisms, from yeast to humans (Kung, 2005). MscL is the largest of the known MS channels. It assembles as homopentamer, each subunit (136 AA) containing two transmembrane domains. For activation a much stronger membrane tension is necessary than it is the case for MscS and MscM. The threshold level of the membrane tension that activates MscL is reached at imminent cell lysis. Accordingly, MscL acts as emergency valve activated at the last moment to allow an extremely fast compensation of the osmotic gradient. Deletion of *mscL* in *E. coli* shows no significant differences concerning growth or survivability upon hypoosmotic stress compared to the wild type. Thus, lack of MscL function seems to be compensated by the other MS channels. MscS activity in *E. coli* is composed of two different channel activities. The gene product of *yggB*, MscS, constitutes the main part of activity, while *kefA* encodes a potassium regulated MS channel (MscK). MscS belongs to a family of small membrane proteins of about 300 AA (*E. coli* MscS: 286 AA). However, MscK is part of a family of larger membrane proteins of more than 700 AA (*E. coli* MscK: 1120 AA). *E. coli* mutants lacking MscL and MscS are not able to survive severe osmotic downshifts. However, lack of MscK (also KefA) has no influence on the survivability (Levina *et al.* 1999; Perozo and Rees 2003; Pivetti *et al.*, 2003). Besides sensing membrane stretches (activation threshold is about 50 % of MscL) MscS is able to detect changes of the membrane potential (Sukarev, 2002). The crystal structure revealed that MscS assembles a homoheptamer (Fig. 1.5) (Bass *et al.*, 2002).

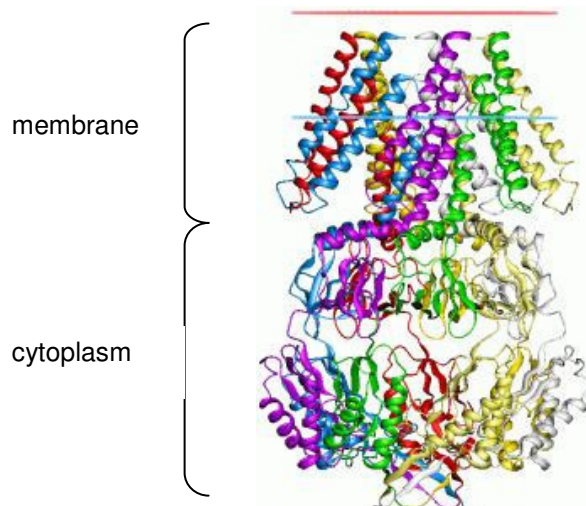


**Fig. 1.5: *E. coli* MscS heptamer**  
(side view).

*E. coli* MscS assembles as homoheptamer. Each subunit is shown in a different colour. The periplasmic part (N-terminus) is displayed at the top, the cytoplasmic part (C-terminus) at the bottom.

From: Bass *et al.*, 2002

Each MscS subunit contains 286 AA assembling three transmembrane helices and an additional large, cytoplasmic C-terminal domain. However, some MscS homologs are predicted to have more than three transmembrane (TM) spans which are observed in *E. coli* MscS (Pivetti *et al.*, 2003). While the TM1 and TM2 domains act probably as sensor of changes in membrane tension and membrane potential, the TM3 domains of each subunit pack tightly in the heptameric complex to line a pore. In the crystal structure (Fig. 1.5), this pore has a diameter of about 8 – 11 Å at the narrowest point generated by the side chains of Leu105 and Leu109, which form the hydrophobic seal in the closed channel (Bass *et al.* 2002, Miller *et al.* 2003). The pore forming TM3 helix contains a conserved glycine- and alanine-rich motif that forms a helix-helix interface. The smooth glycine face allows a sliding of the opposite TM3 helices across each other inducing a conformational change that opens the channel (Edwards *et al.*, 2005). It was proposed that opening and closing of the channel is caused by an iris-like rotation of the helices in the membrane. The current model suggests that under outwardly directed turgor pressure, the density of lipids in the cytoplasmic membrane is decreased. Thereupon, TM1 and TM2 adjust their conformation to increase their buried volume. This rotation of TM1 and TM2 might lead to a shift of TM3. Movement of TM3 withdraws the side chains of Leu105 and Leu109 from the central pore allowing solvated ion transport (Wang *et al.*, 2008). Single amino acid exchanges within the three TM domains important for channel gating often have a high impact on channel activation. For MscS several loss-of-function (LOF - difficult or no channel opening), and gain-of-function (GOF - easy or flickering channel opening) mutants are described (Nomura *et al.*, 2006; Okada *et al.*, 2002; Miller *et al.*, 2003; Edwards *et al.*, 2005; Wang *et al.*, 2008). GOF-mutations can especially have severe consequences for the cell as a permanently open channel would cause cell death.

In contrast to the MS channels known for *E. coli* which release different molecules in a very unspecific way, *C. glutamicum* MS channels show much higher substrate specificity for compatible solutes, mainly betaine and proline (Ruffert *et al.*, 1997). As mentioned above, two different conductances were observed in patch clamp analysis of *C. glutamicum* membrane fragments (Ruffert *et al.*, 1999). Two putative MS channel genes, *mscL* and *yggB*, identified by sequence homologies to the *E. coli* MS channels, were further characterized by Nottebrock *et al.* (2003). While a deletion of *mscL* showed no phenotype, the absence of *yggB* led to a reduced ability to release betaine upon osmotic downshift. A double mutation had an intermediate phenotype concerning its ability to cope with hypoosmotic stress indicating the existence of a third efflux channel, not identified yet

(Nottebrock *et al.*, 2003). This assumption was further supported by the fact that the double deletion in *C. glutamicum* was not lethal upon severe hypoosmotic conditions. However, deletion of *yggB* also included an essential regulatory sequence, located upstream the genes of isoleucine/valine biosynthesis. This additional deletion resulted in a strain auxotroph for isoleucine, leucine, and valine. Side effects on the phenotype due to this auxotrophy could not be completely excluded (Nottebrock *et al.*, 2003).

As described above, MscS of *E. coli* has been under intensive investigation by several research groups. The *C. glutamicum* homolog YggB, on the contrary, has been poorly investigated. Therefore, not much knowledge exists about its function as MS channel. Furthermore, there is still no proof, e.g. using patch clamp analysis, that the YggB protein really harbors the functions of a MS channel.

#### **1.4 Glutamate production by *C. glutamicum***

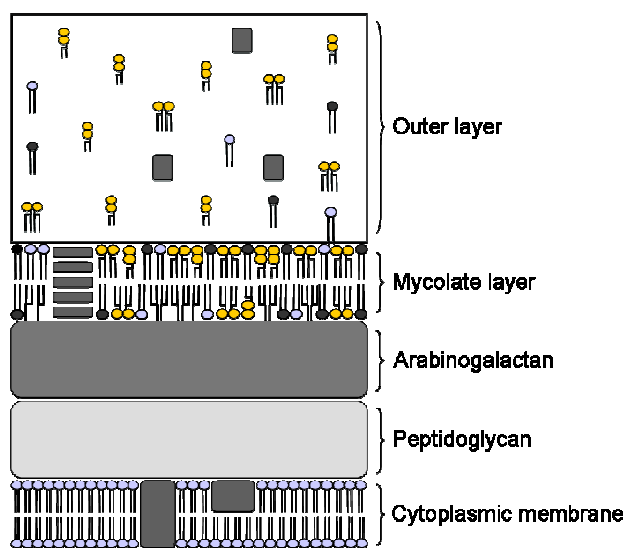
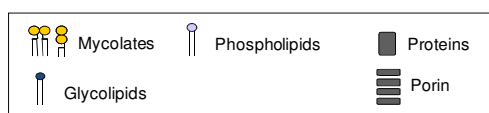
Among the amino acids produced by microbial fermentation, L-glutamic acid in the form of monosodium glutamate (MSG) is the one with the highest production rate. MSG has a unique flavor, which is called *umami* in Japanese, and is used as flavor-enhancer. About 2.0 million tons of MSG is currently produced worldwide per year by fermentation using coryneform bacteria (Shirai *et al.*, 2005; Sano, 2009). The fermentation process is carried out under strictly controlled conditions (temperature, pH, aeration) using sugar cane syrup as the most common carbon source. The L-glutamic acid excreted by the bacteria into the fermentation solution is then obtained by crystallization (Leuchtenberger *et al.*, 2005).

To induce glutamate productive conditions several treatments are known since *C. glutamicum* does not excrete any glutamate under normal growth conditions. As described below all these treatments somehow alter the cell wall. Consequently, the structure of the cell wall and its regulation is supposed to have significant influence on amino acid efflux (Eggeling *et al.*, 2008). A schematic model of the *C. glutamicum* cell wall is shown in figure 1.6. The cytoplasm is surrounded by the cytoplasmic membrane composed of phospholipids in which the membrane proteins, e.g. importers and exporters, are embedded. The peptidoglycan–arabinogalactan is arranged on top in outward direction. The mycolate layer consists of one layer of mycolic acids (mainly dimycolates) which are esterified with arabinogalactan, and of one layer of non-covalently bound trehalose mycolates. This upper layer is already part of the outer layer containing also a large quantity of soluble lipids, such as trehalose di- and monomycolates. The mycolate layer

has a highly ordered structure that leads to a cell wall of unusually low permeability (Puech *et al.*, 2001; Eggeling and Sahn, 2001).

**Fig. 1.6: Cell wall composition of *C. glutamicum*.**

On top of the cytoplasmic membrane the peptidoglycan is located. To the peptidoglycan a layer of arabinogalactan is linked. To the ends of the arabinogalactan mycolic acids (mainly dimycolates) are esterified which together with soluble mycolic acids in the form of trehalose monomycolates and trehalose dimycolates form an outer layer.



The conditions of normal growth of *C. glutamicum* can be changed towards glutamate productive conditions by several treatments. In general, two major modifications of (a) the cell wall structure and (b) the metabolic flux between tricarboxylic acid (TCA) cycle and glutamate synthesis are involved in glutamate production by *C. glutamicum*. One possibility to induce glutamate overproduction is limited supply of biotin which is necessary for growth (Shiio *et al.*, 1962). Glutamate excretion triggered by biotin limitation is explained by the inhibition of fatty acid synthesis which leads to a decreased availability of phospholipids and consequently to membrane alterations. In the presence of sufficient biotin, glutamate excretion can be induced by the addition of fatty acid ester surfactants such as Tween 40 (polyoxyethylene sorbitan monopalmitate) or Tween 60 (polyoxyethylene sorbitan monostearate) (Takinami *et al.*, 1965; Duperray *et al.*, 1992). However, monolaurate or monooleate esters (Tween 20 and 80, respectively) are not effective. Further triggering methods are the addition of (a) the beta-lactam antibiotic penicillin inhibiting cell wall biosynthesis by binding to penicillin-binding proteins, which catalyze the transglycosylation and transpeptidation of peptidoglycan (Nunheimer *et al.*, 1970); (b) the antimycobacterial drug ethambutol targeting a series of arabinosyltransferases, and therefore causing a decreased arabinan deposition in the cell wall (Radmacher *et al.*, 2005); (c) local anesthetics, e. g. chlorpromazine, tetracaine, butacaine, and benzocaine, which change the order of the lipid bilayer by insertion into the membrane (Lambert *et al.*, 1995). It becomes quickly obvious that all these treatments or

conditions alter the cell envelope of *C. glutamicum*. The amount of mycolic acids is reduced by up to approximately 40 % under glutamate production conditions. Additionally, the spectrum of mycolic acids, normally consisting of 30, 32 or 34 carbons is altered to much shorter mycolic acids containing 22 and 24 carbons (Hashimoto *et al.*, 2006). However, not only treatments directly altering the cell wall induce glutamate production, but also genetic manipulations of the cell wall via fatty acid synthesis can trigger glutamate excretion. Here it has to be mentioned that trehalose becomes covalently linked to fatty acids forming trehalosemono- and dimycolates (Tropis *et al.*, 2005). A mutant lacking the trehalose synthesis genes *treS*, *otsA*, and *treY* is devoid of the mycolic acid layer under distinct cultivation conditions. This lack of mycolates is sufficient to induce continuous glutamate excretion (Gebhardt *et al.*, 2007). Additionally, the overexpression or inactivation of the genes involved in lipid synthesis results in a strong alteration of the phospholipid composition and as a consequence of the modified lipid synthesis in a dramatically changed glutamate efflux (Nampoothiri *et al.*, 2002).

Several genes are up- or downregulated under glutamate productive conditions (Kataoka *et al.*, 2006). One is the gene *dtsR1* encoding a homolog of the  $\beta$ -subunit of some biotin-containing enzyme complexes (Kimura *et al.*, 1996). The expression of the *dtsR1* gene and therefore the cellular concentration of the protein are decreased under biotin limited conditions and upon Tween 40 addition. A disruption of the *dtsR1* gene results in a strain strictly auxotroph for fatty acids (oleic acid). The  $\Delta dtsR$  mutant produced glutamate efficiently also in excess of biotin (Kimura *et al.*, 1997). Although the related protein DtsR1 has no biotin-binding motif, it seemed very likely that it might form a complex with another subunit that contains biotin. The two carboxylases identified in *C. glutamicum* which were shown to be essential for fatty acid and mycolic acid synthesis (Gande *et al.*, 2007) were assumed to be counterparts of DtsR1 forming a complex including biotin molecules as co-factors.

As mentioned above, also a change in metabolic flux is involved in glutamate production by *C. glutamicum*. On the metabolic level a reduced specific activity of the 2-oxoglutarate dehydrogenase complex (ODHC) was observed in the *dtsR1* disruptants (Kimura, 2002). Interestingly, such a decrease in the specific activity of the ODHC was also observed under biotin limitation inducing glutamate production. Therefore, the ODHC seems to be a key enzyme in glutamate production, which is located at the metabolic branch point between the glutamate biosynthesis pathway and the TCA cycle where it catalyzes the oxidative decarboxylation of 2-oxoglutarate to succinyl-CoA (Kawahara *et al.*, 1997). It was shown

that the activity of the ODHC was also decreased under glutamate productive conditions induced by several other treatments than biotin limitation, while the activity of the glutamate dehydrogenase (GDH), catalyzing ammonia assimilation of 2-oxoglutarate to form glutamate, was mainly unchanged. Furthermore, the level of ODHC activity seemed to be inversely correlated to the yield of glutamate (Kawahara *et al.*, 1997). Metabolic flux analysis indicated that attenuation of ODHC activity is the factor with the greatest impact on glutamate formation in the metabolic network (Shirai *et al.*, 2005). ODHC consists of three subunits, one the 2-oxoglutarate dehydrogenase subunit E1 $\alpha$  encoded by the gene *odhA* (Usada *et al.*, 1996). Deletion of *odhA* results in the elimination of any ODHC activity. The  $\Delta$ *odhA* mutant produces glutamate spontaneously under normal growth conditions. In this mutant no alteration in the fatty acid composition of the cells was observed. Glutamate production by this mutant additional to the basal glutamate excretion could be triggered by several treatments (Asakura *et al.*, 2007). However, overexpression of *odhA* leading to an increased ODHC specific activity results in dramatically reduced glutamate production despite Tween 40 addition (Kim *et al.*, 2009). These results suggest that decrease in ODHC activity is an important factor for glutamate production by *C. glutamicum*, leading to increased metabolic flux towards glutamate biosynthesis. Thus, it is very interesting how reduction of the ODHC activity and alterations of the cell envelope are correlated.

Recently, a novel regulation mechanism of ODHC was discovered. The 15 kDa protein OdhI in its unphosphorylated form is responsible for the inhibition of ODHC by direct interaction with the E1 $\alpha$  subunit (OdhA). OdhI is phosphorylated by the Ser/Thr protein kinase PknG (Niebisch *et al.*, 2006). Phosphorylated OdhI is inactive and cannot bind to the ODHC. Dephosphorylation of OdhI is catalyzed by the phosphoprotein phosphatase Ppp. PknG is a soluble protein which is assumed to be membrane associated whereas Ppp is a membrane-integral protein. These proteins might function as sensors and their de-/phosphorylation activity is thought to be dependent on the absence or presence of specific stimuli. Deletion of the *odhI* gene nearly abolishes glutamate production. However, the effect of a *pknG* deletion varies depending on the inducing conditions but can lead to a significantly increased glutamate production. The positive influence of the *pknG* deletion on glutamate production might be caused by an increased level of unphosphorylated OdhI, resulting in an increased inhibition of ODHC activity and therefore a higher flux of 2-oxoglutarate towards glutamate synthesis (Schultz *et al.*, 2007).

Taken together glutamate overproduction seems to be the result of a combination of cell wall alteration, possibly mediating the activation of a glutamate excretion system, and metabolic alteration towards efficient glutamate synthesis. A model to combine all effects connected with the induction of glutamate production involves sensing of cell wall alterations, a regulatory cascade up to the central metabolism, and activation of a specific glutamate export system (Fig. 1.7)

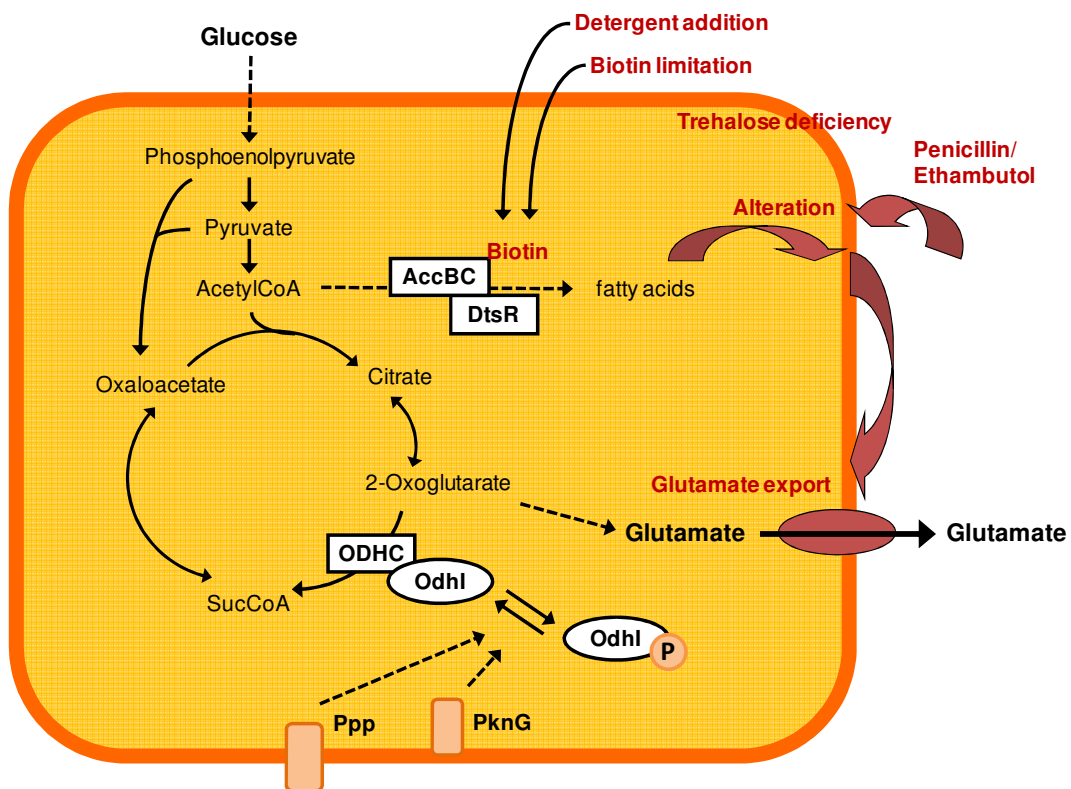


**Fig. 1.7: Model for the induction of glutamate production by *C. glutamicum*.**

Treatments triggering glutamate production alter the cell envelope of *C. glutamicum*. Biotin limitation and detergent addition alter the membrane by inhibiting fatty acid synthesis. Genetic manipulations resulting in effects like trehalose deficiency or changed fatty acid synthesis also change the composition of the cell wall. Addition of penicillin or ethambutol inhibits cell wall biosynthesis. These cell wall alterations might be sensed by the glutamate export carrier itself or by other membrane bound proteins, like PknG and Ppp. These proteins could regulate the ODHC activity via the phosphorylation status of OdhI.

Modified from Nakamura *et al.*, 2007 and Eggeling *et al.*, 2008

## 1.5 Glutamate export

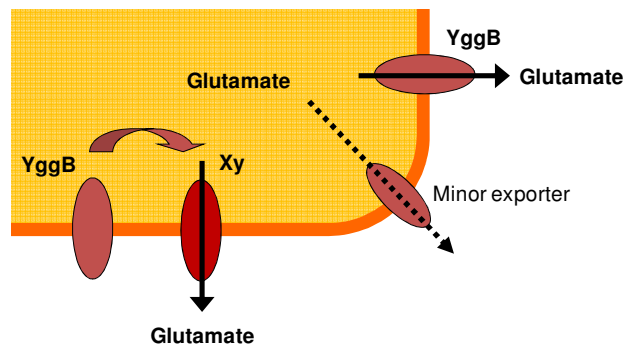
Since *C. glutamicum* is used for the industrial production of various amino acids, which have to cross the cell membrane on their way into the external medium, a main focus of research laid on the identification of the corresponding export systems. Several exporters have been identified so far, such as LysE exporting the basic amino acids L-lysine and L-arginine (Vrljic *et al.*, 1996), BrnFE exporting branched chain amino acids and L-methionine (Kennerknecht *et al.*, 2002; Trötschel *et al.*, 2005), and ThrE exporting L-threonine (Simic *et al.*, 2001). For the export of glutamate the situation slightly differs. Because all the triggers known at the time being affected the cell surface of *C. glutamicum*, it was initially assumed that glutamate passively leaks through the membrane and cell wall ('leak model'). However, it was shown that membrane permeability does not change during glutamate production, since other amino acids, as well as acetate and ions ( $H^+$ ,  $K^+$ , and  $Cl^-$ ) do not leak from the cell (Hoischen and Krämer, 1989; 1990). Furthermore, the leak model itself could not explain the accumulation of external glutamate. Therefore, the presence of a specific glutamate export system in the membrane was proposed (Hoischen and Krämer, 1989; Gutmann *et al.*, 1992). However, this export carrier for the industrial important glutamate was not known for decades.

Recently, the MS channel homolog YggB of *C. glutamicum* was connected to the export of glutamate (Nakamura *et al.*, 2007). As previously mentioned, the activity of the ODHC is significantly decreased under glutamate producing conditions. Therefore, the construction of *odhA* disruptants was one strategy to increase glutamate productivity. However, these mutants showed a reduced ability to grow on minimal medium and had an extremely unstable phenotype resulting in suppressor mutations. To identify such a mutation in a glutamate producing mutant, a Sau3AI library of wild-type *C. glutamicum* chromosomal DNA was used. The gene which restored normal growth and abolished glutamate production was identified by sequencing as *NCgl1221* (*yggB*). Several *odhA* disruptants showing elevated levels of glutamate production revealed mutations within the *yggB* gene. One mutant with a *yggB* (V419::IS1207) gene leading to a protein with a C-terminal truncation of 110 AA showed continuous glutamate production without induction. Overexpression of *yggB* from a plasmid resulted in increased glutamate production only upon induction by various triggers. The deletion of *yggB* was followed by a dramatically decrease in glutamate production. However, a small residual excretion of glutamate could still be observed. Based on the obtained results, Nakamura and co-workers proposed the following model for the role of YggB in glutamate production by *C. glutamicum*: (a)

several treatments inducing glutamate production cause changes in membrane tension, (b) the structure of YggB is altered by these changes so that YggB becomes activated, and (c) allows glutamate excretion. However, YggB is localized in the cytoplasmic membrane, while most of the treatments which induce glutamate production, alter the cell wall of *C. glutamicum*. Here the unique C-terminal elongation provides an interesting candidate to sense and transduce these changes of the cell wall under the assumption that it is localized in the periplasmic space. The reduced ODHC activity might be only a consequence of glutamate production and not an activator. However, a decrease in ODHC activity can then further increase glutamate productivity. Besides the proposed major glutamate export system YggB, a second minor glutamate export carrier might exist. However, the existence of another so far unknown glutamate export system is also possible. In this case YggB might just function as regulator of this glutamate exporter Xy (Fig. 1.8) (Nakamura *et al.*, 2007).

**Fig. 1.8: Possible functions of YggB in the export of glutamate.**

YggB might either function as glutamate exporter together with a minor export system responsible for residual glutamate excretion of the *yggB* deletion strain or as regulator of another unknown export system (shown here as protein Xy).



## 1.6 Thesis objective

The aim of this work was a detailed characterization of the protein YggB of *C. glutamicum*. Research on YggB is interesting because a dual function of the protein was proposed as mechanosensitive channel under hypoosmotic conditions on the one hand and an involvement in the export of the industrial important amino acid glutamate on the other. MS channels can sense alterations of the membrane tension and transduce these alterations into a conformational change allowing solute efflux. As all treatments inducing glutamate production go along with an alteration of the cell envelope, a MS channel harboring the mentioned properties might be a good candidate to be involved in the sensing of these alterations.

However, the actual function of YggB as MS channel has still to be proven. An approved method to show mechanosensitive properties of a channel are electrophysiological analyses via the patch clamp technique. Additionally, YggB should be physiologically characterized under different osmotic stress conditions to gain a comprehensive understanding of its properties. Regarding the proposed involvement of YggB in the export of glutamate the main question is if YggB is the glutamate exporter itself or whether it is just a regulator of another so far unknown glutamate export system. To answer this question, several physiological and biochemical attempts are made to characterize the role of YggB under glutamate productive conditions. In addition to a functional characterization of YggB, the correct topology of the protein in the membrane should be determined. Depending on the computer program used, the existence of a fourth transmembrane domain was predicted which would localize the C-terminal elongation in the periplasm.

## 2 Materials and Methods

### 2.1 Bacterial strains and plasmids

All strains used in this work are listed in table 2.1.

**Table 2.1: Bacterial strains**

Strain	Genotype	Reference
<b><i>E. coli</i></b>		
DH5 $\alpha$ mcr	<i>endA1 supE44 thi-1 <math>\lambda</math>- recA1 gyrA96 relA1 deoR <math>\Delta</math>(lacZYA-argF) U196 <math>\phi</math>80DlacZ <math>\Delta</math>M15mcrA <math>\Delta</math>(mmr hsdRMS mcrBC)</i>	Grant <i>et al.</i> 1990
BL21 (DE3)	F- <i>ompT gal [dcm] [lon] hsdSB</i> (rB –mB –; an <i>E. coli</i> B strain) with DE3, a $\lambda$ prophage carrying the T7 RNA polymerase gene	Novagen, Darmstadt
Frag 1	F–, <i>rha, thi, gal, lacZ</i>	Epstein and Kim, 1971
MJF455	Frag1, $\Delta$ <i>mscL::Cm, <math>\Delta</math>yggB</i>	Levina <i>et al.</i> 1999
MJF465	Frag1, $\Delta$ <i>mscL::Cm, <math>\Delta</math>yggB, <math>\Delta</math>kefA::Km</i>	Levina <i>et al.</i> 1999
<b><i>C. glutamicum</i></b>		
ATCC 13032	wild type	Abe <i>et al.</i> 1967
ATCC 13032 $\Delta$ <i>mscL</i>	Derivative of ATCC 13032 with an <i>in frame</i> -deletion of the <i>mscL</i> gene	Nottebrock <i>et al.</i> 2003
ATCC 13032 $\Delta$ <i>yggB</i>	Derivative of ATCC 13032 with an <i>in frame</i> -deletion of the <i>yggB</i> gene	this work
ATCC 13032 $\Delta$ <i>mscL <math>\Delta</math>yggB</i>	Derivative of ATCC 13032 with <i>in frame</i> -deletions of the <i>mscL</i> and <i>yggB</i> genes	this work
ATCC 13032 $\Delta$ <i>Cgl0590<math>\Delta</math>yggB</i>	Derivative of ATCC 13032 with <i>in frame</i> -deletions of the <i>Cgl0590</i> and <i>yggB</i> genes	this work
ATCC 13032 $\Delta$ <i>Cgl2211<math>\Delta</math>yggB</i>	Derivative of ATCC 13032 with <i>in frame</i> -deletions of the <i>Cgl2211</i> and <i>yggB</i> genes	this work
ATCC 13032 $\Delta$ <i>Cgl2211<math>\Delta</math>Cgl0590</i>	Derivative of ATCC 13032 with <i>in frame</i> -deletions of the <i>Cgl2211</i> and <i>Cgl0590</i> genes	this work
ATCC 13032 $\Delta$ <i>Cgl2211<math>\Delta</math>Cgl0590 <math>\Delta</math>yggB</i>	Derivative of ATCC 13032 with <i>in frame</i> -deletions of the <i>Cgl2211</i> , <i>Cgl0590</i> , and <i>yggB</i> genes	this work
ATCC 13032 IS:: <i>Cgl0063</i>	Derivative of ATCC 13032 with an <i>insertion</i> -deletion of the <i>Cgl0063</i> gene, <i>Cgl0063::Am</i>	Elena Jolkver

## Material and Methods

ATCC 13032 <i>Δkup ΔCglK</i>	Derivative of ATCC 13032 with <i>in frame</i> -deletions of the <i>kup</i> and <i>CglK</i> genes	Follmann <i>et al.</i> , 2009
---------------------------------	--	-------------------------------

All plasmids used in this work are listed in table 2.2.

**Table 2.2: Plasmids**

Plasmid	Features	Reference
pET29b	Km <sup>R</sup> , P <sub>T7</sub>	Novagen, Inc. Madison, USA
pET29b_yggB-his	pET29b containing <i>yggB</i> -his6 for overexpression of <i>yggB</i> with C-terminal (His) <sub>6</sub> -tag fusion in <i>E. coli</i>	Nina Möker
pET29b_yggB Δ110-his	pET29b containing <i>yggB</i> Δ110-his6 for overexpression of <i>yggB</i> with a C-terminal truncation of 110 AA and a (His) <sub>6</sub> -tag fusion in <i>E. coli</i>	Nina Möker
pET29b_yggB Δ132-his	pET29b containing <i>yggB</i> Δ132-his6 for overexpression of <i>yggB</i> with a C-terminal truncation of 132 AA and a (His) <sub>6</sub> -tag fusion in <i>E. coli</i>	Nina Möker
pET29b_yggB Δ247-his	pET29b containing <i>yggB</i> Δ247-his6 for overexpression of <i>yggB</i> with a C-terminal truncation of 247 AA and a (His) <sub>6</sub> -tag fusion in <i>E. coli</i>	Nina Möker
pEKex2	Km <sup>R</sup> , tac promotor, ori <sub>V.E.c.</sub> , ori <sub>V.C.g.</sub>	Eikmanns <i>et al.</i> , 1991
pEKex2_yggB	pEKex2 containing <i>yggB</i> for overexpression of <i>yggB</i> in <i>C. glutamicum</i>	this work
pEKex2_yggB-his	pEKex2 containing <i>yggB</i> -his6 for overexpression of <i>yggB</i> with C-terminal (His) <sub>6</sub> -tag fusion in <i>C. glutamicum</i>	this work
pEKex2_yggB Δ110-his	pEKex2 containing <i>yggB</i> Δ110-his6 for over expression of <i>yggB</i> with a C-terminal truncation of 110 AA and a (His) <sub>6</sub> -tag fusion in <i>C. glutamicum</i>	this work
pEKex2_yggB Δ132-his	pEKex2 containing <i>yggB</i> Δ132-his6 for overexpression of <i>yggB</i> with a C-terminal truncation of 132 AA and a (His) <sub>6</sub> -tag fusion in <i>C. glutamicum</i>	this work
pEKex2_yggB Δ247-his	pEKex2 containing <i>yggB</i> Δ247-his6 for overexpression of <i>yggB</i> with a C-terminal truncation of 247 AA and a (His) <sub>6</sub> -tag fusion in <i>C. glutamicum</i>	this work
pEKex2_Cgl0590	pEKex2 containing <i>Cgl0590</i> for overexpression of <i>Cgl0590</i> in <i>C. glutamicum</i>	this work
pEKex2_Cgl0590-His	pEKex2 containing <i>Cgl0590</i> -his6 for overexpression of <i>Cgl0590</i> with a (His) <sub>6</sub> -tag fusion in <i>C. glutamicum</i>	this work
pEKex2_Cgl2211-His	pEKex2 containing <i>Cgl2211</i> -his6 for overexpression of	this work

Material and Methods

	<i>Cgl2211</i> with a (His) <sub>6</sub> -tag fusion in <i>C. glutamicum</i>	
pMS3	pEKex2 fused with a β-galactosidase alkaline phosphatase reporter cassette for topology studies	Seidel <i>et al.</i> , 2007
pMS3_yggB	pEKex2 containing <i>yggB</i> fused to a β-galactosidase alkaline phosphatase reporter cassette for overexpression in <i>E. coli</i> and in <i>C. glutamicum</i>	this work
pMS3_yggB Δ110	pEKex2 containing <i>yggB</i> Δ110 fused to a β-galactosidase alkaline phosphatase reporter cassette for overexpression in <i>E. coli</i> and in <i>C. glutamicum</i>	this work
pMS3_yggB Δ132	pEKex2 containing <i>yggB</i> Δ110 fused to a β-galactosidase alkaline phosphatase reporter cassette for overexpression in <i>E. coli</i> and in <i>C. glutamicum</i>	this work
pMS3_yggB Δ247	pEKex2 containing <i>yggB</i> Δ110 fused to a β-galactosidase alkaline phosphatase reporter cassette for overexpression in <i>E. coli</i> and in <i>C. glutamicum</i>	this work
pEKex2_mscS	pEKex2 containing <i>E. coli mscS</i> for overexpression of <i>mscS</i> in <i>C. glutamicum</i>	this work
pEKex2_mscS-His	pEKex2 containing <i>E. coli mscS</i> -his6 for overexpression of <i>mscS</i> with C-terminal (His) <sub>6</sub> -tag fusion in <i>C. glutamicum</i>	this work
pEKex2_mscS/CtyggB	pEKex2 containing <i>E. coli mscS</i> fused to the C-terminal domain of YggB for overexpression of <i>mscS/CtyggB</i> in <i>C. glutamicum</i>	this work
pEKex2_mscS/CtyggB-His	pEKex2 containing <i>E. coli mscS</i> fused to the C-terminal domain of YggB-his6 for overexpression of <i>mscS/CtyggB</i> with C-terminal (His) <sub>6</sub> -tag fusion in <i>C. glutamicum</i>	this work
pEKex2_mscS-His I37N/L86N	pEKex2 containing <i>E. coli mscS</i> I37N L86N-his6 for overexpression of <i>mscS</i> I37N L86N with C-terminal (His) <sub>6</sub> -tag fusion in <i>C. glutamicum</i>	this work
pEKex2_mscS/CtyggB-His I37N/L86N	pEKex2 containing <i>E. coli mscS</i> I37N L86N fused to the C-terminal domain of YggB-his6 for overexpression of <i>mscS/CtyggB</i> I37N L86N with C-terminal (His) <sub>6</sub> -tag fusion in <i>C. glutamicum</i>	this work
pEKex2_mscS-His A51N/F68N	pEKex2 containing <i>E. coli mscS</i> A51N F68N-his6 for overexpression of <i>mscS</i> A51N F68N with C-terminal (His) <sub>6</sub> -tag fusion in <i>C. glutamicum</i>	this work
pEKex2_mscS/CtyggB-His A51N/F68N	pEKex2 containing <i>E. coli mscS</i> A51N F68N fused to the C-terminal domain of YggB-his6 for overexpression of <i>mscS/CtyggB</i> A51N F68N with C-terminal (His) <sub>6</sub> -tag fusion in <i>C. glutamicum</i>	this work

pEKex2_mscS-His V40D	pEKex2 containing <i>E. coli</i> <i>mscS</i> V40D-his6 for overexpression of <i>mscS</i> V40D with C-terminal (His) <sub>6</sub> -tag fusion in <i>C. glutamicum</i>	this work
pEKex2_mscS/CtyggB-His V40D	pEKex2 containing <i>E. coli</i> <i>mscS</i> V40D fused to the C-terminal domain of YggB-his6 for overexpression of <i>mscS/CtyggB</i> V40D with C-terminal (His) <sub>6</sub> -tag fusion in <i>C. glutamicum</i>	this work
pEKex2_mscS-His A106V	pEKex2 containing <i>E. coli</i> <i>mscS</i> A106V-his6 for overexpression of <i>mscS</i> A106V with C-terminal (His) <sub>6</sub> -tag fusion in <i>C. glutamicum</i>	this work
pEKex2_mscS/CtyggB-His A106V	pEKex2 containing <i>E. coli</i> <i>mscS</i> A106V fused to the C-terminal domain of YggB-his6 for overexpression of <i>mscS/CtyggB</i> A106V with C-terminal (His) <sub>6</sub> -tag fusion in <i>C. glutamicum</i>	this work
pEKex2_mscS-His L109S	pEKex2 containing <i>E. coli</i> <i>mscS</i> L109S-his6 for overexpression of <i>mscS</i> L109S with C-terminal (His) <sub>6</sub> -tag fusion in <i>C. glutamicum</i>	this work
pQE60	Am <sup>r</sup> , T5 promotor, Col E1	Qiagen, Hilden
pREP	Km <sup>r</sup> , <i>lacI</i>	Qiagen, Hilden
pQE60-lacI	pQE60 with integrated <i>lacI</i> gene	this work
pQE60-lacI_yggB	pQE60-lacI containing <i>yggB</i> for overexpression of <i>yggB</i> in <i>E. coli</i>	this work
pQE60-lacI_yggB-His	pQE60-lacI containing <i>yggB</i> -His for overexpression of <i>yggB</i> with C-terminal (His) <sub>6</sub> -tag fusion in <i>E. coli</i>	this work
pQE60-lacI_yggB Δ110	pQE60-lacI containing <i>yggB</i> Δ110 for overexpression of <i>yggB</i> Δ110 in <i>E. coli</i>	this work
pQE60-lacI_yggB Δ132	pQE60-lacI containing <i>yggB</i> Δ132 for overexpression of <i>yggB</i> Δ132 in <i>E. coli</i>	this work
pQE60-lacI_yggB Δ247	pQE60-lacI containing <i>yggB</i> Δ247 for overexpression of <i>yggB</i> Δ247 in <i>E. coli</i>	this work

## 2.2 Media and growth conditions

*E. coli* strains DH5α<sub>mc</sub>r (Grant, 1990) and MJF strains (Levina *et al.* 1999) as well as *C. glutamicum* wild type strain ATCC13032 (Abe, 1967) and its derivatives (this work) were cultivated in shaking flasks (125 rpm) under aerobic conditions. *E. coli* was grown at 37 °C in Luria-Bertani (LB) medium, *C. glutamicum* at 30 °C in brain heart infusion (BHI, Difco, Detroit, USA) or in CgXII MOPS minimal medium, pH 7.0. The cell density of bacterial cultures was measured photometrical at 600 nm (OD<sub>600</sub>) (Spektrophotometer Novaspec II,

Pharmacia Biotech Inc.). An OD<sub>600</sub> of 1 equates approximately 10<sup>9</sup> cells per ml (Miller, 1992) or a cell dry weight of 0.34 mg/ml. Unless otherwise stated, *C. glutamicum* cells were grown in BHI medium for about 8 h. This culture was washed twice in 0.9 % NaCl and used to inoculate CgXII MOPS, pH 7.0 to an optical density (OD<sub>600</sub>) of 0.2 - 0.5 for adaptation to the minimal medium. Protein expression was already induced in the overnight (o/n) culture by addition of 25 or 200 μM IPTG, respectively. After ~ 16 h this culture was used to inoculate the main cultures. For growth under different osmolalities MM1 medium, pH 7.0 was used containing different salt concentrations.

Antibiotics were added in concentrations of 100 μg/ml for *E. coli* and 25 μg/ml for *C. glutamicum*.

For a general approach to look for the excretion of amino acids besides glutamate, cells were grown in BHI + 500 mM NaCl for about 8 h to let the cells accumulate different solutes. After washing twice, cells were resuspended in CgXII MOPS at an OD<sub>600</sub> of about 10. Following incubation at 30 °C for 30' samples were taken, centrifuged and the supernatant analyzed by HPLC.

### **For 1 L:**

<b>LB</b>	10 g tryptone, 5 g yeast extract, 10 g NaCl
<b>CgXII MOPS</b>	20 g (NH <sub>4</sub> ) <sub>2</sub> SO <sub>4</sub> , 5 g urea, 1 g KH <sub>2</sub> PO <sub>4</sub> , 1.6 g K <sub>2</sub> HPO <sub>4</sub> , 42 g MOPS, 2.9 g NaCl, 4 % glucose, 0.25 g MgSO <sub>4</sub> , 0.01 g CaCl <sub>2</sub> , 0.2 mg biotin, 30 mg protocatechuate, 1 ml trace elements
<b>MM1</b>	5 g (NH <sub>4</sub> ) <sub>2</sub> SO <sub>4</sub> , 5 g urea, 2 g KH <sub>2</sub> PO <sub>4</sub> , 2 g K <sub>2</sub> HPO <sub>4</sub> , 3 g NaCl, 4 % glucose, 0.25 g MgSO <sub>4</sub> , 0.01 g CaCl <sub>2</sub> , 0.2 mg biotin, 30 mg protocatechuate, 1 ml trace elements
<b>Trace elements</b>	10 g FeSO <sub>4</sub> x 7 H <sub>2</sub> O, 10 g MnSO <sub>4</sub> x H <sub>2</sub> O, 1 g ZnSO <sub>4</sub> x 7 H <sub>2</sub> O, 0.2 g CuSO <sub>4</sub> x 5 H <sub>2</sub> O, 20 mg NiCl <sub>2</sub> x 6 H <sub>2</sub> O

## **2.3 Molecular biological approaches**

### **2.3.1 Preparation of competent *E. coli* cells and transformation**

To prepare competent *E. coli* cells, 5 ml LB medium were inoculated from an agar plate of the respective *E. coli* cells and cultivated for 8 h at 37 °C. Subsequently, this culture was used to inoculate 125 ml SOB medium. After 16 h, the cultures were chilled on ice for 10 min, before harvested by centrifugation (2500 rpm, 4 °C, 10 min). The cell pellet was

resuspended in 40 ml TB buffer, chilled on ice for 10 minutes and again centrifuged. The pellet was now resuspended in 10 ml TB puffer, 700  $\mu$ l DMSO was added drop wisely and chilled on ice for 10 min. Aliquots of 100  $\mu$ l were transferred into pre-cooled reaction tubes, immediately frozen in liquid nitrogen and stored at -80 °C.

Prior to transformation, an aliquot of competent *E. coli* cells was thawed on ice. Plasmid DNA was added and the cells were incubated on ice for 30 min. Heat shock at 42 °C for 30 sec was followed by the addition of 800  $\mu$ l LB medium. The cell suspension was cultivated for 1 h at 37 °C. Subsequently, the cell suspension was plated on a LB plate containing the appropriate antibiotic.

**SOB (1L)**     5 g tryptone, 1.25 g yeast extract, 0.125 g NaCl, 2.5 mM KCl • H<sub>2</sub>O, 10 mM Mg Cl<sub>2</sub>

**TB**            10 mM Pipes, 15 mM CaCl<sub>2</sub>, 250 mM KCl, 55 mM MnCl<sub>2</sub>

### 2.3.2 Preparation of competent *C. glutamicum* cells and transformation

To prepare competent *C. glutamicum* cells, 5 ml LB medium plus 2 % glucose were inoculated from an agar plate of the respective *C. glutamicum* cells and cultivated for ~ 16 h at 30 °C. Subsequently, this culture was used to inoculate 25 ml LB medium plus 2 % glucose, which was again inoculated for ~ 8 h. This culture was now used to inoculate 250 ml LB medium supplemented with 4 g/l isonicotinic acid hydrazide, 2.5 % (w/v) glycine, and 0.1 % (v/v) Tween 80 to an OD<sub>600</sub> of 0.3. The cells were cultivated at 20 °C, 140 rpm. After ~ 16 h, the cultures were chilled on ice for 20 min, before harvested by centrifugation (4000 rpm, 4 °C, 10 min). The cells were washed five times in ice-cold 10 % glycerol. After the final washing step, the cell pellet was resuspended in 1 ml ice-cold 10 % glycerol. Aliquots of 55  $\mu$ l were transferred into pre-cooled reaction tubes, immediately frozen in liquid nitrogen and stored at -80 °C.

Prior to transformation, an aliquot of competent *C. glutamicum* cells was thawed on ice. Plasmid DNA was added and the cells were transferred to a pre-cooled electroporation cuvette (PepLab, Erlangen). Electroporation was performed with a Gene-Pulser (Biorad, München) at 2.5 kV, 600  $\Omega$ , and 25  $\mu$ F for at least 5 msec. 1 ml BHIS medium (BHI + 0.5 M sorbitol) was added immediately and the cell suspension was transferred to a cultivation tube. The cells were cultivated for 1 – 2 h at 30 °C. Subsequently, the cell suspension was plated on a BHI plate containing the appropriate antibiotic.

### 2.3.3 DNA techniques

#### 2.3.3.1 Isolation of plasmid DNA from *E. coli* and *C. glutamicum*

The isolation of plasmid DNA was performed following the principle of alkaline lysis. For this purpose, 5 ml rich medium was inoculated with a single colony from an *E. coli* or *C. glutamicum* plate and inoculated overnight. For the isolation of plasmid DNA from these cultures, the NucleoSpin® Plasmid DNA Purification kit (Macherey-Nagel, Düren) was used as recommended by the supplier. For plasmid isolation from *C. glutamicum* cells a pre-incubation step in resuspension buffer A1 containing 15 mg/ml lysozyme for 1 – 2 h at 37 °C was necessary.

#### 2.3.3.2 Isolation of genomic DNA from *E. coli* and *C. glutamicum*

The isolation of genomic DNA was performed using the phenol-chloroform extraction method. For this purpose, 5 ml rich medium was inoculated with a single colony from an *E. coli* or *C. glutamicum* plate and cultivated o/n at 37 °C or 30 °C, respectively. Cells were harvested and the pellet resuspended in 200 µl ddH<sub>2</sub>O. Subsequently, 200 µl phenol was added and the cell suspension was incubated for 10 min at 65 °C followed by a 2 min incubation step on ice. Then, 200 µl chloroform was added and the suspension was vortexed generously. The supernatant was separated from the cell debris (15,300 rpm, 5 min, 4 °C) and 200 µl chloroform was added. After another centrifugation step the supernatant contained the extracted DNA and was stored at -20 °C.

#### 2.3.3.3 Gel electrophoresis and extraction of DNA from agarose gels

Gel electrophoresis of DNA was performed using 0.9 % agarose gels in 1x TAE buffer as described by Sambrook *et al.* (1989). For this purpose, DNA samples were mixed with 5x Loading Dye (MBI Fermentas, St. Leon-Roth). After electrophoresis, DNA was stained with ethidium bromide. For detection of stained DNA, the Image Master VDS system (Amersham Biosciences, Freiburg) was used. DNA was isolated from agarose gels using the NucleoSpion® Extract kit (Macherey-Nagel, Düren) as recommended by the supplier.

**1x TAE**      40 mM Tris, 1 mM EDTA, pH (acetic acid) = 8.0

#### 2.3.3.4 Polymerase chain reaction (PCR)

The amplification of specific DNA fragments was performed by the polymerase chain reaction (PCR, Mullis *et al.*, 1986) using the 2.5x Eppendorf Master Mix (Eppendorf, Hamburg) as recommended by the supplier. Therefore, two primers were used, flanking the DNA region, which should be amplified. Primers were diluted to a concentration of 10 pmol/ $\mu$ l in ddH<sub>2</sub>O. The annealing temperature was chosen with respect to the forward and reverse primer. For each guanine and cytosine 4 °C, for each adenine and thymine 2 °C are required to separate the hydrogen bonds. As template, chromosomal DNA, plasmid DNA, or a colony was used. The PCR reaction was performed using the thermocycler Mastercycler® gradient (Eppendorf, Hamburg) or FlexCycler (analytikjena, Jena).

##### PCR reaction mixture

4  $\mu$ l 2.5x Eppendorf Master-Mix  
 1  $\mu$ l forward primer  
 1  $\mu$ l reverse primer  
 1  $\mu$ l template  
 ddH<sub>2</sub>O ad 10  $\mu$ l

##### PCR amplification program

94 °C_3 min	} 30 cycles
94 °C_15 sec	
Annealing temperature_15 sec	
72 °C_60 sec per 1000 bp	
72 °C_10 min	
4 °C	

If necessary, the PCR product was purified either with the NucleoSpin® Extract Kit (Macherey-Nagel, Düren) as recommended by the supplier, or by gel electrophoresis as described in section 2.3.3.3.

All primers (oligonucleotides) used in this study were manufactured by Eurofins MWG Operon (Ebersberg) and are listed in table 7.1 in the supplement.

#### 2.3.3.5 Restriction, ligation, and sequencing of DNA

For restriction of DNA, restriction enzymes were used as recommended by the suppliers (NEB, Frankfurt/Main; MBI Fermentas, St. Leon-Roth). If dephosphorylation of 5' ends

was necessary, 1  $\mu$ l antarctic phosphatase (NEB, Frankfurt/Main) was added to the samples. For refill of 3'-end overhangs, the DNA Polymerase I, Large (Klenow) Fragment (NEB, Frankfurt/Main) was used. After restriction, dephosphorylation, and/or blunting, DNA was purified either with the NucleoSpin® Extract kit (Macherey-Nagel, Düren) following the supplier's protocol or by gel electrophoresis as described in section 2.3.3.3. For the ligation of DNA fragments into restricted vectors, the T4 DNA ligase (MBI Fermentas, St. Leon-Roth) was used as recommended by the supplier. For direct ligation of PCR products into the pDrive vector by T/A-cloning, the QIAGEN PCR Cloning kit (Qiagen, Hilden) was used. After ligation, 5  $\mu$ l of the reaction mix was used to transform competent *E. coli* cells as described in section 2.3.1.

DNA sequence analyses were carried out by GATC Biotech (Konstanz).

#### 2.3.4 Construction of deletion strains and plasmids

The construction of several deletion strains was performed according to the methods of cross over PCR (Jakoby *et al.*, 1999) and double homologous recombination using the suicide vector pK19mobsacB (Rübenhagen *et al.*, 2001). The correct deletion of the gene was verified by PCR analysis.

Plasmids were constructed by standard molecular genetic methods and confirmed by DNA sequence analysis. To overexpress YggB in the deletion mutant the *yggB* gene was amplified via PCR using ATCC 13032 chromosomal DNA as template. The amplified fragment was cleaved with BamHI and SalI and ligated to BamHI/SalI-cleaved pEKex2, resulting in pEKex2\_*yggB*. According to that *E. coli mscS* was amplified via PCR using MG1655 chromosomal DNA as template. The amplified fragment was cleaved with BamHI and NotI and ligated to BamHI/NotI-cleaved pEKex2, resulting in pEKex2\_*mscS*-His. The fusion of the *E. coli mscS* gene and the C-terminal domain of *C. glutamicum yggB* was constructed by PCR using the named template DNAs as described previously (Yon and Fried, 1989).

Different truncations of *yggB* were subcloned from pET29b (plasmids constructed by Nina Möker) into the *E. coli C. glutamicum* shuttle vector pEKex2. Therefore, fragments were cleaved with BlnI and XbaI. Upon refill of 3'-end overhangs fragments were ligated into Ecl136II-cleaved pEKex2.

All these plasmids were introduced into ATCC 13032  $\Delta$ *yggB* by electroporation.

### 2.3.5 Site-directed mutagenesis

Site-directed mutagenesis was performed using the Stratagene Quickchange Site-Directed Mutagenesis protocol to introduce single amino acid exchanges. Mutagenic primer pairs are listed in table 7.2 in the supplement. Subsequent to the PCR, the methylated initial template DNA was digested by addition of 1  $\mu$ l DpnI and the residual DNA was transformed into *E. coli* DH5 $\alpha$  competent cells.

**PCR reaction mixture**

- 5  $\mu$ l Pfu buffer (10x)
- 2.5  $\mu$ l of each primer
- 5  $\mu$ l plasmid (1:100 dilution)
- 6  $\mu$ l dNTPs (2 mM)
- 1  $\mu$ l Pfu Turbo polymerase
- ddH<sub>2</sub>O ad 50  $\mu$ l

**PCR amplification program**

- 95 °C\_30 sec
- 95 °C\_30 sec
- 55 °C\_60 sec
- 68 °C\_15 min
- 68 °C\_7 min
- 4 °C

} 18 cycles

## 2.4 General analytic methods

### 2.4.1 Cell disruption and membrane preparation

To control the extent of protein expression, cells were disrupted using a Ribolyser (FastPrep<sup>TM</sup>, Waltham, USA) three times at maximum speed of 6.5 for 45 sec. The cell debris was separated from the supernatant by centrifugation (20 min, 13,000 rpm, 4 °C). The supernatant was then again centrifuged (20 min, 80,000 rpm, 4 °C) and membranes were resuspended in PBS buffer, pH 7.5.

**PBS**            137 mM NaCl, 2.7 mM KCl, 4.3 mM Na<sub>2</sub>HPO<sub>4</sub>, 1.4 mM KH<sub>2</sub>PO<sub>4</sub>, pH (NaOH) = 7.5

### 2.4.2 Determination of protein concentrations

Protein concentrations of cell or membrane extracts were measured by the Bradford spectrophotometric technique (Bradford, 1976). For this purpose, 1 to 10 µg of protein were diluted in 100 µl ddH<sub>2</sub>O and supplemented with 900 µl Bradford reagent. Known concentrations of bovine serum albumine (BSA; NEB, Frankfurt/Main) were used as standard. The optical density of the samples was measured at 595 nm and the concentration of the protein solution could be determined by the use of the BSA calibration curve.

**Bradford reagent** 35 mg Coomassie Brilliant Blue G250, 50 ml phosphoric acid, 25 ml ethanol, ddH<sub>2</sub>O ad 500 ml

### 2.4.3 SDS-Polyacrylamide Gel Electrophoresis (PAGE)

For the electrophoretic analyses of proteins under denaturing conditions, cell extract or membrane preparations were diluted in loading dye and subjected to SDS-PAGE using 12 % SDS polyacrylamide gels (Laemmli *et al.*, 1970).

**12 % Separation gel** 1.5 ml separation gel buffer, 2.21 ml ddH<sub>2</sub>O, 2.5 ml acrylamide: bisacrylamide (30 : 0.8), 40 µl APS (100 mg/ml), 4 µl TEMED

**Stacking gel** 0.625 ml stacking gel buffer, 1.465 ml ddH<sub>2</sub>O, 0.41 ml acrylamide : bisacrylamide (30 : 0.8), 11.25 µl APS (100 mg/ml), 3.75 µl TEMED

Gel electrophoresis was performed in Minigel-Twin Electrophoresis Units (Biometra, Göttingen) at 50 V for about 40 min and subsequently at 160 V up to 2 h.

**Separation gel buffer** 1.5 M Tris, 0.4 % SDS, pH (HCl) = 8.8

**Stacking gel buffer** 0.5 M Tris, 0.4 % SDS, pH (HCl) = 6.76

**1x Electrophoresis buffer** 25 mM Tris, 192 mM glycine, 3.5 mM SDS, pH (HCl) = 8.2

**5x Loading buffer** 4 % SDS, 20 % glycerol , 10 % 2-mercaptoethanol, 0.01 % serva blue G, 25 % separation gel buffer

#### 2.4.4 Staining of SDS-gels - Coomassie Brilliant Blue staining

Via SDS-PAGE separated proteins were routinely made visible by Coomassie Brilliant Blue staining (Sambrook *et al.*, 1989). For this purpose, the SDS-gels were incubated in staining solution for 1 to 16 h, followed by decolorizing of the gels using 10 % acetic acid.

**Staining solution**     2.5 g Serva Blue G-250, 454 ml ddH<sub>2</sub>O, 454 ml methanol, 10 % acetic acid

#### 2.4.5 Immunoblot analyses

The expression level of specific proteins was determined by means of immuno blotting. After SDS-PAGE, the proteins were transferred from the SDS-gels to a PVDF membrane (Millipore Immobilon P, Roth, Karlsruhe) by semi dry blotting. For this purpose, the membrane was first incubated in methanol and then equilibrated in transfer buffer. Following, the membrane was placed on top of three chromatography papers (Whatman, Dassel), which were equilibrated in the same buffer. After removal of the stacking gel the SDS-gel was applied on top of the membrane and covered with another three filters, which were equilibrated in transfer buffer. The protein transfer reaction was carried out inside of a semi dry blotter (Pharmacia Biotech, GE Healthcare, München) for 45 min at 0.8 mA / cm<sup>2</sup>. After shaking for 1 h in blocking buffer 1, the membrane was incubated for another 1 h in blocking buffer 1 containing the first antibody raised against 6xHis-tag (1:2000 dilution) (Qiagen, Hilden) or against YggB (1:1000 dilution) (produced by Eurogentech, Köln). After 3 washing steps with TBST buffer for 10 min each, as second antibody anti-Mouse IgG alkaline phosphatase (1:10,000 dilution in blocking solution 2) or anti-Rabbit IgG alkaline phosphatase (1:10,000 in blocking solution 1) (Sigma-Aldrich, Deisenhofen) was used and incubated for 1 h at RT. After 4 further washing steps (10 min each), the signal detection was achieved by the addition of the alkaline phosphatase substrate BCIP/NBT (final concentration 0.0165 % and 0.033 %, Roth, Karlsruhe) in AP buffer. Depending on the desired signal intensity, the membrane was incubated for 5 to 60 min in the dark, before the reaction was stopped by the addition of ddH<sub>2</sub>O.

**Transfer buffer**             10 mM CAPS, 10 % (v/v) methanol, pH (NaOH) = 11  
**1x TBS**                         10 mM Tris, 150 mM NaCl, pH (HCl) = 7.5  
**1x TBST**                        20 mM Tris, 500 mM NaCl, 0.05 % (v/v) Tween 20, 0.2 % (v/v) Triton-X-100

<b>Blocking buffer 1</b>	3 % BSA in TBS
<b>Blocking buffer 2</b>	10 % milk powder in TBS
<b>AP buffer</b>	100 mM Tris, 100 mM NaCl, 5 mM MgCl <sub>2</sub> , pH (HCl) = 9.5

#### 2.4.6 Determination of osmolality

To determine the osmolality of any buffer or medium an osmometer (Osmomat 030, Gonotec, Berlin) was used as recommended by the suppliers. Calibration solutions of 0.4 and 1.2 osmol/kg were used as recommended by the suppliers.

#### 2.4.7 HPLC (high-performance liquid chromatography) – analysis

Glutamate concentrations were determined using the HPLC systems Agilent HP1100 and VWR/Hitachi EliteLaChrom. Samples were diluted to a range between 10 and 250 µM. Glutamate solutions of 10, 50, 100 and 250 µM were used to obtain a calibration curve. A derivatization of glutamate with o-Phtaldialdehyd/Borat/2-Mercaptoethanol (OPA) was performed previously, which could be detected by a fluorescence detector. Samples were separated via a reversed-phase precolumn (Multospher 40x4mm, CS-Chromatographie) followed by a reversed phase main column (Nucleodur RP-18, 125x4mm, Macherey & Nagel). The program used is displayed in table 2.3.

**OPA (100 ml)** 90 ml ddH<sub>2</sub>O, 2.5 g boric acid, pH (KOH) = 10.4, 0.3 ml Brij 35 (30 % (w/v)), 0.244 ml mercato-propion acid, OPA (80 mg in 1 ml MeOH), ad 100 ml with ddH<sub>2</sub>O

**Table 2.3: HPLC-program used for determination of glutamate concentrations.**

Time [min]	Buffer A [%]	Buffer B [%]
0.0	90	10
3.0	80	20
3.5	70	30
5.5	62	38
12	90	10

Flow rate: 1 ml/min

**Buffer A** 40 mM sodium acetate, 0.06 % sodium azide, 5 % (v/v) MeOH:Acetonitrile (1:1)

**Buffer B** MeOH:Acetonitrile (1:1)

Complete amino acid analysis was performed under the same conditions described above, using the program displayed in table 2.4. To detect the amino acid proline derivatization with Fmoc (fluorenylmethyloxycarbonyl chloride) was used additionally to OPA.

**Table 2.4: HPLC-program used for complete amino acid analysis.**

Time [min]	Buffer A [%]	Buffer B [%]
0.0	93	7
3.1	93	7
5.0	93	7
7.0	90	10
15	85	15
22	50	50
25	40	60
28	30	70
29	20	80
30	50	50
31	80	20
32	93	7

Flow rate: 1 ml/min

## 2.5 Biochemical approaches

### 2.5.1 Enzyme assays

For alkaline phosphatase and  $\beta$ -galactosidase activity determinations, LB o/n cultures of *E. coli* BL21 (DE3) cells harboring the pMS3 plasmid with different *yggB* truncations were diluted to an OD<sub>600</sub> of 1 with LB. Cells were permeabilized by addition of 70  $\mu$ l 0.1% sodium deoxycholate and 70  $\mu$ l toluol. After incubation for 30 min at 37 °C, 1ml assay buffer was added. The enzyme reaction was started by addition of 200  $\mu$ l substrate (each 4 mg/ml, OPNG in 0.1 M KH<sub>2</sub>PO<sub>4</sub>, BCIP in DMSO) and stopped after a yellow or rather blue coloration became visible by addition of 1 ml Na<sub>2</sub>CO<sub>3</sub> or K<sub>2</sub>CO<sub>3</sub>, respectively. Alkaline phosphatase activity was assayed essentially as described by Brickman and Beckwith (1975), except using an extinction coefficient of  $\epsilon_{405\text{nm}} = 1.85 \times 10^{-4} \text{ M}^{-1}\text{cm}^{-1}$  with 5-bromo-4-chloro-3-indolyl phosphate disodium salt (BCIP) as a substrate, whereas  $\beta$ -galactosidase was assayed according to Miller (1992) with o – nitrophenyl  $\beta$ -D-galactopyranoside (OPNG) using an extinction coefficient of  $\epsilon_{420\text{nm}} = 2.13 \times 10^{-4} \text{ M}^{-1}\text{cm}^{-1}$ . Enzyme activities were then determined using the Lambert-Beer-Law:

$$\text{Enzyme activity } [\mu\text{M}/\text{min}] = \Delta A \cdot 3.34 \cdot (\text{dilution factor}) \cdot 10^6 / (\epsilon \cdot d \cdot \Delta t)$$

<b>Assay buffer for AP</b>	10 mM Tris, 10 mM MgSO <sub>4</sub> , pH 8
<b>Assay buffer for <math>\beta</math>-Gal</b>	37 mM NaH <sub>2</sub> PO <sub>4</sub> , 63 mM Na <sub>2</sub> HPO <sub>4</sub> , 1 mM MgSO <sub>4</sub> , 0.2 mM MnSO <sub>4</sub>

### 2.5.2 Analysis of cell viability

Survival rates of *E. coli* cells after an osmotic downshift were determined using the LIVE/DEAD<sup>®</sup> BacLight<sup>™</sup> Bacterial Viability Kit as recommended by the supplier (Molecular Probes, Leiden, The Netherlands). Cultivation of MJF455 was performed as described earlier (Levina *et al.*, 1999). *O/n* cultures were grown at 37 °C in MacIlvaine medium + 0.4 g/l glucose for ~ 16 h. Subsequently, 2 g/l glucose was added and cells were incubated for 1 h at 37 °C. Cells were then diluted with MacIlvaine medium + 2 g/l glucose to an OD<sub>600</sub> of 0.05 and grown at 37 °C to an OD<sub>600</sub> of 0.2 – 0.3. A second *o/n* culture was inoculated in MacIlvaine medium (2 g/l glucose) + 500 mM NaCl at an OD<sub>600</sub> of 0.025 and incubated at 25 °C. Subsequently, 0.2 mM IPTG was added for 2-3 hours. 1 ml of the cultures was harvested and resuspended in isoosmotic buffer (50 mM MOPS, pH 7.0 adjusted to an osmolality of 1.12 osmol/kg with sorbitol) or in hypoosmotic buffer (50 mM MOPS, pH 7.0 adjusted to an osmolality of 0.19 osmol/kg with sorbitol). After incubation for 10 min, cells were diluted in the identical buffer to an OD<sub>600</sub> of 0.03 and incubated for 15 min in the dark with a mixture of SYTO 9 and propidium iodide. The fluorescence emission spectra of the samples (excitation 470 nm, emission 490-700 nm) were measured in a fluorimeter (SLM Aminco, Rochester, USA). The ratio of the integrated intensity of the spectrum between 510 and 540 nm and that between 620 and 650 nm was determined for each sample and the percentage of live cells was calculated by comparing this ratio with a standard curve of live/dead *E. coli* cells.

<b>MacIlvaine (1L)</b>	8.58 g NaH <sub>2</sub> PO <sub>4</sub> , 1.34 g citric acid, 0.87 g KH <sub>2</sub> PO <sub>4</sub> , 1 g NH <sub>4</sub> SO <sub>4</sub> , 0.1 g MgSO <sub>4</sub> , 0.002 g (NH <sub>4</sub> ) <sub>2</sub> SO <sub>4</sub> • FeSO <sub>4</sub> • 6 H <sub>2</sub> O, 0.001 g thiamine
------------------------	--

### 2.5.3 Efflux of glutamate upon **hypoosmotic shock**

The standard pre-cultivation scheme was used. Main cultures were inoculated with an OD<sub>600</sub> of about 2 and cultivated at 30 °C, 125 rpm. After reaching of an OD<sub>600</sub> of about 6, solid NaCl was added to a final concentration of 750 mM and the cultures were further

incubated for 20 minutes to induce internal glutamate accumulation. Subsequently, the cells were stored on ice and pre-heated for 3 min. at 30 °C prior to use. To determine external glutamate concentrations after an osmotic downshift, cells were centrifuged, the supernatant discarded and the pellet resuspended within seconds in 100 mM Mes/Tris, pH 8.0, containing NaCl at concentrations up to 0.9 M. After 15 seconds 200 µl samples were withdrawn and cells were rapidly separated from the surrounding medium by silicone oil centrifugation with perchloric acid in the bottom layer (oil density of 1.09 kg/l for osmolalities > 1.2 osmol/kg and 1.03 kg/l for osmolalities < 1.2 omol/kg). The external glutamate concentration could be measured in the supernatant by HPLC-analysis.

#### 2.5.4 Efflux of glycine betaine upon **hypoosmotic shock**

The enzymatic synthesis of labeled glycine betaine was performed according to Landfald and Strom (1986) and has been described previously (Peter *et al.*, 1996). *C. glutamicum* strains were grown aerobically at 30 °C, 125 rpm o/n in BHI medium containing 500 mM NaCl for hyperosmotic growth conditions. Cells were harvested by centrifugation and washed twice with chilled downshock buffer. The hypoosmotic washing step resulted in efflux of the majority of compatible solutes which were taken up or synthesized during the prior growth period. Uptake of the labeled betaine was performed by incubating the cells at an OD<sub>600</sub> of 4 for 80 min at 30 °C in a hyperosmotic uptake buffer. Shortly after transfer into the uptake buffer, [<sup>14</sup>C]-glycine betaine at a final concentration of 1 mM (25,000 cpm/ml) was added. Subsequently, the cells were stored on ice and pre-heated for 3 min. at 30 °C prior to use. To measure betaine efflux, cells were centrifuged, the supernatant discarded and the pellet resuspended within seconds in 100 mM Mes/Tris, pH 8.0, containing NaCl at concentrations up to 0.9 M. After 15 seconds 200 µl samples were withdrawn and cells were rapidly separated from the surrounding medium by silicone oil centrifugation with perchloric acid in the bottom layer (oil density of 1.09 kg/l for osmolalities > 1.2 osmol/kg and 1.03 kg/l for osmolalities < 1.2 omol/kg). The radioactivity of 150 µl of the supernatant and of the whole cell suspension supplemented with 3.8 ml Rotiszint ecoplus (Roth, Karlsruhe) was determined by liquid-scintillation counting (Beckman, München) for the amount of excreted and total glycine betaine, respectively.

**Downshock buffer**                    100 mM Mes/Tris, pH 8.0, 5 mM Na<sub>2</sub>HPO<sub>4</sub>, 5 mM K<sub>2</sub>HPO<sub>4</sub>,  
(4 °C)

**Uptake buffer**                      100 mM Mes/Tris, pH 8.0, 0.9 M NaCl, 30 mM glucose, 30 mM urea, 30 mM KCl

### 2.5.5 Betaine uptake and efflux under **hyperosmotic** conditions

*C. glutamicum* strains were cultured, washed and resuspended in uptake buffer as described for betaine efflux (section 2.5.4). Shortly after transfer into the uptake buffer, [<sup>14</sup>C]-glycine betaine at a final concentration of 1 mM (25,000 cpm/ml) was added. After different time intervals (up to 90 min after the addition of betaine), samples were taken and filtered rapidly through glass fibre filters (Typ GF5, Schleicher und Schuell, Dassel). The filters were washed with uptake buffer, and the radioactivity was determined by liquid scintillation counting. To visualize net betaine efflux in the stationary phase an excess of unlabeled betaine to a final concentration of 50 mM was added and samples were taken at times indicated. This surplus of unlabeled betaine masked betaine uptake as only unlabeled betaine was taken up after the addition. The net efflux of betaine could therefore be calculated via the change of radioactivity inside the cells.

### 2.5.6 Betaine uptake rate during osmotic compensation

*C. glutamicum* strains were cultured, washed and resuspended in uptake buffer as described for betaine efflux (section 2.5.4). Shortly after transfer into the uptake buffer [<sup>14</sup>C]-glycine betaine at a final concentration of 4 mM (25,000 cpm/ml) was added. After different time intervals (up to 90 min after the addition of betaine), samples were taken and filtered rapidly through glass fibre filters. A parallel culture was incubated with 4 mM non-labeled betaine. After 3, 30, 60, and 90 minutes an aliquot was taken and tracer-free label (25,000 cpm/ml) in uptake buffer was added. To determine the betaine uptake rate samples were taken immediately after 20, 40, 60, and 80 seconds and filtered rapidly through glass fibre filters. The filters were washed with uptake buffer, and the radioactivity was determined by liquid scintillation counting.

### 2.5.7 Determination of membrane potential

The membrane potential was determined as described earlier (Ebbighausen *et al.*, 1991, Krämer *et al.*, 1990). Therefore, the lipophile radioactiv labeled permeant cation [<sup>14</sup>C]-tetraphenylphosphonium bromide (TPP) (Hartmann Analytic, Braunschweig) was used. TPP is able to permeate the cytoplasmic membrane and is accumulated within the cell.

This accumulation depends on the electric potential over the membrane and occurs until an equilibrium is reached. At the equilibrium state the chemical potential of TPP is equal to the electric membrane potential. Consequently, the membrane potential can be calculated based on the intra- and extracellular TPP concentration.

$$\Delta\psi = (- 2.303 RT/F) \log ([\text{TPP}^+]_{\text{in}}/[\text{TPP}^+]_{\text{ex}})$$

To exclude unspecific accumulation of TPP the ionophores valinomycin and nigericin which provoke the breakdown of the membrane potential were used. The still intracellular accumulated TPP binds unspecific within the cell and its concentration has to be abstracted. Different pre-cultivation schemes were used to investigate the membrane potential under various conditions. Depending on the experimental setup 20  $\mu\text{l}$   $^{14}\text{C}$ -TPP<sup>+</sup> working solution (10  $\mu\text{M}$ ,  $2.21 \times 10^9$  D/min mmol) per 1 ml cell suspension was added. At distinct time points 200  $\mu\text{l}$  cells were separated from the medium by silicone oil centrifugation with perchloric acid in the bottom layer. Radioactivity of 150  $\mu\text{l}$  supernatant was determined by liquid scintillation counting. The internal TPP concentration was obtained by measuring the radioactivity of the whole cell suspension.  $\text{TPP}_{\text{internal}} = \text{TPP}_{\text{total}} - \text{TPP}_{\text{external}}$ . The obtained values of membrane potential were corrected for unspecific probe binding by addition of the uncoupler valinomycin and nigericin at final concentrations of 20  $\mu\text{M}$  and 5  $\mu\text{M}$ , respectively.

### 2.5.8 Determination of the internal pH and the pmf (proton motive force)

The pH gradient was determined via the distribution of a weak acid over the cell membrane or a weak base, respectively. This method is based on the assumption that the membrane is permeable for the neutral form of the molecule but not for the ionic form. Depending on the internal pH an equilibrium is adjusted between internal and external amounts of the molecule. In this case, the external pH of the loading buffer (pH = 8.0) was expected to be higher than the internal pH. Therefore, radio-labeled  $^{14}\text{C}$ -methylammonium ( $\text{pK}_{\text{A}} = 10.65$ ) (Hartmann Analytic, Braunschweig) was used as probe. For the determination of internal and external methylammonium concentrations a final concentration of 15  $\mu\text{M}$  methylammonium (specific activity 3.3 mCi/mmol) was added to the cells and samples were taken before and 15 minutes after addition of 1 mM betaine and separated by rapid silicon oil centrifugation with perchloric acid in the bottom layer. Previously the cells were treated as described for betaine efflux experiments (severe

osmotic downshock followed by resuspension in high osmolality buffer). Radioactivity in the supernatant as well as in the resuspended cells was determined by liquid scintillation counting. To exclude unspecific binding 0.022 % CTAB (cetyltrimethylammoniumbromide) was added as control. With the internal and external methylammonium concentrations the pH gradient as well as the internal pH could be calculated:

$$\Delta\text{pH} = \text{pH}_{\text{ex}} - \text{pH}_{\text{in}} = \log \left( \frac{[\text{methylammonium}^+]_{\text{in}}}{[\text{methylammonium}^+]_{\text{ex}}} \right)$$

$$\text{pH}_{\text{in}} = -\log \left( \frac{[\text{methylammonium}_{\text{total}}]_{\text{in}}}{[\text{methylammonium}_{\text{total}}]_{\text{ex}}} \left( 10^{-\text{pKs}} + 10^{-\text{pHex}} \right) - 10^{-\text{pKs}} \right)$$

The determination of membrane potential and pH gradient over the cytoplasmic membrane allows the calculation of the pmf :

$$\Delta p \text{ (pmf)} = \Delta\psi - z \Delta\text{pH}$$

$$\Delta p = \text{electrochemical proton potential [mV]}$$

$$\Delta\psi = \text{membrane potential [mV]}$$

$$z = 2,3 \text{ RT/F} \sim 61 \text{ mV at } 30 \text{ }^\circ\text{C}$$

### 2.5.9 Test for pyruvate efflux

For this assay the inhibitor aminoethyl-phosphinate was used. Within the cell aminoethyl-phosphinate is converted to acetylphosphinate which inhibits the pyruvate dehydrogenase. As result high amounts of pyruvate are accumulated within the cell and an increased export of pyruvate occurs (Laber and Amrhein, 1987). To perform this assay, respective strains were grown in MM1 minimal medium, inoculated from a MM1 o/n culture with an OD<sub>600</sub> of about 1. Simultaneously, aminoethyl-phosphinate was added to a final concentration of 300 μM. Pyruvate concentrations in the external medium were determined by HPLC analysis at different time points.

### 2.5.10 Test for K<sup>+</sup> permeability

To test K<sup>+</sup> permeability due to expression of *yggB* Δ110-His, a strain completely unable to transport K<sup>+</sup> was used. Recently, it was shown that *C. glutamicum* requires potassium for pH homeostasis at low pH values and is therefore not able to grow under these conditions in the absence of potassium. While wild type cells recover after the addition of KCl the K<sup>+</sup>-transport negative mutant Δ*kup*Δ*CgIK* does not. This mutant lacks all import systems for

potassium ions and is so not able to import potassium ions necessary for pH homeostasis at low pH (Follmann *et al.*, 2009). The ability of YggB  $\Delta$ 110 to restore growth in the  $\Delta$ kup $\Delta$ CglK was tested. For this purpose cells were grown o/n in normal, potassium containing MM1 medium, pH 7.0. This culture was used to inoculate potassium-free MM1 medium containing 250 mM MES at a pH of 6.0 on the one hand and 250 mM MOPS, pH 6.5 on the other. Although there was no potassium in the medium due to contaminations there are always very low amounts of potassium present. Cultures were incubated at 30 °C for 4 hours before 20 mM KCl was added and the further growth was monitored via the OD<sub>600</sub>.

### 2.5.11 Susceptibility of antibiotics

One indicator for the general permeability of the cell wall is the susceptibility to different antibiotics. Using Etest<sup>®</sup> strips (AB Biodisk, Solna, Sweden) containing different antibiotics the minimum inhibitory concentrations (MIC) could be determined. The strips had a MIC scale on one side and an immobilized exponential grade of antibiotic on the other side. When an Etest strip is applied to an inoculated agar surface the antibiotic gradient diffuses into the agar. After incubation, whereby bacterial growth becomes visible, a symmetrical ellipse centered along the strip occurs. Here the antibiotics erythromycin, ethambutol, and penicillin were used. For inoculation, a CgXII MOPS o/n culture was diluted to an OD<sub>600</sub> of 1 and spread with a cotton swab over the CgXII agar plates containing 25 µg/ml kanamycin and 25 µM IPTG. The inoculated plates were incubated at 30 °C until growth became visible.

### 2.5.12 Glutamate production

The standard pre-cultivation scheme was used. Main cultures were inoculated with an OD<sub>600</sub> of about 2 and cultivated at 30 °C, 125 rpm. Glutamate excretion was induced during the exponential growth phase (OD<sub>600</sub> 5 – 6) by the addition of 0.15 % Tween 60 or 6 U/ml Penicillin G, respectively (both Sigma-Aldrich, Deisenhofen). For biotin-limited conditions an additional 24 hours pre-culture in CgXII MOPS minimal medium, pH 7.0 containing 0.5 µg/l biotin was necessary. Samples were centrifuged (5-8 min, 13,000 rpm, RT) to separate the cells from the supernatant. Concentrations of external glutamate in the supernatant were determined by HPLC analysis.

In order to perform an osmolality shift during glutamate production, cells were grown in CgXII MOPS minimal medium, pH 7.0 as described before. Glutamate excretion was

induced by addition of 0.15 % Tween. After 2 hours of incubation parts of the main culture were diluted 1:1 with media of different osmolalities (ddH<sub>2</sub>O, CgXII MOPS and CgXII MOPS + 622.5 mM NaCl) resulting in osmolalities of 0.566, 1.132 (isoosmolar), and 1.726 osmol/kg. Glutamate concentrations in the external medium were measured as described above.

### 2.5.13 Hypoosmotic stress response under glutamate productive conditions

*C. glutamicum* strains were grown aerobically at 30 °C, 125 rpm o/n in BHI medium containing 500 mM NaCl for hyperosmotic growth conditions. Cells were harvested by centrifugation and washed twice with chilled downshock buffer analog to the procedure for the betaine efflux experiments (section 2.5.4). Then, the experiment was split into two parts. In the first part cells were loaded with [<sup>14</sup>C]-labeled betaine at a final concentration of 1 mM (25,000 cpm/ml) under hyperosmotic conditions (CgXII MOPS + 400 mM NaCl (1.839 osmol/kg)) by incubating the cells at an OD<sub>600</sub> of 4 for 80 min at 30 °C. In the second part cells were just incubated in the same manner but without labeled betaine. Upon loading, glutamate production was induced by the addition of Tween 60 and cells were incubated for 3 more hours at 30 °C. The cells were then incubated at decreasing external osmolalities as described in section 2.5.4. After 15 seconds 200 µl samples were withdrawn and cells were rapidly separated from the surrounding medium by silicone oil centrifugation (oil density of 1.09 kg/l for osmolalities > 1.2 osmol/kg and 1.03 kg/l for osmolalities < 1.2 omol/kg). For determination of betaine efflux, the radioactivity of 150 µl of the supernatant and of the whole cell suspension supplemented with 3.8 ml Rotiszint ecoplus (Roth, Karlsruhe) was measured by liquid-scintillation counting (Beckman, München) for the amount of excreted and total glycine betaine, respectively. For determination of glutamate efflux from the experimental setup without labeled betaine, the external glutamate concentrations were measured directly in the supernatant by HPLC-analysis. For the internal glutamate concentrations the cell pellet was resuspended in 120 µl ddH<sub>2</sub>O and 100 µl silicone oil was added. The cells were disrupted by ultrasonification for 15 min. After centrifugation (13,000 rpm, 20 min, 4 °C) the aqueous supernatant was used for HPLC-analysis as well.

## 2.6 Electrophysiological approaches

### 2.6.1 Preparation of giant spheroplasts

Spheroplasts were prepared from *E. coli* strain MJF465 lacking MscL, MscS, and MscK and expressing the plasmid-encoded *yggB* of *C. glutamicum* in a manner similar to that described previously (Ruthe and Adler, 1985; Martinac *et al.*, 1987). Since the MJF465 strain already harbors a kanamycin and chloramphenicol resistance a new vector was constructed. The pQE60 vector (ampicillin resistance) was fused to the *lacI* gene normally encoded on a second plasmid. The *yggB* gene was amplified via PCR using ATCC 13032 chromosomal DNA as template. The amplified fragment was cleaved with NcoI and BamHI and ligated to NcoI/BamHI-cleaved pQE60-*lacI*. A culture of MJF465 containing the respective pQE60-*lacI* was grown in LB medium at 37 °C up to an OD<sub>600</sub> of 0.4 – 0.5, then diluted 1:10 into LB medium, and cephalixin was added to 60 µg/ml. The culture was then incubated at 42 °C for 2-2½ until single-cell filaments reached sufficient length (50-150 µm) for formation of giant spheroplasts (5-10 µm in diameter). Afterwards, IPTG (final concentration 100 µM) and glycerol was added (0.4 %) and cells were incubated at 25 °C, 180 rpm for about 1 hour. Then filaments were harvested by centrifugation, and the pellet was rinsed without resuspension by gentle addition of 1 ml of 0.8 M sucrose (0.4 % glycerol). After a second centrifugation step, the supernatant was removed, and the pellet was resuspended in 2.5 ml of 0.8 M sucrose (0.4 % glycerol). The following reagents were added in order: 150 µl of 1 M Tris (pH 7.2); 120 µl of lysozyme (5 mg/ml); 50 µl of DNase I (5 mg/ml); 150 µl of 0.125 M EDTA. This mixture was incubated at room temperature for 3-5 min to hydrolyze the peptidoglycan layer, and the progress of spheroplast formation was followed under the microscope. At the end of this incubation, 1 ml of a solution containing 20 mM MgCl<sub>2</sub> (to remove the EDTA and activate the DNase), 0.7 M sucrose, 0.4 % glycerol, and 10 mM Tris (pH 7.2) was added. The mixture was then diluted with 5 ml solution containing 10 mM MgCl<sub>2</sub>, 0.8 M sucrose, 0.4 % glycerol and 10 mM Tris (pH 7.2). Aliquots were made and stored at -20 °C.

### 2.6.2 Electrical Recording

Single-channel analysis was performed on giant *E. coli* spheroplasts (Martinac *et al.*, 1987). Spheroplasts (1.5-3 µl) were placed in a bath containing, unless otherwise stated, 250 mM KCl, 90 mM MgCl<sub>2</sub>, and 5 mM Hepes (pH 7.2). Borosilicate glass pipettes (Drummond Scientific Co., Broomall, USA) were pulled using a Flaming/Brown pipette puller (P-87, Sutter Instrument Co., Novato, USA) to a diameter which corresponded to a

pipette resistance between 3.0 and 6.0 M $\Omega$ . The pipettes were filled with 200 mM KCl, 90 mM MgCl<sub>2</sub>, and 5mM Hepes (pH 7.2). All recordings were made by use of standard patch-clamp technique (Hamill *et al.*, 1981) at room temperature (19-23° C). Negative pressure (suction) recorded in mm Hg was applied to patch pipettes by using a syringe and was monitored using a piezoelectric pressure transducer (Omega Engineering, Stamford, USA). Ion currents arising from activation of the proteins using suction were recorded using an Axon 1D patch-clamp amplifier (Axon Instruments), filtered at 2 kHz and digitized at 5 kHz. Single channel analysis was done using pCLAMP10 software (Axon Instruments).

### 3 Results

#### 3.1 Recombinant YggB proteins

The *C. glutamicum* YggB protein consists of 533 amino acids (AA) including an N-terminal part (~ 286 AA) similar to other proteins of the MscS-type family and an additional C-terminal domain of 247 AA absent in the *E. coli* homolog MscS (see figure 7.1 in the supplement for alignment comparing the primary sequence of *C. glutamicum* YggB and *E. coli* MscS). Using YggB as template only six other members of the MscS-type family with a similar protein length (450 – 600 AA) were found, all belonging to strains of the genus *Corynebacterium*. Homology search using only the C-terminal part results in the same six species. Furthermore, no homology of the C-terminal domain to any other sequence was found, indicating that this C-terminal domain is a characteristic feature of *C. glutamicum* YggB and its close relatives. In order to investigate the functions of YggB, several recombinant *C. glutamicum* strains were constructed, one harboring a deletion of the *yggB* gene as well as another one with a deletion of the *mscL* gene and a double deletion lacking both mechanosensitive (MS) channel genes. These strains were the prerequisite to investigate the role of YggB in the cell's response to osmotic stress conditions on the one hand in the production of glutamate on the other.

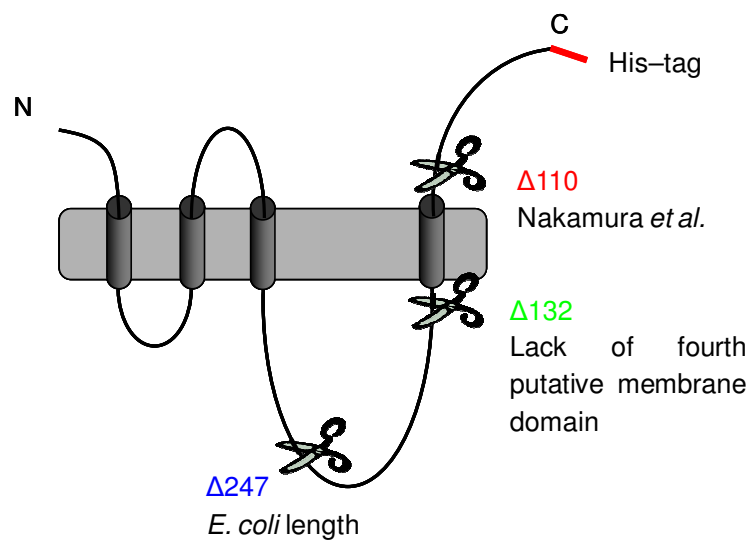


**Fig. 3.1: Topology model of YggB indicating different truncations.**

Different truncated forms of YggB were analyzed, namely the  $\Delta 110$  mutant (423 AA) excreting glutamate spontaneously, the  $\Delta 132$  mutant (401 AA) lacking a fourth putative transmembrane domain, and the  $\Delta 247$  mutant assembling the length of the *E. coli* homolog MscS (286 AA). All genes were recombinantly expressed in the *yggB* deletion strain. All truncation mutants as well as the full length protein carried a C-terminally added 6xHis-tag.

Using the shuttle-vector pEKex2 different plasmid-encoded variants of *yggB* were expressed in the *yggB* deletion strain, including a native *yggB* gene, a His-tagged version of the *yggB* gene, as well as several truncations (Fig. 3.1). The truncated versions of *yggB* were supposed to provide more information about the role of the C-terminal domain of YggB. Additionally, the homologous *E. coli* gene *mscS* and a *mscS/CtyggB* fusion gene was expressed in the *yggB* deletion strain. The *mscS/CtyggB* fusion gene encodes a protein containing the *E. coli* MscS which is 286 AA in length fused to the additional 247 C-terminal AA of YggB. The expression efficiency of the various constructs using different IPTG concentrations is summarized in figure 3.2. Not only in the *yggB* deletion mutant but also in the wild type, which carries a genomic copy of *yggB*, the YggB protein could not be visualized. This indicates a naturally very low expression of *yggB*. However, such a low protein level in the cell was also reported for MscS in *E. coli*, where approximately 3 – 5 channels per cell occur (Booth, personal communication). The *yggB*-His construct on the other hand was extremely overexpressed. Even without IPTG induction a clear signal was detectable. However, based on the low expression of *yggB* in the wild type, all constructs were overexpressed.

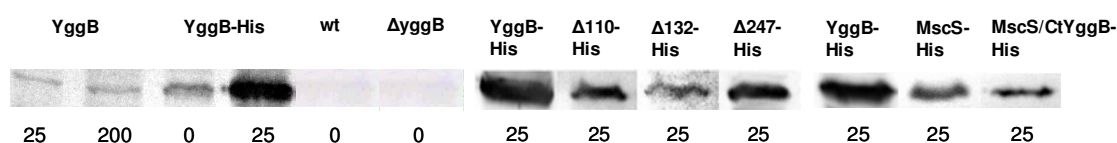


**Fig. 3.2: Western blot analysis of different YggB and MscS constructs.**

wt – wild type strain harboring only the genomic copy of *yggB*,  $\Delta yggB$  – *yggB* deletion strain, all constructs were expressed from the vector pEKex2 in *C. glutamicum*  $\Delta yggB$ . 30  $\mu$ g of membrane extract (60  $\mu$ g for  $\Delta 132$ -His) were loaded to each gel. Below the blot lanes, the concentration of IPTG used for gene expression is indicated. The six lanes on the left were developed using anti-YggB antibody, for all the other lanes anti-(penta)-His antibody was used.

For the complementation of the *yggB* deletion phenotype the expression of the plasmid-encoded *yggB* gene was initially induced by the addition of 200  $\mu$ M IPTG as a standard concentration used for gene expression in *C. glutamicum*. However, expression of the different *yggB* variants by addition of 200  $\mu$ M IPTG led to peculiar growth phenotypes (Fig. 3.3). The  $\Delta 110$ -His mutant showed a strongly delayed onset of growth reaching a final OD<sub>600</sub> after o/n cultivation of only 8.2. The YggB-His strain had also an impaired growth but to a smaller extent (o/n OD<sub>600</sub> 20.8). Under the same conditions the  $\Delta 247$ -His mutant reached an o/n OD<sub>600</sub> of 39.5 which was just very slightly decreased compared to the wild type (o/n OD 46.6) (Fig. 3.3). The growth of the  $\Delta 132$ -His mutant showed no

significant difference compared to the wild type (data not shown). A concern was the fact that at least the  $\Delta 110$ -His strain started to grow normally after several hours of incubation. In this phase no more synthesis of the YggB  $\Delta 110$ -His protein was detected. Due to this observation in the majority of the described experiments 25  $\mu$ M IPTG was used to induce gene expression. MscS-His and MscS/CtYggB strains had no growth phenotype under the later used conditions (data not shown).

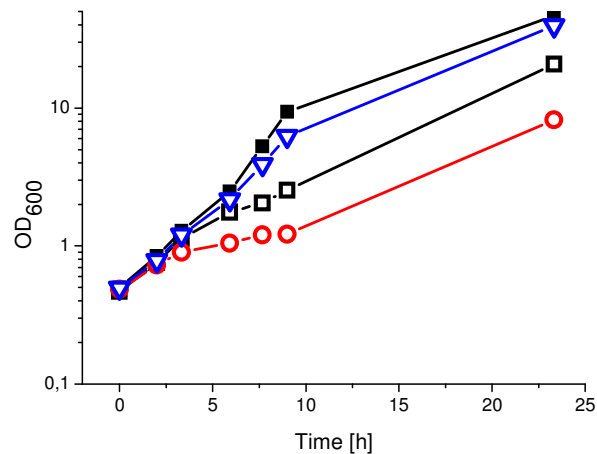


**Fig. 3.3: Growth curves of *C. glutamicum* strains.**

Shown is the increase of optical density (OD) at a wave length of 600 nm. Variants of *yggB*-His were expressed in the *C. glutamicum yggB* deletion and strains were grown in CgXII MOPS minimal medium, pH 7.0 containing 25  $\mu$ g/ml kanamycin and 200  $\mu$ M IPTG). wt (■), YggB-His (□),  $\Delta 110$ -His (○),  $\Delta 247$ -His (▽).

### 3.2 Topology of *C. glutamicum* YggB

YggB harbors three N-terminally located transmembrane domains which show high sequence homology to their counterparts in *E.coli* MscS (see figure 7.1 in the supplement for sequence alignment). The N-terminal end of *E.coli* MscS is localized in the periplasm while the C-terminal end faces the cytoplasm. However, depending on the computer program used, for YggB of *C. glutamicum* a fourth transmembrane segment was predicted which would localize the C-terminal end of YggB in the periplasm instead. In order to reveal the correct topology of the protein, *yggB* gene variants encoding the full length protein as well as the different truncated forms were fused to an alkaline phosphatase- $\beta$ -galactosidase reporter cassette (Seidel *et al.* 2007). This system enables to localize the fusion point to the periplasmic side when alkaline phosphatase is active and  $\beta$ -galactosidase is inactive or to the cytoplasmic side when the enzyme activities are reversed. The *E. coli C. glutamicum* shuttle vector pMS3 containing such an alkaline

phosphatase- $\beta$ -galactosidase reporter cassette was provided by the group of Lothar Eggeling, Forschungszentrum Jülich (Germany). This pMS3 vector containing the different truncated forms of *yggB* was transformed in *E. coli* BL21 (DE3) cells. With the resulting strains  $\beta$ -galactosidase as well as alkaline phosphatase activity assays were performed. Table 3.1 summarizes the ratios of the  $\beta$ -galactosidase/alkaline phosphatase activity for the different truncations. Due to the genomic copy of the *lacZ* gene, the absolute values for both enzyme activities were quite different. However, the ratio clearly demonstrates that YggB harbors a fourth transmembrane domain. In the *yggB* and  $\Delta 110$  variants the alkaline phosphatase activity was much higher than in the  $\Delta 132$  and  $\Delta 247$  mutants indicating a periplasmic localization of the C-terminal domain. Vice versa,  $\Delta 132$  and  $\Delta 247$  had a highly increased  $\beta$ -galactosidase activity compared to the other two mutants. Based on these results, it was proven that *C. glutamicum* YggB harbors a fourth transmembrane domain and that consequently the elongated C-terminal end is localized in the periplasm.

**Table 3.1:** Ratio of  $\beta$ -galactosidase and alkaline phosphatase activity [ $\Delta\mu\text{M}/\text{min}$ ] of *E. coli* BL21 (DE3) heterologously expressing the respective *yggB* variant. Mean values from three independent experiments.

	Ratio $\beta$ -Gal/AP	Standard deviation
<b>yggB</b>	<b>1.31</b>	<b>0.59</b>
<b><math>\Delta 110</math></b>	<b>1.17</b>	<b>0.59</b>
<b><math>\Delta 132</math></b>	<b>10.66</b>	<b>3.33</b>
<b><math>\Delta 247</math></b>	<b>14.74</b>	<b>6.96</b>

### 3.3 Electrophysiological characterization of YggB

Although YggB was proposed to function as MS channel, a final proof was still missing. Patch clamp analysis is the accepted technique for the characterization of channel proteins. A small glass electrode tip is tightly sealed onto a patch of cell membrane, thereby making it possible to record the flow of current through individual ion channels or pores in the patch (Hamill *et al.*, 1981). For electrophysiological analysis of *C. glutamicum* YggB using the patch clamp technique *E. coli* giant spheroplasts (cells in which the cell wall was removed) were used. For spheroplast preparation *yggB* wt,  $\Delta 110$ ,  $\Delta 132$ ,  $\Delta 247$  and *yggB*-

6xHis were expressed in the *E. coli* triple knock out strain MJF465 lacking MscL, MscS and MscK. The pQE60 vector fused to the *lacI* gene was used. Subcloning of *yggB* into pQE60 resulted in a single amino acid exchange from isoleucine to valine since the NcoI restriction site had to be used. As they are both nonpolar amino acids, no effect of this exchange was expected.

Electrical recordings were made from single channels of the prepared spheroplasts. To form a tight (1-2 G $\Omega$ ) seal strong suction was used to move the spheroplast onto the tip of the pipette. After seal formation suction was released. When a spheroplast was lifted out of the bath solution and returned very quickly, the spheroplast was destroyed, leaving only a small patch of membrane across the opening of the pipette (excised patch) (Martinac *et al.*, 1987).

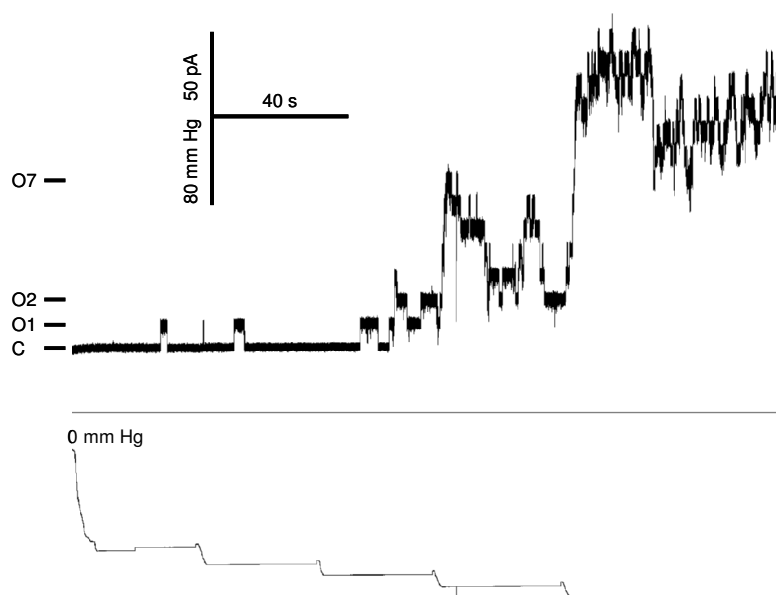


**Fig. 3.4: Gating behavior of YggB in *E. coli* spheroplasts.**

The trace was recorded under asymmetrical conditions (200 mM KCl, 40 mM MgCl<sub>2</sub>, 5 mM HEPES, pH 7.2 in the pipette and 250 mM KCl, 90 mM MgCl<sub>2</sub>, 5 mM HEPES, pH 7.2 in the bath) at + 50 mV applied voltage. Increasing tension opened more channels. C and O<sub>n</sub> denote the closed and open state of n number of channels.

Patch clamp analysis of inside-out excised patches from the spheroplasts revealed the presence of stretch-activated channels. Upon stepwise increasing tension several channels opened, the first channel upon a negative pressure of about – 80 mm Hg. However, this value differed depending on the patch. With increasing pressure more and more channels opened and remained open for several minutes (Fig. 3.4). In contrast to *E. coli* MscS no desensitization (inactivation) occurred. Instead, an oscillating behavior of channel activity was observed indicating the closure of some channels reopening after a further period. As

there were hundreds of channels in a single patch their number was difficult to ascertain. Therefore, no Boltzmann curve (open probability vs. tension) was obtained. As shown in figure 3.5 the channel strongly rectifies, meaning that the conductance is different depending on the direction of ion flux. Measuring the currents upon voltages from  $-90$  mV up to  $+90$  mV in steps of  $10$  mV allows the display of the current/voltage relationship (I/V plot) of YggB (Fig. 3.6).

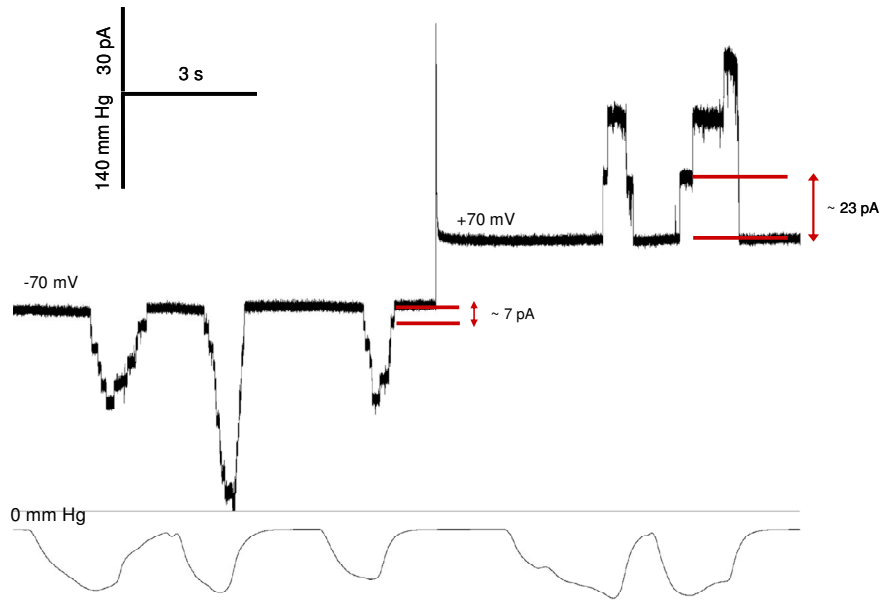


**Fig. 3.5: Effects of positive and negative voltages on YggB conductance.**

The channel showed higher conductance at positive voltages (about  $23$  pA at  $+70$  mV) than at negative voltages (about  $7$  pA at  $-70$  mV). The trace was recorded under asymmetrical conditions ( $200$  mM KCl,  $40$  mM  $MgCl_2$ ,  $5$  mM Hepes, pH  $7.2$  in the pipette and  $250$  mM KCl,  $90$  mM  $MgCl_2$ ,  $5$  mM Hepes, pH  $7.2$  in the bath).

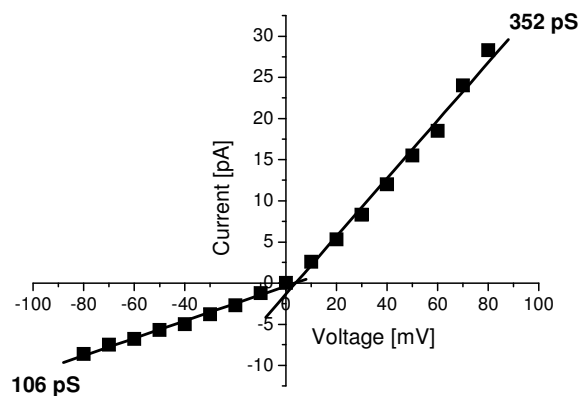


**Fig. 3.6: I/V plot of YggB in *E. coli* spheroplasts.**

This exemplary I/V plot was obtained under asymmetrical conditions ( $200$  mM KCl,  $40$  mM  $MgCl_2$ ,  $5$  mM Hepes, pH  $7.2$  in the pipette and  $250$  mM KCl,  $90$  mM  $MgCl_2$ ,  $5$  mM Hepes, pH  $7.2$  in the bath). Straight lines represent linear regression.

The slope at negative and positive voltages represents the conductance of the channel. The conductance was about  $346.3 \pm 22.5$  pS ( $n = 8$ ) at positive voltages and  $99.5 \pm 4.5$  pS ( $n = 8$ ) at negative voltages. Although the conductances described for the *E. coli* homolog MscS (950 pS and 650 pS) are higher, YggB showed the same rectifying behavior with the conductance at negative voltages being only about 30 % of that at positive voltages. Thus, *C. glutamicum* YggB is clearly a MS channel related to *E. coli* MscS, but with several different properties. Additionally, the behavior of the channel under several other conditions was determined. The I/V plot shown in figure 3.7a was obtained under symmetric conditions (250 mM KCl, 90 mM MgCl<sub>2</sub>, 5 mM Hepes, pH 7.2). Holding the patch and substitution of the buffer in the bath to 250 mM NaCl, 90 mM MgCl<sub>2</sub>, 5 mM Hepes, pH 7.2 had no significant impact on the conductance of the channel or its pressure sensitivity. Conductance was also measured in NaCl solutions only (250 mM in the bath and 200 mM in the pipette). Here again, no significant difference was detected (Fig 3.7b), indicating that the channel has no preference for either potassium or sodium ions.

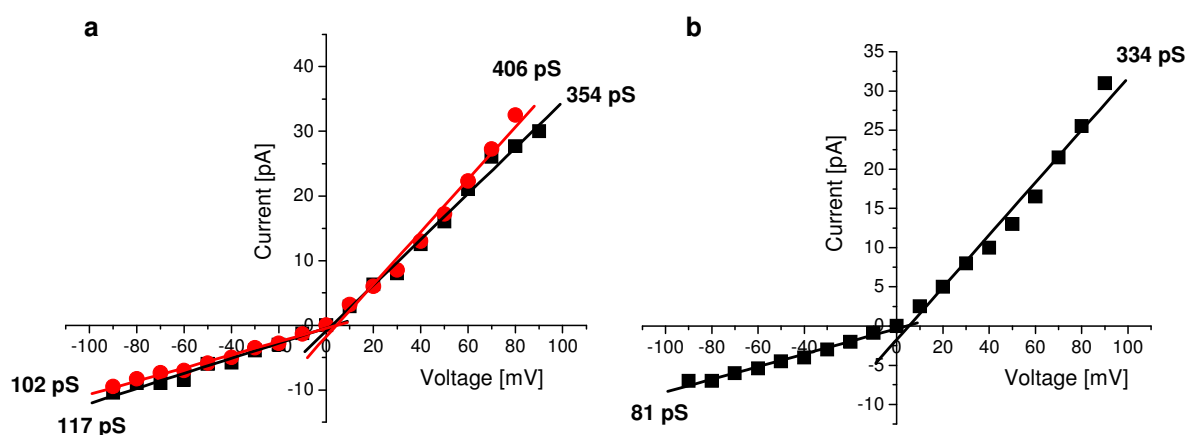


**Fig. 3.7: Ionic preference for potassium or sodium ions.**

(a) The I/V plot was obtained under symmetric conditions (250 mM KCl, 90 mM MgCl<sub>2</sub>, 5 mM Hepes, pH 7.2) (■) followed by a substitution of bath solution to buffer containing 250 mM NaCl. (●); (b) The I/V plot was obtained in sodium containing buffers (200 mM NaCl, 40 mM MgCl<sub>2</sub>, 5 mM Hepes, pH 7.2 in the pipette and 250 mM NaCl, 90 mM MgCl<sub>2</sub>, 5 mM Hepes, pH 7.2 in the bath). Straight lines represent linear regression.

As YggB became interesting due to its possible role in the export of glutamate, also the conductivity of the channel for glutamate was tested. Seal formation was always performed under asymmetric conditions of 250 mM KCl or NaCl, 90 mM MgCl<sub>2</sub>, 5 mM Hepes, pH 7.2 in the bath and 200 mM KCl or NaCl, 40 mM MgCl<sub>2</sub>, 5 mM Hepes, pH 7.2 in the pipette. The solution in the bath was then substituted by 430 mM KGlu or NaGlu (5 mM

Hepes, pH 7.2). As illustrated in figure 3.8a and b, glutamate is able to pass the channel. However, the conductance for glutamate is much lower than for chloride ions. Additionally, the organic acid pyruvate, related to glutamate roughly in size and charge, was tested to allow a better comparison with a more similar substrate. As was the case with glutamate, pyruvate also passed through the channel. Correlating to the slightly smaller size of pyruvate, the conductance upon positive voltage (at 175 pS) was even higher than observed for glutamate (data not shown).

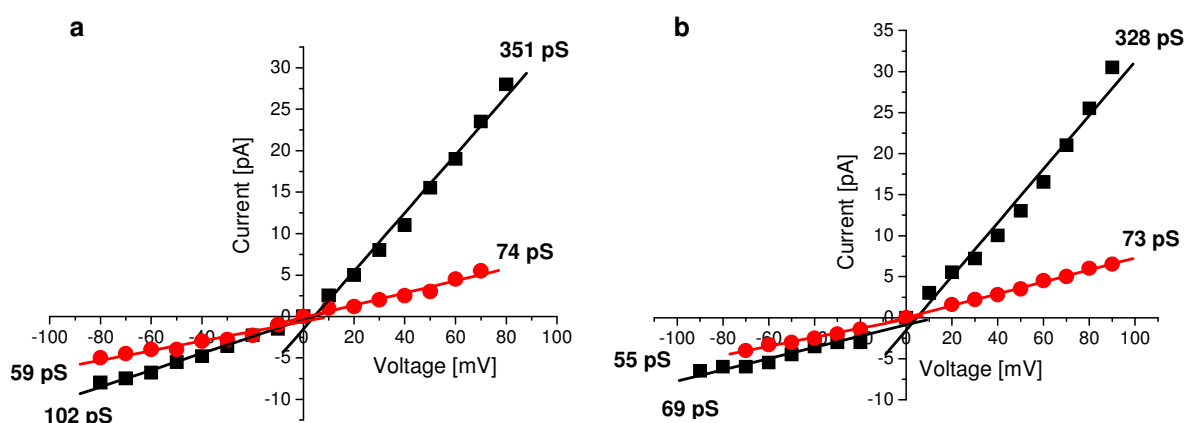


**Fig. 3.8: Channel conductance for glutamate.**

The I/V plots were obtained under standard conditions with either KCl (a) (■) or NaCl (b) (■) followed by a substitution of bath solution with 430 mM KGlutamate or NaGlutamate, 5 mM Hepes, pH 7.2 (●). Straight lines represent linear regression.

*E. coli* MscS shows a slight anionic preference for chloride over potassium ( $P_{Cl}/P_K \sim 1.5 - 3.0$ ) (Martinac *et al.*, 1987). To examine if a similar preference for the ion species could be observed for *C. glutamicum* YggB, the channel behavior was recorded in symmetric solutions in bath and pipette of 200 mM KCl, 40 mM  $MgCl_2$ , 5 mM Hepes, pH 7.2 followed by an increase of the KCl concentration in the bath to 400 mM. Due to the concentration gradient, ions flew from the bath towards the pipette, resulting in a shift of about 8 mV of the zero current potential in the positive direction (Fig 3.9a, b). This positive shift revealed that more potassium ions were able to pass the channel. Consequently, the rightward shift of the I/V plot indicates a channel preference for cations over anions with a selectivity ratio for potassium over chloride of  $P_K/P_{Cl} \sim 3.0$ .

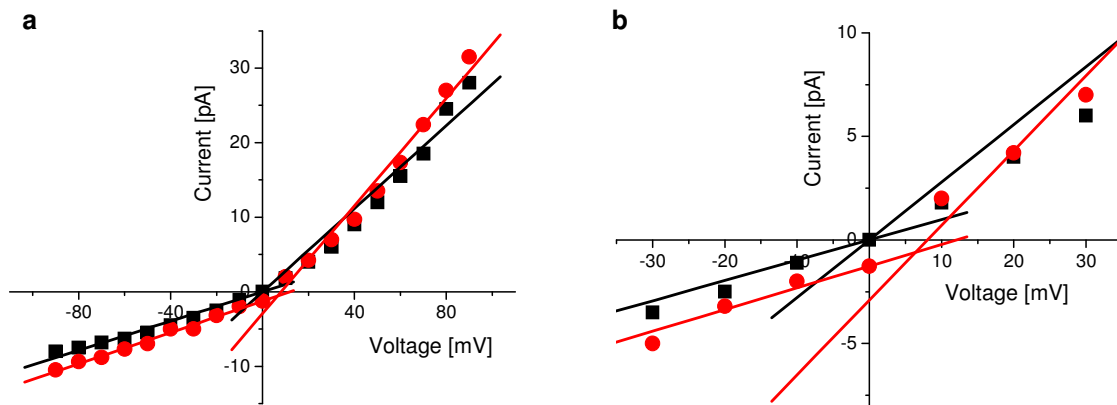


**Fig. 3.9: Preference for anions or cations.**

(a) The I/V plot was obtained under symmetric conditions (200 mM KCl, 40 mM MgCl<sub>2</sub>, 5 mM Hepes, pH 7.2) (■) followed by substitution of bath solution to 400 mM KCl (●). 15 b shows an enlargement of the intersection points with the axes visualizing a ~ 8 mV shift of the zero-current potential. Straight lines represent linear regression.

Additionally, the channel conductance as a dependence on different ion concentration were tested. Therefore, symmetric solutions in bath and pipette were used containing KCl concentrations from 100 mM to 400 mM as well as 40 mM MgCl<sub>2</sub>, 5 mM Hepes, pH 7.2. As displayed in figure 3.10 the conductance increased with increasing KCl concentration. However, this dependency was not linear. At concentrations over 250 mM KCl the conductance became saturated at positive pipette voltage while the conductance at negative pipette voltage was not affected. This indicates that the conductance threshold of the channel was reached.

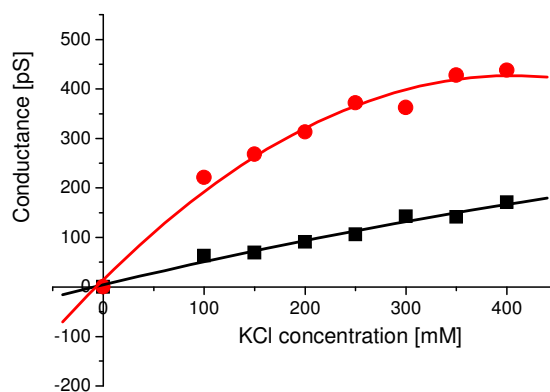


**Fig. 3.10: Conductance vs. KCl concentration.**

Single channel conductance as a function of specific buffer conductivity measured in symmetrical conditions containing different mM concentrations of KCl, 40 mM MgCl<sub>2</sub>, 5 mM Hepes, pH 7.2. Dependency of the conductance is shown upon negative (■) and positive (●) voltages.

All other YggB constructs ( $\Delta 110$ ,  $\Delta 132$ ,  $\Delta 247$ ) as well as YggB-His were just briefly analyzed. However, the conductance of all these constructs was comparable to the wt conductance (Table 3.2). This result suggests that the pore of the channel itself is not affected by different truncations. If indeed there is an effect concerning the regulation or selectivity of the channel this has still to be investigated.

**Table 3.2: Conductance values of different YggB channel constructs.**

Conductance was determined via I/V plots obtained under standard conditions (200 mM KCl, 40 mM MgCl<sub>2</sub>, 5 mM Hepes, pH 7.2 in the pipette and 250 mM KCl, 90 mM MgCl<sub>2</sub>, 5 mM Hepes, pH 7.2 in the bath).

<b>Strain</b>	<b>Conductance [pS]</b>
<b><math>\Delta 110</math></b>	<b>97</b>
	<b>353</b>
<b><math>\Delta 132</math></b>	<b>98</b>
	<b>369</b>
<b><math>\Delta 247</math></b>	<b>118</b>
	<b>321</b>
<b>YggB-His</b>	<b>106</b>
	<b>353</b>

### 3.4 Functionality of *C. glutamicum* YggB in *E. coli*

Using the patch clamp technique the functionality of *C. glutamicum* YggB in the membrane of the *E. coli* triple knock out strain MJF465 lacking MscL, MscS and MscK was shown. To complete studies in *E. coli* also the ability of YggB to rescue the *mscL*, *yggB* double deletion strain MJF455, which is not able to survive upon severe hypoosmotic stress (Levina *et al.*, 1999), under physiological conditions was tested. This experiment was aimed to help understanding the differences of the *C. glutamicum* YggB and the *E. coli* MscS protein, which should be mainly caused by the C-terminal elongation of YggB. Genes coding for T7 polymerase were integrated via  $\lambda$ DE3 phages ( $\lambda$ DE3 Lysogenization Kit, Novagen) into the genome of *E. coli* Frag1 (wt) and MJF455 to allow expression of *C. glutamicum* YggB variants encoded on the plasmid pET29b (work of Nina Möker). However, upon induction of *yggB*  $\Delta 110$ -His and  $\Delta 132$ -His gene expression in the high osmolality medium, necessary for an osmotic downshift, no protein could be detected in

the cells. However, the ability of the other *C. glutamicum* YggB variants to compensate the lack of MS channels in *E. coli* and enable the cells to survive an osmotic downshift was investigated. Therefore, cells were adapted to high osmolality medium and gene expression was induced by the addition of IPTG. Afterwards, a severe hypoosmotic shock from 1.028 osmol/kg to 0.056 osmol/kg was performed by resuspension in the respective buffer. Using the LIVE/DEAD cell viability Kit (Invitrogen) survival rates were determined (Fig. 3.11). Surprisingly, only about 50 % of wild type cells (Frag 1) survived an osmotic downshift, while the MJF455 double deletion mutant showed almost no survival upon hypoosmotic shock. However, expression of *yggB*  $\Delta$ 247 (corresponding to the length of *E. coli* MscS) could fully complement this phenotype. Complementation with the full length YggB protein could only be shown in few experiments probably caused by the fact that the *yggB* gene was unsteadily expressed in *E. coli* under these conditions (data not shown). Thus, while the MJF455 phenotype could be fully complemented by the presence of YggB  $\Delta$ 247, complementation with the YggB full length protein could not be shown definitely.

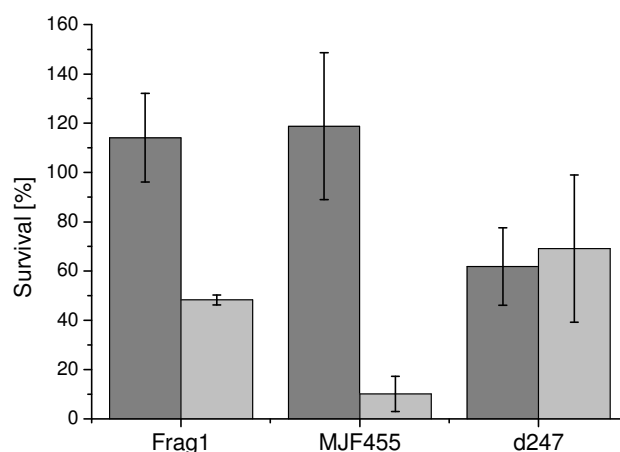


**Fig. 3.11: Survival rates of *E. coli* strains upon osmotic downshift.**

Survival of different *E. coli* strains is monitored after resuspension in isoosmolar buffer (dark grey) and after a severe hypoosmotic shock from 1.028 osmol/kg to 0.056 osmol/kg (light grey). Survival rates were determined using the LIVE/DEAD cell viability Kit. Mean values from three independent experiments.

Frag1 – wt; MJF455 –  $\Delta$ *mscL* $\Delta$ *yggB*; d247 – *yggB*  $\Delta$ 247 expressed in MJF455.

### 3.5 Function of YggB under osmotic stress conditions

#### 3.5.1 Glutamate efflux upon osmotic downshift

The solute efflux mediated by the *C. glutamicum* MS channels upon osmotic downshift was described as quite specific, releasing preferentially betaine and proline (Ruffert *et al.*, 1997). Since YggB was recently linked to the glutamate excretion by *C. glutamicum*

(Nakamura *et al.*, 2007), the efflux of glutamate upon different osmotic downshifts was tested. Therefore, salt stress was applied for a short period of time to induce internal accumulation of glutamate. The cells were then transferred into buffer of decreasing external osmolalities down to very low values and the concentration of glutamate in the external medium was determined immediately (15 sec) after transfer, using HPLC-analysis. Depending on the extent of the downshift increasing amounts of glutamate were released (Fig. 3.12).

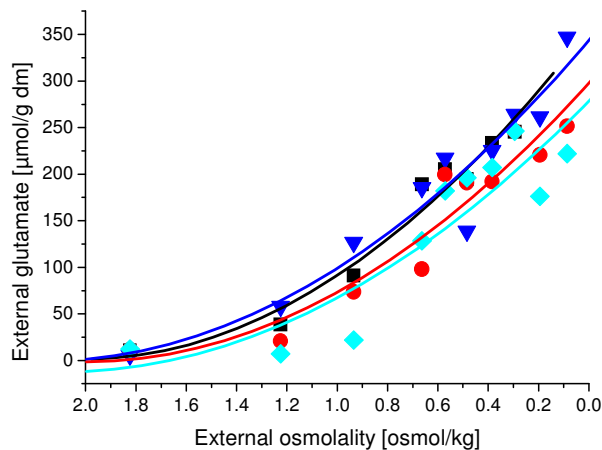


**Fig. 3.12: Glutamate efflux upon hypoosmotic shock.**

Efflux of glutamate was quantified after salt stress-induced accumulation of glutamate (internal amount of glutamate  $\sim 350 - 400 \mu\text{mol/g dm}$ ). Cells were exposed to buffers of different osmolalities and efflux of glutamate was measured 15 sec after the dilution into hypoosmotic buffer. wt (■),  $\Delta yggB$  (●),  $\Delta mscL$  (▼),  $\Delta mscL\Delta yggB$  (◆).

Prior to the downshift the cells had accumulated about  $350 - 400 \mu\text{mol/g dm}$  of glutamate. A strong hypoosmotic shock of about  $\Delta 1.7 \text{ osmol/kg}$  led to the release of most of this internal glutamate. Comparison of the wild type with the  $\Delta yggB$  deletion mutant as well as with the  $\Delta mscL$  deletion and the  $\Delta mscL\Delta yggB$  double deletion strains indicated that these deletions have not a large effect on the ability of the cell to release glutamate. Strains lacking the *yggB* gene released slightly less glutamate (Fig. 3.12). However, the cells still showed considerable glutamate efflux. Nevertheless, it was shown that glutamate efflux occurs upon hypoosmotic stress, although an involvement of YggB in this efflux is not essential.

### 3.5.2 Betaine efflux upon osmotic downshift

In order to investigate the efflux of betaine by *C. glutamicum* cells upon osmotic downshift, cells were pre-incubated in high osmolality medium to induce full expression of importers accumulating compatible solutes. Upon release of all internal solutes, the cells were first loaded with radioactively labeled betaine before they were transferred into buffer of decreasing external osmolalities starting at isoosmolar conditions of 1.8 osmol/kg down to very low osmolality values. Lack of the YggB protein resulted in a reduced betaine efflux upon the same extent of hypoosmotic stress compared to the wild type, meaning that stronger osmotic downshifts were required to detect the same amounts of external betaine (Fig. 3.13). However, deletion of the *mscL* gene had no influence on the efflux pattern compared to the wild type (data not shown) and accordingly no additional effect in the  $\Delta mscL\Delta yggB$  double deletion mutant was observed. This result indicated the existence of at least one additional MS channel in *C. glutamicum*, which was already suggested previously (Nottebrock *et al.*, 2003).

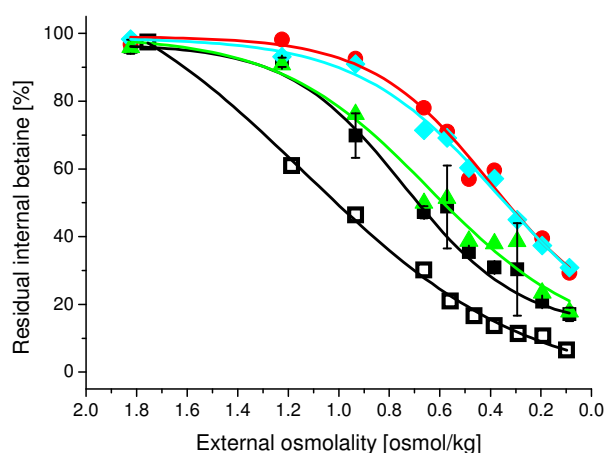


**Fig. 3.13: Betaine efflux upon hypoosmotic shock.**

Efflux of the compatible solute glycine betaine (in radiolabeled form) was quantified after preloading *C. glutamicum* cells under hyperosmotic conditions (1.8 osmol/kg). Cells were exposed to media at different osmolalities and efflux of betaine is measured 15 sec after the dilution into hypoosmotic buffer. Plasmid-encoded gene expression was induced by addition of 25  $\mu$ M IPTG. wt (■),  $\Delta yggB$  (●), YggB (▲),  $\Delta mscL\Delta yggB$  (◆), YggB-His (◻).

The phenotype of the  $\Delta yggB$  mutant could be fully complemented by the expression of the *yggB* gene from a plasmid. Different IPTG concentrations of 25  $\mu$ M and 200  $\mu$ M used for induction of gene expression had no influence on the efflux pattern in this case. However, for the expression of the *yggB*-His construct 0  $\mu$ M and 25  $\mu$ M IPTG were used, which had a high impact on the protein level (Fig. 3.2). Concerning the function as MS channel, the

strain harboring moderate amounts of YggB-His (0  $\mu$ M IPTG) revealed a similar betaine efflux pattern as the complementation (YggB) strain (data not shown). On the contrary, the high overexpression of *yggB*-His (25  $\mu$ M IPTG) led to a much stronger betaine efflux upon the same extent of hypoosmotic stress compared to the wild type and the complementation strain (Fig. 3.13).

For the purpose of investigating the role of the C-terminal domain of YggB, the different truncations of the protein were also tested regarding their function as MS channel. The same experiment using labeled betaine as in figure 3.13 was performed. Figure 3.14a displays the efflux patterns of the strains expressing different *yggB* variants. The increased betaine efflux of YggB-His (25  $\mu$ M IPTG) was already shown in figure 3.13. However, also the other mutants showed a significantly changed betaine efflux. The phenotype of the  $\Delta$ 132-His mutant was comparable to the *yggB* deletion, indicating an inactive or non-functional channel. On the contrary, betaine efflux of the  $\Delta$ 110-His mutant started at an already lower level of internal betaine. The  $\Delta$ 247-His mutant possessed an intermediate phenotype in between wild type and  $\Delta$ *yggB*. However, when the absolute betaine efflux in counts per minute (cpm) instead of the relative betaine efflux (% of the entire internal betaine) was plotted against the external osmolality, it became obvious that the loading of the different mutants with radio-labeled betaine prior to the hypoosmotic shock differed strongly in respect of the efficiency (Fig. 3.14b).

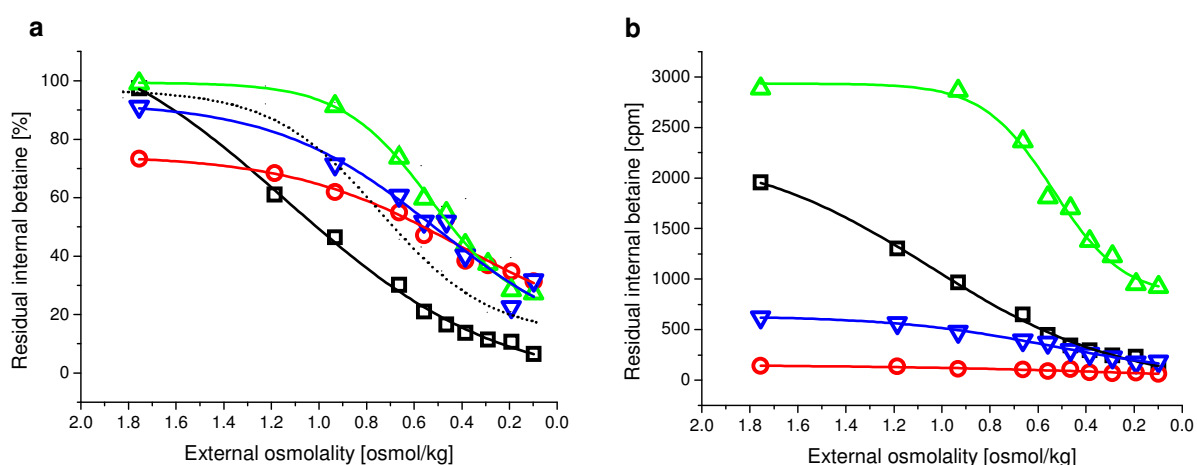


**Fig. 3.14: Betaine efflux upon hypoosmotic shock.**

Efflux of the compatible solute glycine betaine (in radiolabeled form) was quantified after preloading *C. glutamicum* cells under hyperosmotic conditions (1.8 osmol/kg). Cells were exposed to media at different osmolalities and efflux of betaine is measured 15 sec after the dilution into hypoosmotic buffer. Data are displayed as (a) relative efflux in percent and as (b) absolute efflux in cpm. Plasmid-encoded gene expression was induced by addition of 25  $\mu$ M IPTG. YggB-His ( $\blacksquare$ ),  $\Delta$ 110-His ( $\circ$ ),  $\Delta$ 132-His ( $\blacktriangle$ ),  $\Delta$ 247-His ( $\blacktriangledown$ ), wt is shown as dotted line.

The amounts of betaine accumulated under hyperosmotic conditions strongly varied depending on the expressed *yggB* variant. Consequently, the initial amount of internal betaine then detected previous to the osmotic downshift differed significantly. This observation was in contrast to the normal situation under hyperosmotic stress conditions, when cells accumulate compatible solutes until the osmotic gradient is balanced.

Two reasons seemed possible to explain the observed effects. One is an impairment of the main betaine uptake carrier BetP leading to the accumulation of less betaine. However, there was no evidence that the expression of different variants of the *yggB* gene might influence BetP. The other possibility, that some YggB mutants harbor efflux channel activity also under conditions of hyperosmotic stress, seemed much more likely. Therefore, it was now of interest to study the significance of YggB also under conditions of hyperosmotic stress.

### 3.5.3 Betaine accumulation under hyperosmotic conditions

Bacterial cells adapt to hyperosmotic conditions extremely accurate by accumulation of compatible solutes to maintain the ideal cell turgor. To ensure such an exact adjustment, a fine-tuning mechanism including balanced uptake and efflux of these compatible solutes was proposed previously (Grammann *et al.*, 2002). However, the origin responsible for this efflux has not yet been identified. Experimental evidence obtained in this work suggests a possible efflux activity of YggB, also under hyperosmotic conditions. To test this hypothesis the different strains were grown under hyperosmotic conditions analogous to the previous described loading with labeled betaine (see materials & methods) while the uptake of the labeled betaine was monitored (Fig 3.15). As already expected, cells harboring different truncated forms of YggB as well as the highly overexpressed YggB-His had a decreased ability to accumulate betaine. Only the  $\Delta 132$ -His mutant was able to accumulate betaine to amounts comparable to the wild type, *yggB* deletion, and the complementation (YggB) strain expressing a plasmid-encoded *yggB* gene. The strain expressing the  $\Delta 110$ -His truncation was not able to accumulate betaine at all. Also, betaine uptake by cells expressing *yggB*  $\Delta 247$ -His was significantly reduced as well as the uptake by *yggB*-His expressing cells, reaching approximately half of the amount of internal betaine accumulated by wild type cells.

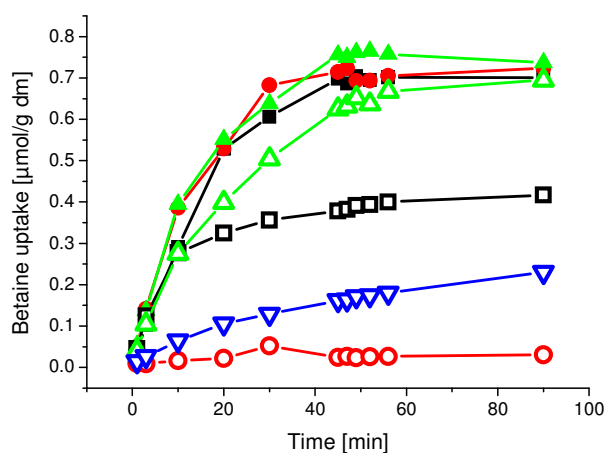


**Fig. 3.15: Betaine accumulation under hyperosmotic conditions.**

Betaine uptake is monitored, the amount of labeled betaine in the cytoplasm of the respective cells was measured by rapid filtration. Plasmid-encoded gene expression was induced by addition of 25  $\mu\text{M}$  IPTG. wt (■),  $\Delta yggB$  (●), YggB (▲), YggB-His (◻),  $\Delta 110$ -His (○),  $\Delta 132$ -His (△),  $\Delta 247$  (▽).

However, with this experiment alone a possible involvement of YggB in the efflux of betaine could not be revealed. Under steady state conditions of internally accumulated betaine no uptake or efflux of betaine can be detected with the described experimental setup. Nevertheless, a balance of uptake and efflux may be assumed to exist during this state. To reveal the net efflux of betaine, a pulse-chase experiment was applied, in which a large excess of unlabeled betaine was added to the cells after reaching the steady state level. This betaine chase masked further uptake of label due to a strongly decreased specific radioactivity in the external buffer and allows separation and quantification of betaine efflux. Importantly for this kind of experiment it has to be mentioned that betaine is not metabolized in *C. glutamicum* cells.

Figure 3.16a shows betaine uptake and efflux visualized by the addition of unlabeled substrate of wild type cells. In the *yggB* deletion mutant the efflux of betaine was slightly but significantly decreased, indicating a contribution of YggB to betaine efflux. The difference of betaine efflux between wild type and the  $\Delta yggB$  mutant displays the portion of betaine efflux mediated by YggB (Fig. 3.16b). The conclusion of YggB as efflux system for betaine was further supported by the strains expressing *yggB* and *yggB*-His induced by different IPTG concentrations (Fig. 3.16c). Strains with moderate protein levels (YggB, YggB-His (0  $\mu\text{M}$  IPTG)) showed normal betaine uptake, but significantly increased efflux. In the strain which highly overexpressed *yggB*-His (25  $\mu\text{M}$  IPTG) the net outward flux was even more enhanced, explaining the explicitly decreased steady state level of betaine accumulation compared to the other strains. Consequently, the YggB protein level and

function in the cell seemed to be directly correlated with the extent of efflux. Taken together, the efflux during the steady state situation of betaine accumulation could be clearly correlated with the presence of YggB.

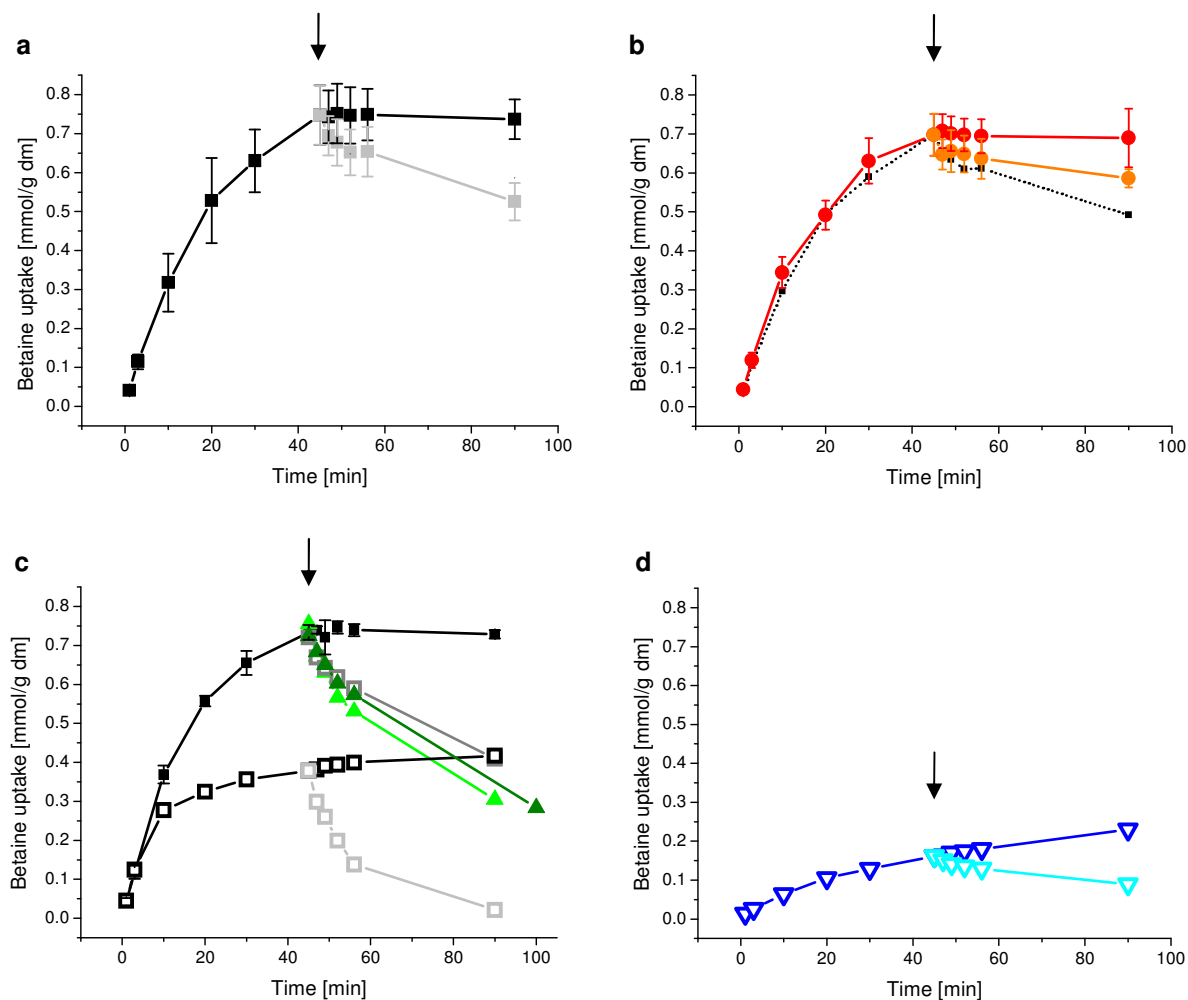


**Fig. 3.16: Kinetic discrimination of betaine uptake and efflux.**

Betaine uptake is monitored until the steady state level. The amount of labeled betaine in the cytoplasm of the respective cells was measured by rapid filtration. The arrow indicates the addition of an excess of unlabeled betaine and the following efflux is visualized. (a) wt uptake (■), chase (□); (b)  $\Delta yggB$  uptake (●), chase (○), for comparison the result for the wt efflux (from a) are added (dotted line). Therefore, the values of the wt were normalized to those of  $\Delta yggB$  by using the mean values of those six measurements from 40 to 90 min without addition of unlabeled betaine in both panels as basis for normalization; (c) YggB (25  $\mu$ M IPTG) chase (▲); YggB (200  $\mu$ M IPTG) chase (▲); YggB-His (0  $\mu$ M IPTG) chase (□); YggB-His (25  $\mu$ M IPTG) uptake (■), chase (□); Betaine uptake by the first three strains was averaged (■). (d)  $\Delta 247$ -His uptake (▼), chase (▽).

Concerning the different YggB truncations,  $\Delta 132$ -His showed the same accumulation/efflux pattern as the *yggB* deletion mutant (Fig. 3.15, data not shown). The  $\Delta 247$ -His mutant which was only able to accumulate little amounts of glutamate, also displayed enhanced efflux upon the betaine chase (Fig. 3.16d). The  $\Delta 110$ -His mutant

accumulated nearly no betaine, making the pulse-chase experiment inapplicable. However, to test if there occurs at least some initial betaine uptake in the  $\Delta 110$ -His mutant the first 60 seconds of betaine accumulation were visualized (Fig. 3.17).

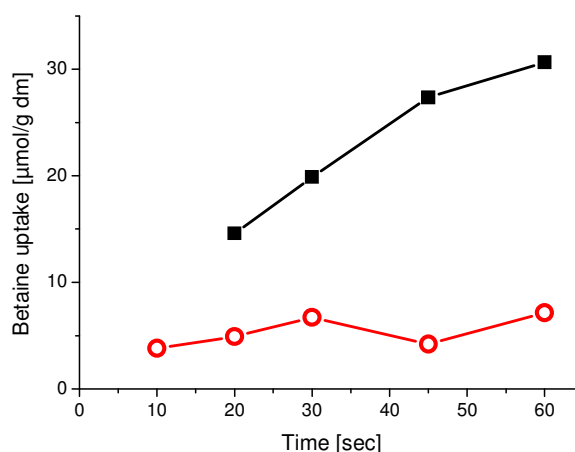


**Fig. 3.17: Initial betaine uptake by the YggB  $\Delta 110$ -His mutant.**

Betaine uptake is monitored during the first 60 sec of betaine accumulation, the amount of labeled betaine in the cytoplasm of the respective cells was measured by rapid filtration. Plasmid-encoded gene expression was induced by addition of 25  $\mu$ M IPTG. wt (■),  $\Delta 110$ -His (○).

But, also within this short period of time no betaine uptake of the cells expressing *yggB*-His  $\Delta 110$  was observed. This might indicate that the  $\Delta 110$  subunits form a basically leaky pore allowing very rapid betaine efflux, at least under the conditions used here. However, such a transiently open pore possibly allowing free flux of several substrates, e. g. protons, would change the energetic situation of the cell resulting in decreased activity of the betaine uptake systems. In order to investigate a possible leakiness of the respective strains the energetic situation of these strains was analyzed further (see section 3.5.3.2).

### 3.5.3.1 BetP activity during osmotic compensation

A possible fine-tuning mechanism of steady state betaine accumulation under hyperosmotic conditions being ensured by a balanced uptake (by BetP) and efflux (via YggB) was proposed in the previous section. The extent of betaine efflux was dependent on the YggB protein level present in the cell. To test a putative feedback of a changed YggB activity on BetP regulation, the adaption of BetP activity during osmotic compensation under the same conditions used before was monitored. Recently, it was shown that BetP activity becomes downregulated when enough compatible solutes,

sufficient to balance the osmotic gradient and maintain ideal cell turgor, were accumulated under hyperosmotic conditions, called osmotic compensation (Botzenhardt *et al.*, 2004). In order to monitor the actual BetP activity during the course of betaine accumulation in the experimental setup used before (see section 3.5.3), the experiment to determine betaine uptake was split into two parallel parts. The first part just monitored the uptake of labeled betaine at high external concentration (4 mM), as described before. In a parallel culture, 4 mM unlabeled betaine was added instead under identical conditions. Betaine uptake and consequently the course of the remaining external betaine concentration could be derived from the first part of the experiment. Consequently, the external betaine concentration at any time point was known and could be transferred to the second part of the experiment. This betaine concentration at the respective time point could then be used to calculate the specific activity of external betaine present in the short term uptake measurements in the second part of the experiment. In this second part pure label was added to an aliquot of cells at different time points and thereupon the uptake kinetics of betaine within a short time (20 – 80 sec) could be monitored resulting in the absolute values of uptake rates at the distinct time point during osmotic compensation. Using this experimental setup, the actual betaine uptake activity of BetP could be monitored at any given time point during betaine accumulation. In wild type cells BetP activity becomes downregulated during osmotic compensation (Botzenhardt *et al.*, 2004) which could be shown for the conditions used here as well (Fig. 3.18).

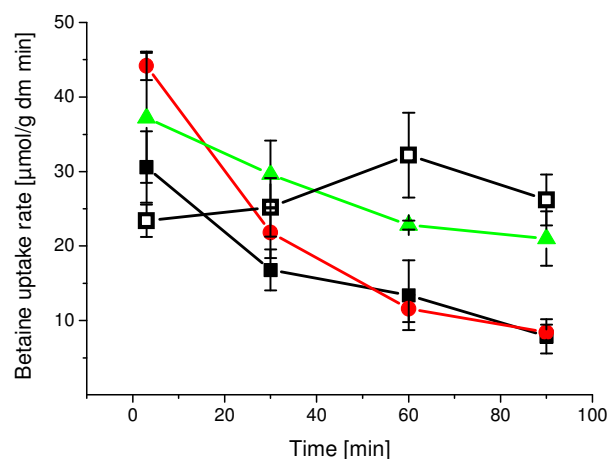


**Fig. 3.18: Actual betaine uptake rate during osmotic compensation.**

Uptake rate of betaine via BetP in the different strains was monitored after initial addition of unlabeled betaine by the addition of pure label at distinct time points. Hyperosmotic conditions were chosen analog to the conditions of the latter experiments. Plasmid-encoded gene expression was induced by addition of 25  $\mu$ M IPTG. wt (■),  $\Delta yggB$  (●), YggB (▲), YggB-His (□), both with 25  $\mu$ M IPTG.

However, in the *yggB* deletion strain this inactivation was observed in a similar manner indicating that the difference in betaine uptake due to the lack of efflux via YggB is too small to be monitored by this kind of experiment. On the contrary, plasmid-encoded expression of *yggB* resulting in an increased betaine efflux had a clear impact on BetP, the activity becoming less downregulated. No decrease of BetP activity was detected in the strain highly overexpressing *yggB*-His which was not able to accumulate sufficient amounts of betaine. Consequently, a direct correlation of YggB efflux activity and BetP uptake activity was demonstrated indicating a tightly connected activity regulation of these two proteins.

### 3.5.3.2 Energetics during betaine accumulation

One important parameter of the energetic situation of the cell is the electrical membrane potential which is also a major contributor of the electrochemical  $\text{Na}^+$  potential, the driving force of betaine uptake via BetP under physiological conditions. In order to investigate whether different YggB truncations result in the formation of a leaky channel the permeability for smaller solutes than betaine and glutamate was tested. Therefore, it was determined if protons as very small molecules pass through these channels by measuring the membrane potential. To determine the membrane potential of a cell the lipophile radioactively labeled cation  $^{14}\text{C}$ -TPP<sup>+</sup> was used. TPP is able to permeate the cytoplasmic membrane and is accumulated within the cell. This accumulation depends on the electric potential over the membrane and occurs until an equilibrium is reached. At the equilibrium state the chemical potential of TPP is equal to the electric membrane potential. Therefore, the membrane potential can be calculated based on the intra- and extracellular TPP concentration.

The membrane potential of several strains was analyzed under the same hyperosmotic conditions used for betaine accumulation experiments described in section 3.5.3 (Fig. 3.19). It was obvious that the membrane potential of the  $\Delta 110$ -His mutant had a much lower value of around 137 mV compared to the other mutants. Also the  $\Delta 247$ -His mutant which was able to accumulate small amounts of betaine showed a decreased membrane potential (~ 160 mV). Indeed, it increased during the uptake of betaine suggesting that the cells started to recover. The strain expressing *yggB*-His (with a potential of about 180 mV) had a slightly lower membrane potential than that expected (200 mV) at a pH value of 8.0 (pH of the loading buffer). This corresponded to the values obtained for the membrane potential of wild type and the  $\Delta 132$ -His mutant.

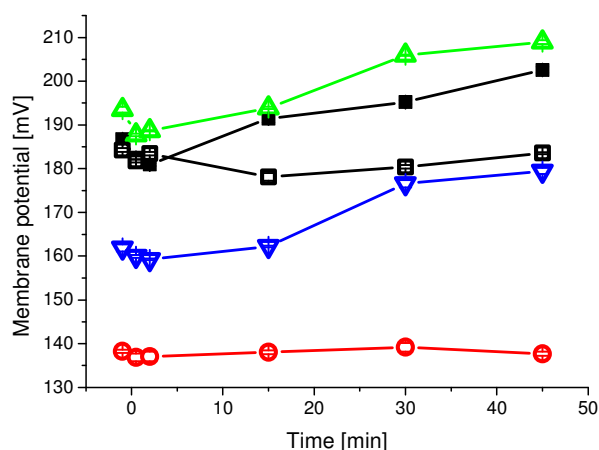


**Fig. 3.19: Membrane potential of different *C. glutamicum* strains.**

Membrane potential was analyzed using the radioactively labeled cation  $^{14}\text{C}$ -TPP<sup>+</sup>, the amount of labeled TPP in the cytoplasm of the respective cells was measured by rapid filtration. The respective strains were cultivated under hyperosmotic conditions causing betaine accumulation. Plasmid-encoded gene expression was induced by addition of 25  $\mu\text{M}$  IPTG. wt (■), YggB-His (■),  $\Delta 110$ -His (○),  $\Delta 132$ -His (△),  $\Delta 247$ -His (▽).

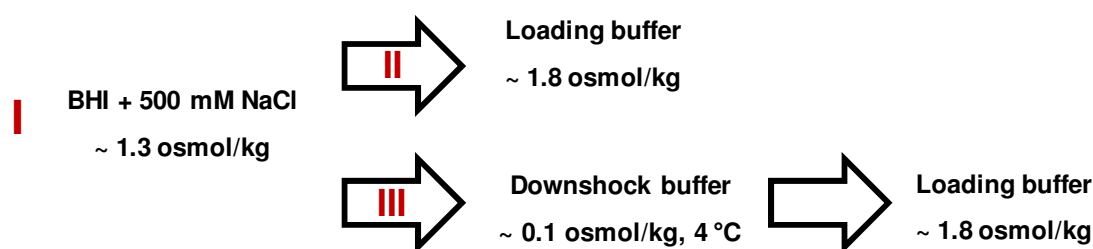
A reduction of the membrane potential leads to a decreased activity of secondary active transporters, such as BetP. Therefore, the low ability of some mutants to accumulate betaine can be caused by diminished BetP activity. Still, evidence was provided previously that betaine leaves the cell through the channel formed by different YggB subunits (see section 3.5.3). Thus, the cause for the low efficiency of the betaine loading by the YggB truncation strains seems to be a combination of reduced betaine uptake as well as immediate outward flux. The cells had to cope with an extreme osmotic downshift prior to betaine loading by application of a high osmolality buffer. Therefore, it was now interesting if the reduced membrane potentials of particularly the  $\Delta 110$ -His and the  $\Delta 247$ -His mutant resembled physiological growth conditions or whether this effect was stress induced.

In order to analyze the energetic situation of the cell under different conditions, the membrane potential was determined before the first osmotic downshift when the cells were adapted to hyperosmotic conditions (Table 3.3, schema I) and when the adapted cells were directly resuspended in loading buffer of higher osmolality without previous osmotic downshift (Table 3.3, schema II). The membrane potentials upon these different treatments compared to the initial membrane potential displayed in figure 3.19 are summarized in table 3.3. Previous to the hypoosmotic shock there was no significant difference between the cells harboring different YggB constructs (Table 3.3, I). Upon direct resuspension in

even higher osmolar loading buffer the membrane potential of nearly all strains was around or slightly above 200 mV. The only exception was the  $\Delta 110$ -His mutant with a reduced membrane potential of 178 mV (Table 3.3, II). However, the decrease in membrane potential of this mutant was not as strong as it was with an extreme osmotic downshift previous to the resuspension in the hyperosmolar loading buffer (Table 3.3, III). The cause for the strong decrease in membrane potential of the  $\Delta 110$ -His mutant and also of the  $\Delta 247$ -His mutant seemed to be a combination of a drastic osmotic downshift (the condition when YggB normally gets activated) followed by an immediate osmotic upshift. This observation suggested that YggB itself was the reason for the decreased membrane potential.

**Table 3.3: Membrane potential of *C. glutamicum* strains upon different combinations of osmotic stress.**

Membrane potential of respective strains was analysed using TPP. The conditions used are displayed schematically: (I) Cells were adapted to hyperosmotic conditions ( $\sim 1.3$  osmol/kg) o/n; (II) cells from I were transferred to hyperosmotic buffer ( $\sim 1.8$  osmol/kg); (III) cells from I were first transferred into hypoosmotic buffer ( $\sim 0.1$  osmol/kg) followed by a transfer to hyperosmotic conditions ( $\sim 1.8$  osmol/kg). Values of membrane potential of the respective *C. glutamicum* strains are summarized in the table below.



Strain	Membrane potential [mV]		
	I	II	III
wt	185	199	187
YggB-His	189	217	184
$\Delta 110$ -His	182	178	138
$\Delta 132$ -His	200	211	193
$\Delta 247$ -His	186	195	162

The membrane potential of bacteria is directly correlated with the proton motive force (pmf) necessary for the generation of ATP. The pmf is the sum of the chemical gradient across the plasma membrane and the membrane potential. To exclude that the decreased membrane potential was caused by a changed internal pH as an adjustment of the pmf, the internal pH

(pH gradient) as well as the pmf was determined. However, there was no difference in the internal pH of the  $\Delta 110$ -His mutant compared to the wild type (data not shown). These results clearly show that the decreased membrane potential of the  $\Delta 110$ -His mutant is not a consequence of a changed internal pH, adjusting the pmf of the cell. Contrary, the pmf itself is significantly decreased in the  $\Delta 110$ -His mutant under hyperosmotic conditions following an osmotic downshift.

#### 3.5.4 Growth at different osmolalities

Strains expressing different truncated forms of *yggB*-His were strongly impaired especially under osmotic stress conditions which was shown via the energetic situation of the respective strains. In the following growth of these strains was monitored under different osmolalities. Therefore, cells were grown in MM1 minimal medium, pH 7.0 additionally containing different amounts of NaCl (0 mM, 100 mM, 200 mM, 300 mM, 400 mM), corresponding to osmolalities of 0.448 osmol/kg, 0.746 osmol/kg, 0.931 osmol/kg, 1.101 osmol/kg, and 1.287 osmol/kg. Growth of cells expressing different *yggB*-His constructs, especially  $\Delta 110$ -His, was significantly changed depending on the osmolality of the medium (Fig. 3.20). Growth of the wild type was nearly independent of the external osmolality. However, the  $\Delta 110$ -His mutant showed an extended lag phase previous to the exponential growth phase. The degree of this lag-phase was clearly dependent on the osmolality of the environment, elongating with increasing osmolality. However, without previous osmotic downshift (as performed in the experiments described before) the cells seemed to be able to overcome this lag-phase indicating that the channel pore formed by YggB  $\Delta 110$  subunits is not likely to be permanently open under these conditions. The same effect was observed for the YggB-His and in a lower extent for the  $\Delta 247$ -His mutant. Altogether, these growth phenotypes were not as much due to different growth during the exponential phase rather than due to the lag phase of distinct duration. These results indicated that the strains expressing the different *yggB* constructs need a certain amount of a special substance or need to reach a defined state before they are able to start growing. Other parameters, such as the pH value, might also have an impact on growth of the mutants. Taken together, this led to the question, what the extended lag phase caused and what made then the following growth phase possible?

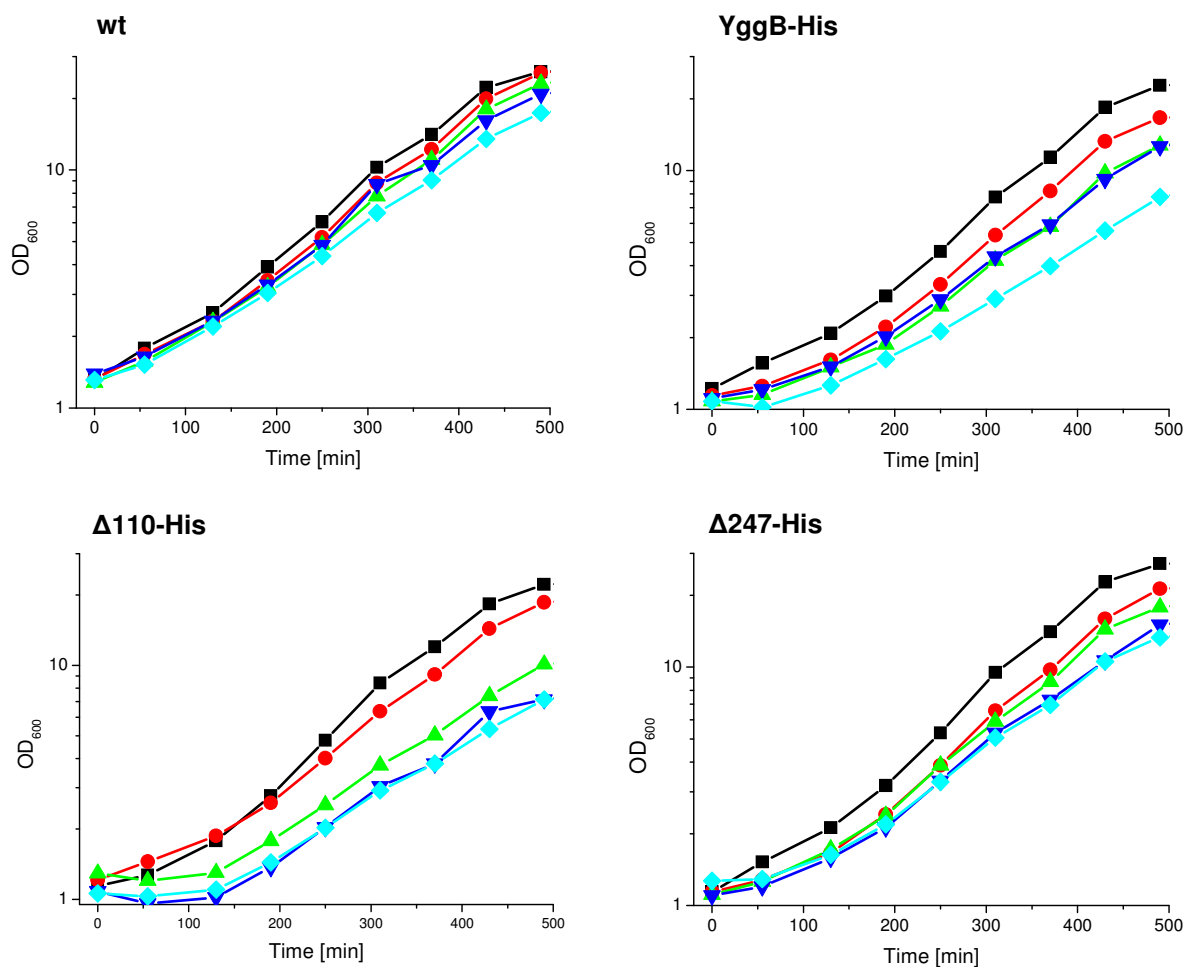


**Fig. 3.20: Growth of *C. glutamicum* strains expressing *yggB*-His and its truncated forms under different osmolalities.**

Growth curves of the respective strains were obtained in MM1 minimal medium, pH 7.0 containing 0 mM, 100 mM, 200 mM, 300 mM, and 400 mM NaCl by monitoring the OD<sub>600</sub>. Related osmolalities of the media were 0.448 (■), 0.746 (●), 0.931 (▲), 1.101 (▼), and 1.287 (◆) osmol/kg. Plasmid-encoded gene expression was induced by addition of 25 μM IPTG

It was tested if the accumulation of any substrate in the external medium is necessary to allow growth of the Δ110-His mutant. Therefore, cells in the exponential growth phase were used to inoculate fresh medium on the one hand and medium containing 25 % of the previously used medium (supernatant without cells) on the other. Although the presence of this ‘used’ medium seemed to support growth in some experiments, this effect could not be definitely shown. Further tests additionally revealed that neither externally added glutamate abolished the lag phase nor a pH shift caused the growth phenotype of the Δ110-His mutant (data not shown).

### 3.5.5 Characterization of leakiness mediated by YggB $\Delta$ 110-His

As described above the presence of YggB variants, especially the  $\Delta$ 110-His mutant, resulted in a strong phenotype regarding growth, accumulation of betaine, and membrane potential under hyperosmotic conditions. Additionally, the  $\Delta$ 110-His mutant was able to excrete glutamate permanently without trigger (Nakamura *et al.*, 2007) as will be described in CgXII MOPS minimal medium, pH 7.0 (~ 1.0 osmol/kg) later (see section 3.6.1). One possible explanation for all these effects might be the formation of a basically or transiently leaky channel by the  $\Delta$ 110 subunits allowing the unspecific release of ions and molecules. Such a transient hole in the membrane might be the reason for the severe problems of the cells mainly under osmotic stress conditions.

To analyze if the permeability of the cell envelope was changed and an unspecific outward flux of ions and molecules occurred in the  $\Delta$ 110-His mutant a number of other solutes were tested for an increased permeability through the plasma membrane. Such an increased permeability could be expected if mutant forms of YggB would form a leaky unspecific channel. HPLC-analysis of culture supernatant resulted in the detection of only very small amounts of glutamine and possibly alanine excreted besides glutamate. Surprisingly, also proline, known as a compatible solute in *C. glutamicum*, seemed not to flow through a possible leaky pore (data not shown).

Additionally, the permeability for a solute, related to glutamate roughly in size and charge, namely the organic acid pyruvate was tested. Therefore, the internal concentration of pyruvate was artificially increased by the addition of the inhibitor aminoethyl-phosphinate (Laber and Amrhein, 1987). Within the cell aminoethyl-phosphinate is converted to acetylphosphinate which inhibits the pyruvate dehydrogenase. Application of this inhibitor led to spontaneous pyruvate excretion, which, however, was not increased in the  $\Delta$ 110-His mutant compared to the wild type (data not shown).

As example for another ion, different from protons, the permeability for  $K^+$  ions was tested. Recently, it was shown that *C. glutamicum* requires potassium for pH homeostasis at low pH values and is therefore not able to grow under these conditions in the absence of potassium. While wild type cells recover after the addition of KCl, the  $K^+$ -transport negative mutant  $\Delta$ kup $\Delta$ CglK does not (Follmann *et al.*, 2009). While addition of the potassium ionophore valinomycin could complement this  $K^+$  deficiency, transformation of the  $\Delta$ kup $\Delta$ CglK mutant with the 'leaky' YggB  $\Delta$ 110-His did not. This result again indicated that potassium ions were not able to permeate the membrane of  $\Delta$ kup $\Delta$ CglK upon expression of yggB  $\Delta$ 110-His. However, it has to be admitted that  $K^+$  ions would have to

permeate the leaky channel in the opposite direction, which would only be possible upon the assumption of a rather unspecific pore in the membrane which seemed not to be the case (data not shown).

Finally, the susceptibility to different antibiotics of cells harboring the YggB  $\Delta$ 110-His mutant compared to the complementation strain (YggB) was tested. In the case of penicillin and ethambutol, which, however, do not need to cross the plasma membrane, the susceptibility of the  $\Delta$ 110-His mutant was slightly increased. Erythromycin, targeting in the cytoplasm, affected growth of the  $\Delta$ 110-His mutant compared to the complementation strain. Although this effect was more pronounced, it was still not fully convincing. If the particular antibiotic really enters the cells through a leaky pore to cause an increased susceptibility or whether this effect is due to general impairment of the cell wall integrity could not be proven by this kind of experiment. It is just another hint that the expression of a truncated version of *yggB* leads to a disturbed cell envelope (data not shown).

Taken together, these results indicated that the pore formed by the  $\Delta$ 110-His mutant is still relatively selective under the conditions used here, although the cell integrity seemed to be significantly impaired. However, severe osmotic stress, such as osmotic up- and downshift, seemed to lead to a more unspecific efflux as shown above for betaine and protons as well as for proline previously (Ruffert *et al.*, 1997). In fact, the permeability of the cells expressing *yggB*  $\Delta$ 110-His for glutamate seemed to be a quite specific effect. None of the tested molecules, like pyruvate, proline, and even  $K^+$  was released by the cell via the proposed leaky pore under the conditions similar to the situation of glutamate production.

### 3.5.6 *E. coli* MscS and MscS/CtYggB in *C. glutamicum* $\Delta$ *yggB*

In addition to the different YggB constructs the mechanosensitive functionality of *E. coli* MscS, the direct structural counterpart of YggB from *C. glutamicum*, and the fusion construct MscS/CtYggB, respectively, present in *C. glutamicum*  $\Delta$ *yggB* was also tested. Although significant level of both proteins could be detected in Western blot analysis (Fig. 3.2), the phenotype of the  $\Delta$ *yggB* mutant was not complemented by either of the proteins (data not shown). Both strains showed a betaine efflux pattern comparable to the *yggB* deletion strain, indicating that *E. coli* MscS as well as the fusion protein MscS/CtYggB does not function as MS channel in *C. glutamicum* mediating betaine efflux. Accordingly, the betaine uptake and efflux behavior under hyperosmotic conditions of either strain was the same as observed for the *yggB* deletion mutant. Additionally, heterologously expressed

*mscS* as well as *mscS/CtyggB* did not influence growth of *C. glutamicum* cells in medium of different osmolalities (data not shown).

### 3.6 Glutamate production

#### 3.6.1 Glutamate production upon different treatments

Glutamate production by *C. glutamicum* can be induced by various treatments. Three different triggers were used to characterize the phenotype of the *yggB* deletion mutant, namely biotin limitation, the addition of Tween 60 and penicillin G. All treatments led to a dramatically decreased glutamate production in the absence of YggB (Table 3.4). However, a residual glutamate production of about 30 % was still detectable in the  $\Delta yggB$  mutant. Additional deletion of *mscL* had no effect on glutamate production (data not shown).

**Table 3.4: Glutamate excretion rates [ $\mu\text{mol}/(\text{min g dm})$ ] after addition of different trigger.**

Glutamate excretion was induced by addition of the respective trigger in the exponential growth phase. Glutamate excretion rates were determined using linear regression of external amounts of glutamate at adequate time points.  $n \geq 3$  for penicillin G and Tween 60. n.d. – not determined

YggB – *yggB* deletion mutant, expressing the *yggB* gene from the vector pEKex2.

	Penicillin G	Tween 60	Biotin limitation
<b>wt</b>	<b>16.62 ± 2.13</b>	<b>10.85 ± 0.79</b>	<b>2.06</b>
<b><math>\Delta yggB</math></b>	<b>5.13 ± 0.82</b>	<b>3.64 ± 1.56</b>	<b>0.66</b>
<b>YggB</b>	<b>20.16 ± 3.96</b>	<b>11.85 ± 2.73</b>	<b>n.d.</b>

Glutamate excretion of the respective strains upon addition of penicillin is shown in figure 3.21. Excretion rates were determined via the linear regression of external glutamate concentrations between one and five hours after induction. As penicillin was most effective, it was used to induce glutamate production in the majority of the following experiments. Plasmid-encoded expression of the *yggB* gene fully complemented the  $\Delta yggB$  phenotype (Fig. 3.21). Indeed, glutamate excretion was slightly enhanced in the complementation strain (YggB), probably due to overexpression of *yggB* compared to the wild type harboring the genomic copy of the gene (Fig. 3.2).

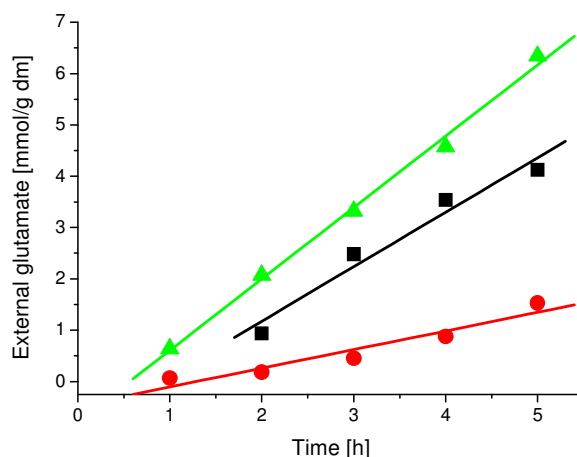


**Fig. 3.21: Induction of glutamate excretion by addition of 6 U/ml penicillin G.**

Glutamate excretion was induced by addition of penicillin ( $t=0$ ) in the exponential growth phase. Amounts of glutamate in the external medium were measured via HPLC-analysis. Straight lines represent linear regressions. Plasmid-encoded gene expression was induced by addition of 25  $\mu$ M IPTG. wt (■),  $\Delta yggB$  (●), YggB (▲).

The extended C-terminal elongation of YggB can only be found in close relatives of *C. glutamicum* and is not present in most MscS channel homologs. To investigate the role of the C-terminal domain strains harboring the truncated derivatives of YggB were analyzed concerning their ability to excrete glutamate without and upon induction (Fig. 3.22). As reported by Nakamura *et al.* (2007) the  $\Delta 110$ -His mutant strain produced highly elevated amounts of glutamate without any induction which could be shown here also in *C. glutamicum* ATCC 13032. It has to be mentioned that the membrane potential of the  $\Delta 110$ -His mutant strain was not changed under the conditions used here, being between 160 – 170 mV (a normal range) and comparable to all other strains (data not shown). Surprisingly, also expression of the full length *yggB* gene with a 6xHis-tag added at the C-terminal end resulted in excretion of remarkable amounts of glutamate without any induction. However, it should be remembered that *yggB*-His is highly overexpressed in *C. glutamicum* (Fig. 3.2, induction of gene expression by addition of 25  $\mu$ M IPTG). Investigation of the glutamate production of the YggB-His strain without induction of gene expression (0  $\mu$ M IPTG) revealed no glutamate excretion without trigger (data not shown). Therefore, the observed effect of the YggB-His strain was due to the high protein level in the cell instead of the added 6xHis-tag possibly interfering with the natural role of the C-terminal domain.

The amount of glutamate accumulated in the external medium without induction started decreasing after 2 – 3 hours of cultivation. This effect could be explained by an on-going growth of the cells during that the uptake of glutamate masked the export. However,

glutamate uptake measurements would be necessary to prove this hypothesis. The  $\Delta 247$ -His mutant excreted only very small amounts of glutamate at an average of about 150 – 200  $\mu\text{mol/g dm}$  compared to the YggB-His and  $\Delta 110$ -His strains. These amounts were still significantly higher as the amounts of glutamate excreted by the wild type or the  $\Delta 132$ -His mutant, being in a low  $\mu\text{molar}$  range ( $< 10 \mu\text{mol}$ ). Here again a possible simultaneous uptake of glutamate could not be measured with this kind of experiment.

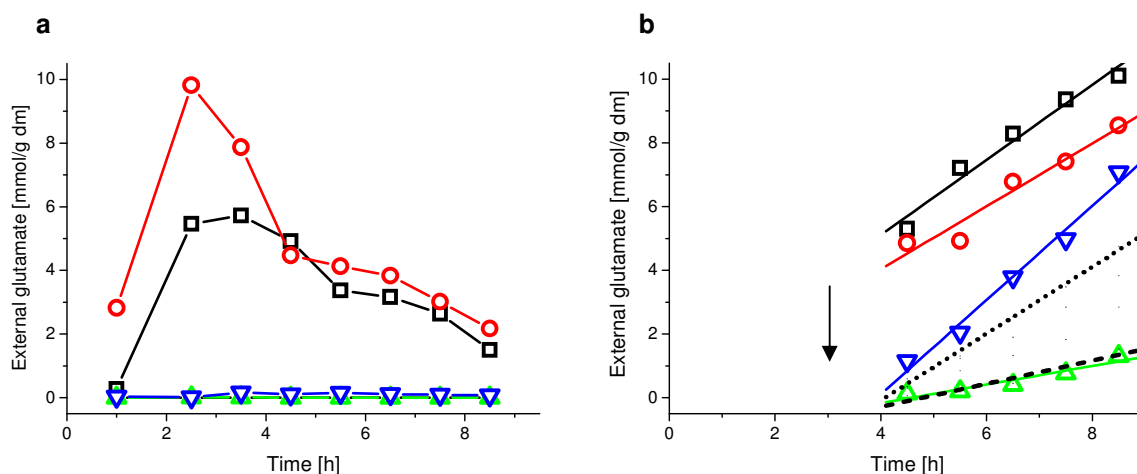


**Fig. 3.22: Glutamate excretion without induction or upon addition of 6 U/ml penicillin G.**

The concentration of glutamate in the external medium (a) without induction and (b) at various time points after induction with penicillin ( $t=3$ ) is displayed.  $T=0$  represents the start of cultivation. Addition of penicillin is indicated by an arrow. Amounts of glutamate in the external medium were measured via HPLC-analysis. Straight lines represent linear regressions. Plasmid-encoded gene expression was induced by addition of 25  $\mu\text{M}$  IPTG. YggB-His ( $\blacksquare$ ),  $\Delta 110$ -His ( $\circ$ ),  $\Delta 132$ -His ( $\blacktriangle$ ),  $\Delta 247$ -His ( $\blacktriangledown$ ). wt is shown as dotted,  $\Delta yggB$  as dashed line; both strains did not excrete any glutamate without induction.

Induction of glutamate production by addition of penicillin resulted in further glutamate excretion in addition to the basal level of all strains (Fig. 3.22b). Starting at a higher level, the glutamate excretion rate of the YggB-His strain was comparable to the wild type, while the  $\Delta 110$ -His mutant had a slightly smaller glutamate excretion rate. The strain expressing *yggB*-His at moderate level (0  $\mu\text{M}$  IPTG) showed a normal glutamate excretion rate similar to the rate determined for the complementation strain (YggB) (Table 3.4 and 3.5). The  $\Delta 247$ -His mutant excreted slightly elevated amounts of glutamate, somehow consistent with the very small amount of glutamate excreted without induction. In the  $\Delta 132$ -His mutant no additional glutamate excretion compared to the *yggB* deletion strain could be induced. This result was consistent with the previous analysis of mechanosensitive function, indicating a non-functional channel assembled by YggB  $\Delta 132$ -His subunits. Glutamate excretion rates of the described strains are summarized in table 3.5.

**Table 3.5: Glutamate excretion rates [ $\mu\text{mol}/(\text{min g dm})$ ] of recombinant *C. glutamicum* strains.**

Glutamate excretion rates of *C. glutamicum*  $\Delta yggB$  expressing truncated forms of *yggB*-His upon addition of 6 U/ml penicillin were determined using linear regression of external amounts of glutamate at adequate time points. If not otherwise stated gene expression was induced by addition of 25  $\mu\text{M}$  IPTG.  $n \geq 3$

<b>Strain</b>	<b>Glutamate excretion rate [<math>\mu\text{mol}/(\text{min g dm})</math>]</b>
<b>YggB-His</b>	<b>17.60 <math>\pm</math> 2.84</b>
<b>YggB-His (0 <math>\mu\text{M}</math> IPTG)</b>	<b>19.12 <math>\pm</math> 3.25</b>
<b><math>\Delta 110</math>-His</b>	<b>13.86 <math>\pm</math> 3.74</b>
<b><math>\Delta 132</math>-His</b>	<b>4.69 <math>\pm</math> 0.30</b>
<b><math>\Delta 247</math>-His</b>	<b>21.11 <math>\pm</math> 4.54</b>

In summary, all modifications of YggB had a more or less pronounced effect on the glutamate production by the respective strains of *C. glutamicum*, indicating an important role of the protein in the process of glutamate excretion. Obviously, the integrity of the C-terminal domain has a strong effect on the inducibility of glutamate production. However, a decision if YggB is really the glutamate exporter or whether it is just a regulator of another so far unknown export system cannot be made based on the experiments described so far.

### 3.6.2 Influence of external osmolality, media, and pH

Due to a possible connection of YggB's function as MS channel and its putative additional function as glutamate exporter, the influence of osmolality changes during glutamate production was investigated. Therefore, glutamate production was induced during exponential growth by the addition of Tween 60. 2 hours after induction the osmolality of the external medium was shifted by 1:1 dilution of the cultures with ddH<sub>2</sub>O or media containing different amounts of NaCl resulting in osmolalities of 0.566, 1.132 (isoosmolar) and 1.726 osmol/kg. Depending on the osmotic conditions after the shift, the glutamate excretion rates of wild type and the *yggB* deletion strain were effected (Fig. 3.23). A decrease of the external osmolality resulted in elevated glutamate excretion while an increase of the external osmolality decreased the amount of glutamate in the medium. A similar effect was already described by Lambert *et al.* (1995) for wild type cells but under

different conditions. Surprisingly, the same dependency was observed for the *yggB* deletion strain, though at a lower level, indicating that the presence of YggB is not required to transduce the impact of osmolality changes on glutamate production.

To exclude other physiological effects besides the osmolality change caused by the dilution in ddH<sub>2</sub>O to reach an osmolality of 0.556 osmol/kg the experiment was repeated in MM1 minimal medium, pH 7.0 possessing a much lower osmolality of about 0.3 osmol/kg than CgXII MOPS. Osmolalities were adjusted with NaCl to the same values used in the first experiment. Thus, a dilution in MM1 was possible to reach a comparable low osmolality. The in MM1 minimal medium detected effects of osmolality changes were similar to the effects described for CgXII MOPS, though the amount of excreted glutamate was less (data not shown).

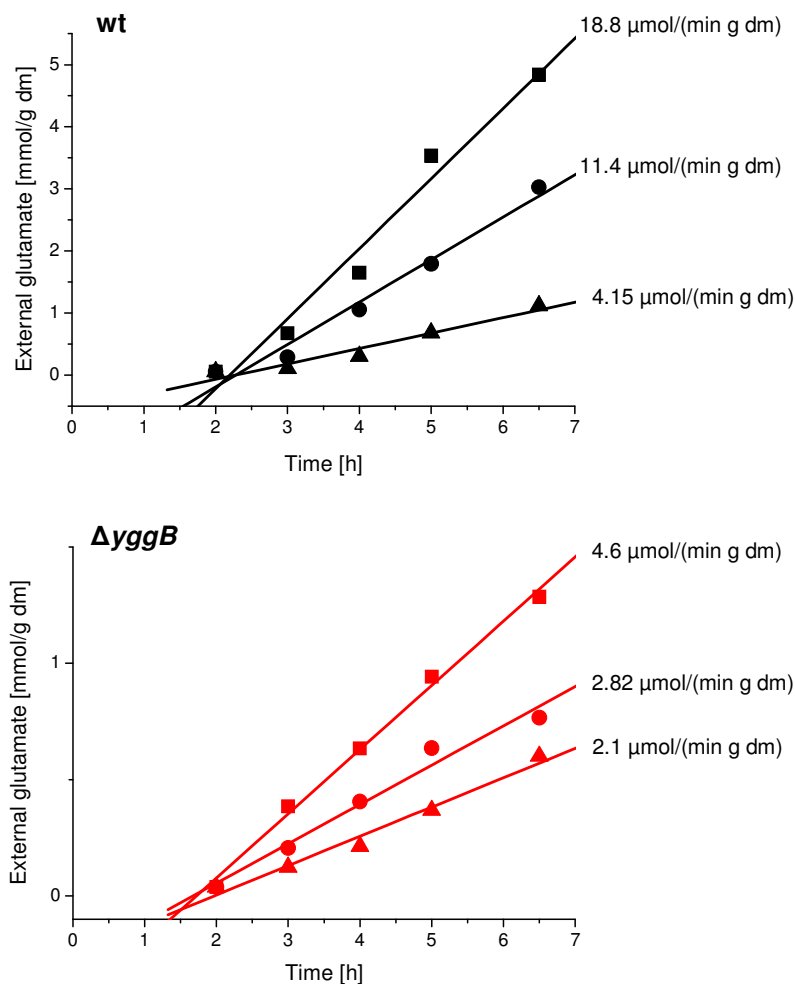


**Fig. 3.23: Effect of osmolality shift on glutamate production.**

Glutamate excretion was induced by addition of 0.15 % (v/v) Tween 60 ( $t=0$ ) in the exponential growth phase. After 2 hours of incubation a shift in external osmolality from 1.132 osmol/kg to 0.566 osmol/kg (squares), 1.132 osmol/kg (isoosmolar, circles), and 1.726 osmol/kg (triangles) was performed. Amounts of glutamate in the external medium were measured via HPLC-analysis. Straight lines represent linear regressions.

Based on the latter described result evidence was provided that there are multiple factors influencing glutamate excretion. CgXII MOPS contained a high amount of MOPS ( $pK_a$  7.2) and thus possessed strong buffer capacity compared to MM1. Obviously related to the present buffer capacity were the pH values of the medium. To investigate the influence of the pH value on glutamate production, MM1 (+ 42 g/l MOPS) with varying pH values of 6.0, 7.0, and 8.0 were used. Changes of pH values during glutamate excretion were measured via a pH electrode (Hydrus 300, Fisher Scientific, Schwerte). During the growth period between inoculation and induction of glutamate production (approximately 3 – 4 hours) the pH value of the external medium was already shifted towards more alkaline values (Fig. 3.24a,  $t=0$ ). However, a dependency of glutamate productivity of the wild type from the external pH was observed (Fig. 3.24b), increasing glutamate excretion being correlated to increasing pH values. Looking at the development of the external pH during glutamate production, the glutamate accumulated externally acidified the medium. The high amount of glutamate excreted by wild type cells decreased the external pH values depending on the initial pH (Fig. 3.24a). Taken together, the efficiency of glutamate production seems to be dependent on the pH of the medium and/or the pre-cultivation conditions. In order to investigate this interesting effect further fermentation experiments have to be performed in which a constant pH can be guaranteed during cultivation.

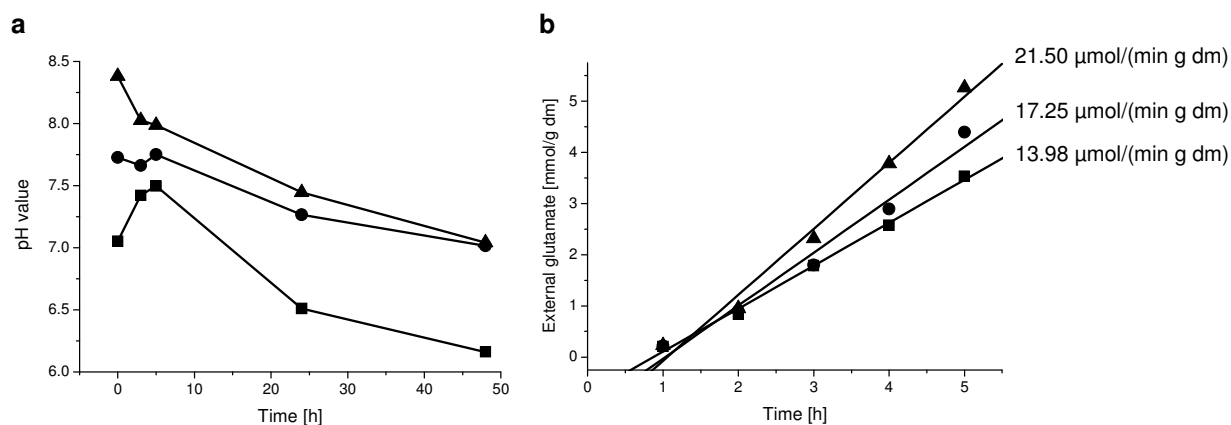


**Fig. 3.24: Glutamate excretion in MM1/MOPS medium of different pH values.**

Glutamate excretion by wild type cells was induced by addition of 6 U/ml penicillin G ( $t=0$ ) in the exponential growth phase. (a) pH values of the external medium during glutamate production, (b) amounts of glutamate in the external medium were measured via HPLC-analysis. Straight lines represent linear regressions. wt, pH 6.0 (■), pH 7.0 (●), pH 8.0 (▲).

### 3.6.3 Influence of on-going glutamate production on hypoosmotic stress response

The influence of an osmolality shift on glutamate production was described in section 3.6.2. Here the influence of on-going glutamate production on the immediate hypoosmotic stress response was also analyzed. Therefore, a similar experiment as described for glutamate and betaine efflux upon osmotic downshift (see sections 3.5.1 and 3.5.2) was split into two parts. In the first part cells were loaded with [ $^{14}\text{C}$ ]-labeled betaine under hyperosmotic conditions (CgXII MOPS + 400 mM NaCl (1.839 osmol/kg)). In the second part cells were incubated in the same medium containing unlabeled betaine. Subsequent to loading, glutamate production was induced for 3 hours by the addition of Tween 60 in both parts. The cells were then incubated at decreasing external osmolalities starting at isoosmolar conditions of 1.8 osmol/kg down to very low osmolality values analog to the experiments described in section 3.5.1 and 3.5.2. Efflux of labeled betaine from the first part of the experiment as well as glutamate from the second part was measured under these conditions. The pattern of betaine efflux of wild type and the *yggB* deletion strain was similar to the betaine efflux upon osmotic downshift shown in figure 3.13 (data not shown). Therefore, on-going glutamate excretion seems not to influence betaine efflux under hypoosmotic conditions. This indicates that betaine is not excreted with glutamate simultaneously before the osmotic downshift was applied, although the internal betaine concentration is suggested to be on a high level due to the previous loading.

Indeed, hypoosmotic efflux of glutamate was decreased in both strains when Tween 60 was added previously to induce glutamate production (Fig. 3.25a). Interestingly, glutamate efflux upon osmotic downshift of the *yggB* deletion strain without previous induction of glutamate production was strongly decreased compared to the wild type. Such a difference was not detected under the conditions used before to investigate glutamate efflux upon hypoosmotic stress (see section 3.5.1). Although the conditions used in section 3.5.1 were slightly different from the conditions used here, an explanation for these unequal results is still missing. The internal amount of glutamate was measured as control and corresponded roughly to the glutamate efflux upon hypoosmotic stress in both strains (pre-induction of glutamate excretion) (Fig. 3.25b, c).

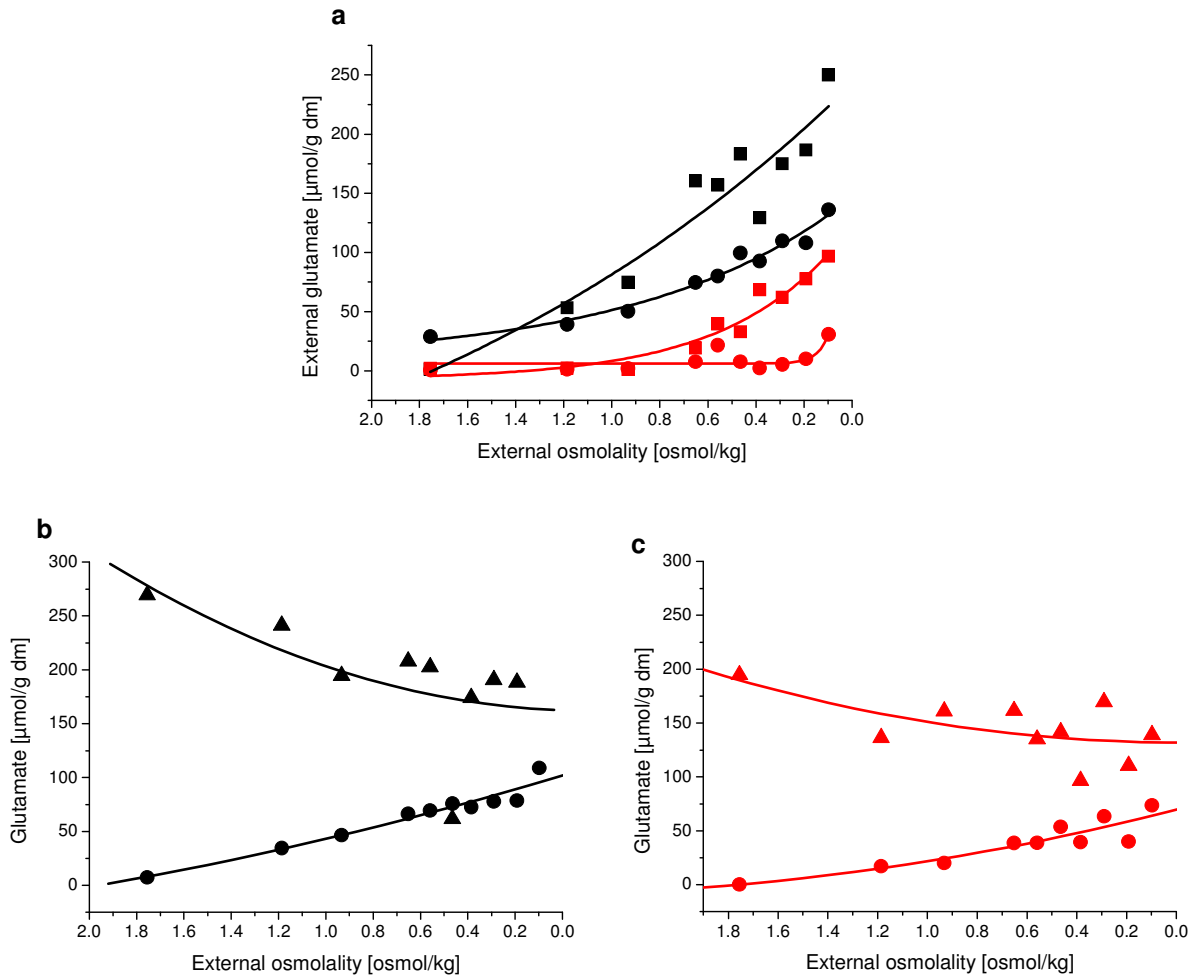


**Fig. 3.25: Glutamate efflux upon osmotic downshift under glutamate productive conditions.**

Efflux of glutamate upon hypoosmotic shock was quantified 3h after glutamate production was induced by addition of 0.15 % Tween 60. Cells were exposed to buffers of different osmolalities and efflux as well as internal amounts of glutamate were measured 15 sec after the dilution into hypoosmotic buffer. (a) Glutamate efflux of wt (black) and *yggB* deletion (red) without previous induction (squares) and after addition of Tween 60 (circles); (b) internal (triangles) and external (circles) amounts of glutamate of wild type cells; (c) internal (triangles) and external (circles) amounts of glutamate of  $\Delta yggB$  cells.

### 3.6.4 Alternative candidates for the glutamate exporter

Based on the previous experiments, the question of the exact role of YggB in the export of glutamate – as exporter or regulator – could not be answered yet. Therefore, also other candidates than YggB were tested to be involved in the export of glutamate.

De Angeli *et al.* (2006) described the member of the chloride channel (CLC) protein family AtCLCa of *Arabidopsis thaliana* being a  $\text{NO}_3^-/\text{H}^+$  antiporter. Additionally, this channel was described to harbor a certain affinity for glutamate. In view of this information the *C. glutamicum* gene *Cgl10063* which was annotated as putative chloride

channel became an interesting candidate for an alternative glutamate export system. Thus, the insertion mutant IS::*Cgl0063* existent in our group was investigated with respect to a possible effect on glutamate productivity upon the addition of Tween 60.

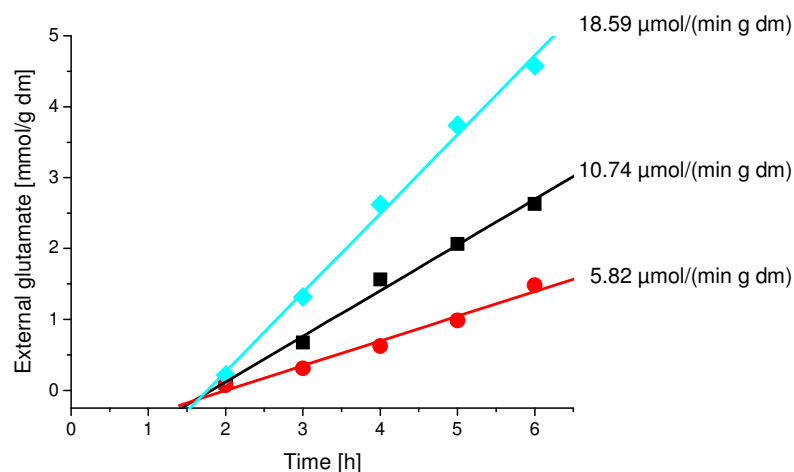


**Fig. 3.26: Glutamate excretion by the IS::*Cgl0063* mutant.**

Glutamate excretion was induced by addition of 0.15 % (v/v) Tween 60 in the exponential growth phase ( $t=0$ ). Amounts of glutamate in the external medium were measured via HPLC-analysis. Straight lines represent linear regressions. wt (■),  $\Delta yggB$  (●), IS::*Cgl0063* (◆).

However, inactivation of the *Cgl0063* gene did not result in decreased glutamate production (Fig. 3.26). In fact, an elevated glutamate excretion rate was detected. Since no decrease of glutamate excretion was detected upon inactivation of *Cgl0063*, the channel encoded by *Cgl0063* seems not to be involved in glutamate excretion triggered by Tween 60. The increased amount of excreted glutamate might be caused by disturbed membrane integrity due to the missing or non-functioning channel. However, this aspect was not investigated further so far.

Due to information from our industry cooperation partner Ajinomoto Co., Inc. two other candidates for the glutamate export carrier were identified in *C. glutamicum*. These were encoded by the genes *Cgl0590* and *Cgl1221*. To test an involvement of the proteins encoded by these two candidate genes in glutamate production the single deletion mutants were constructed. Additionally, several double deletion strains in combination with the *yggB* gene as well as the triple deletion mutant were generated in *C. glutamicum*. The resulting strains were analyzed regarding their ability to excrete glutamate upon induction by penicillin. However, there was no effect of a  $\Delta Cgl0590\Delta Cgl1221$  double deletion on glutamate production of the corresponding strain, excreting similar amounts of glutamate compared to the wild type level. Although all other mutants produced less glutamate there

was no difference compared to the *yggB* single deletion strain indicating that the effect on glutamate excretion is exclusively caused by the *yggB* deletion (Fig. 3.27).

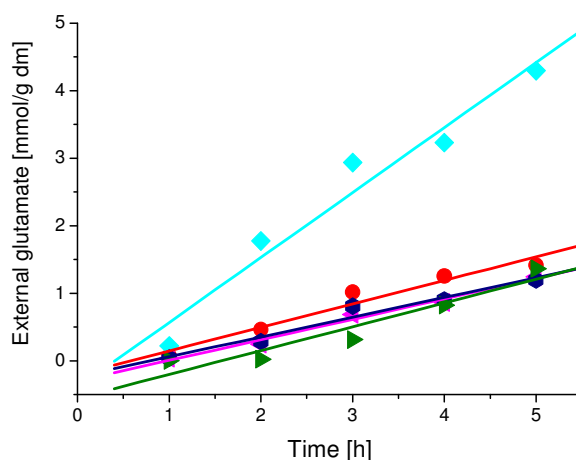


**Fig. 3.27: Glutamate excretion by  $\Delta Cgl0590$  and  $\Delta Cgl2211$  deletion mutants.**

Glutamate excretion was induced by addition of 6 U/ml penicillin ( $t=0$ ) in the exponential growth phase. Amounts of glutamate in the external medium were measured via HPLC-analysis. Straight lines represent linear regressions.  $\Delta yggB$  (●),  $\Delta Cgl2211\Delta Cgl0590$  (◆),  $\Delta Cgl0590\Delta yggB$  (◀),  $\Delta Cgl2211\Delta yggB$  (●),  $\Delta Cgl2211\Delta Cgl0590\Delta yggB$  (▶).

Nevertheless, before a function of the genes *Cgl0590* and *Cgl2211* in glutamate production was completely excluded the effect of overexpression was investigated. Plasmid-encoded expression of the genes *Cgl0590* and *Cgl2211* was induced in the *yggB* deletion mutant. As the C-terminal His tag had a crucial impact on the expression or function in the case of YggB, both of the genes were expressed with as well as without His-tag fusion.

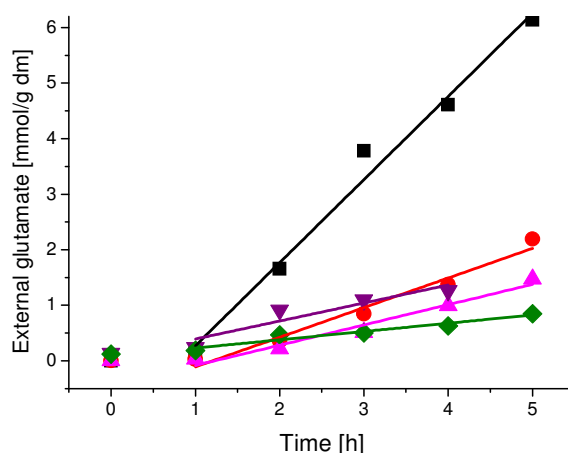


**Fig. 3.28: Glutamate excretion upon *Cgl0590* and *Cgl2211* overexpression.**

Glutamate excretion was induced by addition of 6 U/ml penicillin ( $t=0$ ) in the exponential growth phase. Amounts of glutamate in the external medium were measured via HPLC-analysis. Straight lines represent linear regressions. Plasmid-encoded gene expression was induced by addition of 25  $\mu$ M IPTG. wt (■),  $\Delta yggB$  (●), Cgl0590 (▲), Cgl0590-His (▼), Cgl2211-His (◆).

Expression of the *Cgl0590* gene with/without His-tag led to distinct growth reduction giving a strong hint that protein expression occurred (data not shown). Nevertheless, the amount of excreted glutamate upon overexpression of these proteins was not affected (Fig. 3.28). Although, the strain expressing the His-tagged *Cgl0590* seemed to excrete a slightly increased amount of glutamate 2 hours after the addition of penicillin, there was no significant effect visible. Taken together with the results obtained from the deletion mutants an involvement of the *C. glutamicum* genes *Cgl0590* and *Cgl2211* in the excretion of glutamate is not very likely.

### 3.6.5 *E. coli* MscS and MscS/CtYggB in *C. glutamicum* $\Delta yggB$

On the basis of the experiments described so far, it was still not possible to discriminate between the hypothesis of YggB being the glutamate excretion system on the one hand and the hypothesis of YggB regulating another channel on the other. A further attempt to elucidate whether YggB is the glutamate exporter in *C. glutamicum* was the expression of *E. coli* *mscS* and a fusion construct of *mscS* and the additional C-terminal domain of YggB in the *C. glutamicum* *yggB* deletion mutant. Strains harboring both constructs, MscS and MscS/CtYggB, were analyzed with respect to their ability to restore glutamate production in the *yggB* deletion mutant.

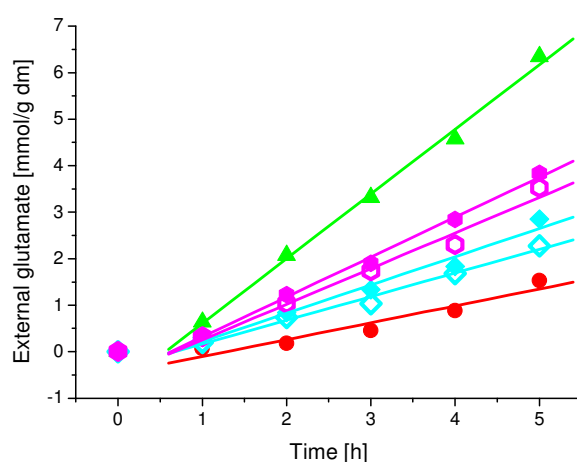


**Fig. 3.29: Glutamate excretion of MscS and MscS/CtYggB strains.**

*E. coli* *mscS* and the *mscS/CtyggB* fusion construct +/- His-tag were expressed in *C. glutamicum*  $\Delta yggB$ . Glutamate excretion was induced by addition of 6 U/ml penicillin ( $t=0$ ) in the exponential growth phase. Amounts of glutamate in the external medium were measured via HPLC-analysis. Straight lines represent linear regressions. Plasmid-encoded gene expression was induced by addition of 25  $\mu$ M IPTG.  $\Delta yggB$  (●), YggB (▲), MscS (◇), MscS-His (◆), MscS/CtYggB (◻), MscS/CtYggB-His (●).

Due to the high impact of a C-terminal His-tag added to the native *yggB* gene expression and consequently on the protein level and glutamate production, the new constructs were expressed with and without His-tag. However, in this case the His-tag had no influence on the glutamate production of the mutants (Fig. 3.29). Therefore, all further experiments were performed with the tagged proteins, since their level could be verified.

The strain MscS-His as well as MscS/CtYggB-His showed significantly increased glutamate production compared to the *yggB* deletion mutant (Fig. 3.29). Nevertheless, the excretion rates were not as high as in the complementation strain (YggB), expressing the untagged *C. glutamicum yggB* gene. The MscS-His mutant showed an increased glutamate production with an excretion rate of 9.85  $\mu\text{mol}/(\text{min g dm})$ . The MscS/CtYggB-His mutant harboring MscS fused to the additional C-terminal domain of YggB showed a glutamate excretion rate at an average of 13.95  $\mu\text{mol}/(\text{min g dm})$  laying in between the mean rates of  $\Delta yggB$  with 5.13  $\mu\text{mol}/(\text{min g dm})$  and the complementation strain (YggB) with 20.16  $\mu\text{mol}/(\text{min g dm})$ . Glutamate excretion rates are summarized in table 3.6. The obtained result indicates that the fusion protein is at least partly able to restore the ability of the cell to produce glutamate upon the induction by penicillin. The presence here of the C-terminal domain of YggB enhanced glutamate excretion.

**Table 3.6: Glutamate excretion rates [ $\mu\text{mol}/(\text{min g dm})$ ] of *C. glutamicum* MscS-His and MscS/CtYggB-His strains.**

Glutamate excretion rates of respective *C. glutamicum* strains upon addition of 6 U/ml penicillin were determined using linear regression of external amounts of glutamate at adequate time points. Gene expression was induced by addition of 25  $\mu\text{M}$  IPTG.  $n \geq 3$

<b>Strain</b>	<b>Glutamate excretion rate [<math>\mu\text{mol}/(\text{min g dm})</math>]</b>
<b>MscS-His</b>	<b>9.85 <math>\pm</math> 0.73</b>
<b>MscS/CtYggB-His</b>	<b>13.95 <math>\pm</math> 0.79</b>
<b>wt</b>	<b>16.63 <math>\pm</math> 2.13</b>
<b>YggB</b>	<b>20.16 <math>\pm</math> 3.96</b>
<b><math>\Delta yggB</math></b>	<b>5.13 <math>\pm</math> 0.82</b>

### 3.6.6 LOF- and GOF mutants of *E. coli* MscS and MscS/CtYggB

The experiments described above provide first evidence that the MscS channel was responsible for glutamate excretion. For MscS several loss-of-function (LOF - difficult or no channel opening), and gain-of-function (GOF - easy or flickering channel opening) mutants are described. In order to confirm the hypothesis of MscS mediating glutamate excretion, several of these mutations were constructed. In the LOF-mutants the hydrophobic residues near either end of the first or the second transmembrane helix (TM1 or TM2) of MscS were replaced by asparagines, leading to a LOF phenotype as described by Nomura *et al.* (2006). *E. coli* strains harboring these MscS A51N/F68N and I37N/L86N mutants in *E. coli* were hardly able to survive an osmotic downshift and no channel openings could be detected in patch clamp analysis. The same point mutations were introduced into *mscS*-His and *mscS/CtyggB*-His, respectively, via site-directed mutagenesis and the resulting genes were expressed in the *C. glutamicum* *yggB* deletion mutant. Upon expression of the four genes, significant level of protein could be detected in Western blot analysis only for three of the proteins (Fig. 3.30). However, no protein was detected upon expression of the *mscS*-His I37N/L86N gene.

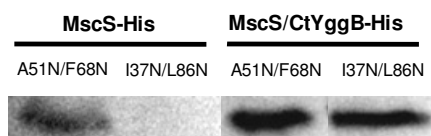


**Fig. 3.30: Western blot analysis of MscS-His and MscS/CtYggB-His LOF-mutants.**

LOF-mutants of *mscS*-His and *mscS/CtyggB*-His were expressed from the vector pEKex2 in *C. glutamicum*  $\Delta yggB$ . 25  $\mu$ M IPTG were used to induce gene expression. 60  $\mu$ g of membrane extract were loaded to each gel. The blot was developed using anti-(penta)-His antibody.

Stains harboring LOF-mutants produced no glutamate in addition to the amount produced by the  $\Delta yggB$  mutant when investigated regarding their ability to excrete glutamate upon the addition of penicillin (Fig. 3.31). The fact that the introduction of LOF-mutations abolished glutamate production observed by expression of wild type *mscS*-His and *mscS/CtyggB*-His, respectively, further supported the hypothesis of glutamate passing through the MscS pore itself. These experiments were not possible using directly the *C. glutamicum* YggB because no LOF-mutants for its mechanosensitive function are known or investigated, respectively.

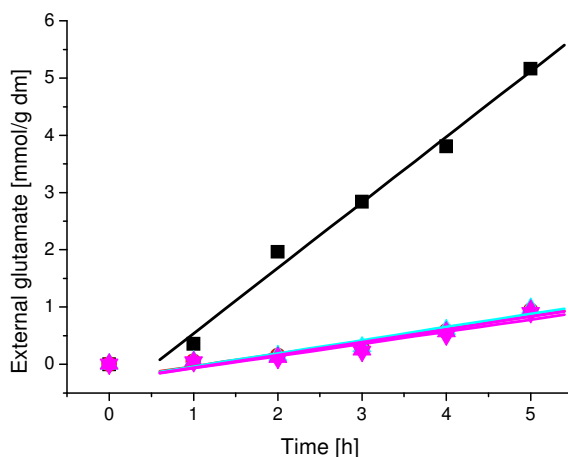


**Fig. 3.31: Glutamate excretion of MscS-His and MscS/CtYggB-His LOF-mutants.** LOF-mutants of *E. coli mscS*-His and the *mscS/CtyggB*-His fusion construct were expressed in *C. glutamicum*  $\Delta yggB$ . Glutamate excretion was induced by addition of 6 U/ml penicillin ( $t=0$ ) in the exponential growth phase. Amounts of glutamate in the external medium were measured via HPLC-analysis. Straight lines represent linear regressions. wt (■),  $\Delta yggB$  (●), MscS-His A51N/F68N (▲) MscS/CtYggB-His A51N/F68N (▲), MscS/CtYggB-His I37N/L86N (▼).

Since LOF-mutants had a significant impact on glutamate production mediated by MscS-His and MscS/CtYggB-His, respectively, also several GOF-mutations described for *E. coli* MscS were investigated regarding their effect on glutamate production in *C. glutamicum*. GOF-mutants of the MscS channel were characterized to require less membrane tension in order to reach the threshold for channel opening and some mutants show also a flickering behavior of channels glutamate opening and closing randomly. The following single amino acid exchanges in MscS were described to result in a GOF phenotype: V40D (Okada *et al.*, 2002), A106V (Edwards *et al.*, 2005; Wang *et al.*, 2008), and L109S (Miller *et al.*, 2003) and were tested in respect to glutamate excretion. The mutations V40D and A106V could be introduced into *mscS*-His and *mscS/CtyggB*, respectively. However, the presence of the respective protein could only be verified for MscS-His A106V, MscS/CtYggB-His V40D, and A106V in Western blot analysis (data not shown). Although a significant level of these proteins was detected no influence on glutamate production was observed. On the contrary, the supposed GOF-mutants had the same effect as the LOF-mutants resulting in no additional glutamate production in the *C. glutamicum*  $\Delta yggB$  strain (data not shown). This indicated that expression in *C. glutamicum* harboring a quite different cytoplasmic membrane as *E. coli* results in the assembling of non-functional channel in the membrane. The reason for this effect remains unclear. The L109S GOF-mutation could so far only be introduced in the MscS-His protein. However, expression of *mscS*-His L109S in *C.*

*glutamicum* led to a strong growth phenotype depending on the IPTG concentration used for gene expression (Fig. 3.32).

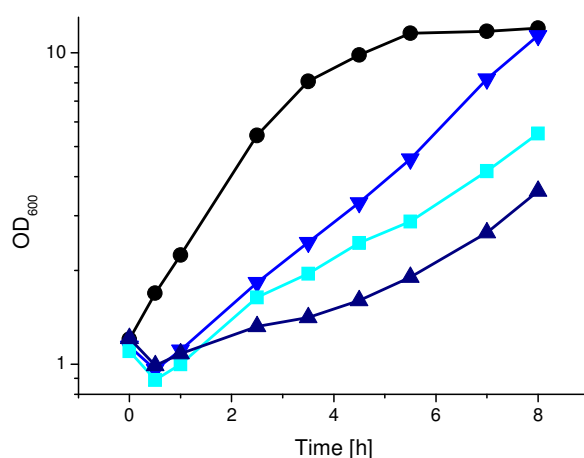


**Fig. 3.32: Growth of *C. glutamicum*  $\Delta yggB$  expressing *mscS*-His L109S.**

Shown is the increase of optical density (OD) at a wave length of 600 nm. Strains were grown in BHI (●) and CgXII MOPS minimal medium, pH 7.0 containing 25  $\mu\text{g}/\text{ml}$  kanamycin. Gene expression in the minimal medium was induced by different IPTG concentrations, 0  $\mu\text{M}$  (▼), 5  $\mu\text{M}$  (■), and 25  $\mu\text{M}$  (▲).

In Western blot analysis only a very low protein level of MscS-His L109S could be detected when gene expression was induced by 25  $\mu\text{M}$  IPTG. Lower IPTG concentration led to protein amounts probably below the detection threshold (data not shown). This observation was consistent with the expression of MscS L109S in *E. coli*. In these experiments the protein was also expressed very poorly compared to other MscS channel mutants investigated in the corresponding study, indicating the presence of a highly active channel (Miller *et al.*, 2003).

Due to the strongly decreased growth upon induction of gene expression with 25  $\mu\text{M}$  IPTG the inoculation schema for the determination of glutamate production was slightly adjusted. Gene expression was induced with 5  $\mu\text{M}$  instead of 25  $\mu\text{M}$  in the pre-culture. The main cultures were split and gene expression was once induced with 5  $\mu\text{M}$  and once with 25  $\mu\text{M}$  IPTG. The latter culture was inoculated at an elevated OD as slow growth was expected. Glutamate production of these two parts without induction and upon addition of penicillin is summarized in figure 3.33. The amount of glutamate which was permanently excreted by the MscS-His L109S mutant was correlated to the protein level. However, the cells that continued growth (without penicillin) probably started to import glutamate again at a distinct time point during growth as seen in the right hand part of figure 3.33. Consequently, it seemed as if the amount of glutamate in the external medium decreased over time for MscS-His L109S (25  $\mu\text{M}$  IPTG). In order to prove the actual occurrence of

glutamate uptake the respective uptake measurements have to be performed. Additional induction of glutamate production by addition of penicillin resulted in glutamate excretion rates of  $6.98 \mu\text{mol}/(\text{min g dm})$  ( $5 \mu\text{M IPTG}$ ) and  $8.62 \mu\text{mol}/(\text{min g dm})$  ( $25 \mu\text{M IPTG}$ ), respectively. The latter rate was comparable to the glutamate excretion rate of  $9.85 \mu\text{mol}/(\text{min g dm})$  obtained for the MscS-His strain. Taken together, the GOF mutant L109S of MscS-His led to continuous glutamate excretion without induction while the glutamate excretion rates upon application of a trigger for glutamate production were not increased compared to wild type MscS-His.

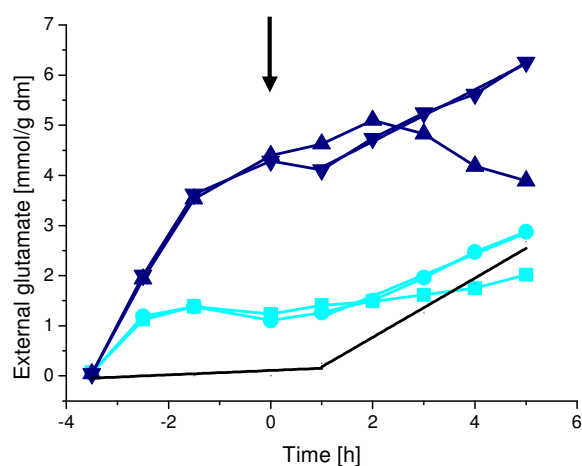


**Fig. 3.33: Glutamate excretion of MscS-His L109S GOF-mutant.**

GOF-mutant L109S of *E. coli mscS* was expressed in *C. glutamicum ΔyggB* using  $5 \mu\text{M}$  or  $25 \mu\text{M}$  IPTG. Glutamate excretion was monitored without induction and after addition of  $6 \text{ U/ml}$  penicillin (Pe) in the exponential growth phase ( $t=0$ , indicated by an arrow). Amounts of glutamate in the external medium were measured via HPLC-analysis. Straight lines represent linear regressions. MscS-His L109S ( $5 \mu\text{M IPTG}$ ) - Pe (■), + Pe (●); L109S ( $25 \mu\text{M IPTG}$ ) - Pe (▲), + Pe (▼); wt MscS-His is shown as black line.

## 4 Discussion

Bacteria respond to sudden decrease in external osmolality by activation of so-called mechanosensitive (MS) channels (Booth *et al.*, 2007). High intracellular osmolality leads to rapid water influx, threatening cell disruption. Consequently increased membrane tension opens MS channels which allow efflux of compatible solutes to protect the cell (Morbach and Krämer, 2002; 2008). Their activity is composed of channels belonging to the MscL- and MscS-type family (Perozo and Rees, 2003). *C. glutamicum* YggB, a structural homolog of the *E. coli* MscS, was suggested to function as MS channel (Ruffert *et al.*, 1999). However, its function has so far been poorly investigated. Recently, YggB was also connected to glutamate export in *C. glutamicum* (Nakamura *et al.*, 2007). *C. glutamicum* is the most important organism in the industrial production of glutamate. Although it has been investigated extensively for decades the export mechanism of glutamate is still unknown. However, several mutation hot spots within the *yggB* gene were identified to be correlated to permanent glutamate excretion. Furthermore, deletion of *yggB* resulted in drastically decreased glutamate production (Nakamura *et al.*, 2007).

In this work the suggested dual function of YggB as MS channel under osmotic stress conditions and in the export of the industrially important amino acid glutamate was investigated. The YggB MS channel homolog MscS of *E. coli* has been studied extensively for years, but only few other members of the MscS-type family have been characterized as functional MS channels. In difference to *E. coli* MscS (286 AA) *C. glutamicum* YggB harbors an elongated C-terminal domain since the protein consists of 533 amino acids (AA). While the N-terminal part of the YggB protein structure is homologous to MscS, including three transmembrane spans, the C-terminal part is quite unique among bacteria. Computer prediction revealed a putative fourth transmembrane domain within this C-terminal domain. Using alkaline phosphatase –  $\beta$ -galactosidase fusions, the topology of YggB was experimentally confirmed in this work. Concerning the question if YggB combines the two functions of a MS channel and a glutamate excretion system the role of the unique C-terminal domain might be crucial. The main question regarding the proposed involvement of YggB in the export of glutamate was, if YggB is the glutamate exporter itself or whether it is a regulator of another, so far unknown, glutamate export system. In order to answer this question several recombinant strains expressing, among others, truncated derivatives of *yggB* were studied.

## 4.1 Topology of YggB

The major difference between *E. coli* MscS and *C. glutamicum* YggB is the additional C-terminal elongation of YggB only found in closely related bacteria. Concerning its structure, the N-terminal half of the protein is highly similar to MscS, thus a comparable topology with the N-terminus located in the periplasmic space was assumed (see Figure 4.2 and figure 7.1 in the supplement for alignment comparing the primary sequence of *C. glutamicum* YggB and *E. coli* MscS). The C-terminal domain only found in close relatives of *C. glutamicum*, e.g. *C. efficiens*, is a characteristic feature of YggB. Regarding its topology, computer predictions differed concerning the existence of a fourth transmembrane domain within the C-terminal elongation of YggB. Using *phoA* and *lacZ* fusions with different truncations of the *yggB* gene, the existence of this fourth transmembrane segment was confirmed. Truncations that localized the fusion point to the periplasmic side showed increased alkaline phosphatase activity while cytoplasmic localization resulted in increased  $\beta$ -galactosidase activity (Seidel *et al.*, 2007). The obtained topology is consistent with results of a recent publication where an  $\alpha$ -amylase was located extracellularly by fusion to YggB  $\Delta$ 110 (Yao *et al.*, 2009). Localization of the unique C-terminal domain of YggB within the periplasmic space may be taken as an indication for a physical connection to the cell wall. With about 110 AA the periplasmic C-terminal part could easily span the periplasmic space reaching the cell wall. As most treatments inducing glutamate production somehow alter the cell envelope of *C. glutamicum* the C-terminal extension of YggB might be involved in sensing of these alterations. However, truncation of the C-terminal domain of YggB resulted in channel proteins that functioned similar to the wild type protein ( $\Delta$ 247 AA) or showed even an enhanced activity ( $\Delta$ 110 AA) concerning glutamate production (see section 3.6.1). These results argue against a function of the C-terminal domain of YggB in sensing of cell wall alterations caused by treatments which trigger glutamate production.

## 4.2 Electrophysiological characterization of YggB

In this work it was shown that YggB harbors the functions of a MS channel. Electrophysiological analysis of *C. glutamicum* *yggB* expressed in *E. coli* giant spheroplasts lacking all native MS channels revealed the presence of a pressure-dependent channel. Like *E. coli* MscS the channel strongly rectifies, meaning that its conductance differs depending on the applied voltage (hyper-, or depolarizing) (Fig. 3.5). However,

with approximately 30 % at positive and 15 % at negative voltages the conductance of YggB in general is much lower than that of MscS. Different conductances of a channel upon positive or negative voltages, respectively, is caused by a different ion permeability of the channel depending on the direction of ion flux. Seal formation in patch clamp analysis of spheroplasts results in inside-out spheroplast patches where the channels are in a right-side-out orientation, meaning that the pipette solution is facing the extracellular side of the spheroplast membrane with the embedded channels (Martinac *et al.*, 1987). Increased ion flux towards the pipette solution then occurs upon application of positive voltage. The higher conductance under these conditions is probably due to the outwardly directed ion flux under physiological conditions as MS channels release solutes from the cell upon hypoosmotic stress (Martinac, 2001).

In contrast to *E. coli* MscS, which becomes desensitized (inactivated) within seconds (Akitake *et al.*, 2005), YggB showed an oscillating behavior with several channels opening and closing constantly over a period of several minutes (Fig. 3.4). Since there were hundreds of channels in a single patch this wave-like behavior might be due to the opening of many channels leading to a decrease of membrane tension. Upon decreasing tension several channels close resulting in higher membrane tension which in turn leads again to channel opening. Not only the high number of channels in a single patch but also the relatively large pore size support such a hypothesis, previously also stated for MscL channels (Martinac, personal communication; Morris, 2002). The activity of the YggB channel was not altered by the presence of sodium ions instead of potassium ions (Fig. 3.7). However, channel conductance for the organic anions glutamate and pyruvate was significantly lower (Fig. 3.8). Nevertheless, it was shown that glutamate is able to pass the channel although not in a highly specific way. Unlike the previously described high specificity of solute efflux upon osmotic downshift (Ruffert *et al.*, 1997), the YggB channel appeared rather unspecific in patch clamp analysis, at least for glutamate and pyruvate as well as for  $K^+$ ,  $Na^+$ , and  $Cl^-$  ions. A further difference of YggB compared to *E. coli* MscS is its conductance saturation at high salt concentrations at positive pipette voltages. For *E. coli* MscS such conductance saturation was not reported up to a concentration of 1.5 M KCl, indicating a wide aqueous pore (Sukharev, 2002). Consequently, the rapid saturation of YggB might in part suggest a smaller or more specific pore. An increase of KCl concentration in the bath led to a shift of the zero current potential. In order to balance the concentration gradient of ions, more positive potassium ions flow towards the pipette indicating a slight preference for cations over anions ( $P_K/P_{Cl}$

~ 3.0, reflecting that YggB passes approximately 3 potassium ions per chloride ion) (Fig. 3.9). *E. coli* MscS, on the other hand, shows a slight preference for anions ( $P_{Cl}/P_K \sim 1.5 - 3.0$ ) (Martinac *et al.*, 1987; Sukarev, 2002), probably caused by the presence of lysine and arginine residues in the C-terminal domain of MscS (Sotomayor, 2007). Accordingly, the presence of a large number of acidic residues in the cytoplasmically located C-terminal portion following the third transmembrane domain enables the preference of YggB for cations over anions (Martinac, personal communication).

### 4.3 Significance of YggB under osmotic stress conditions

The function of YggB as MS channel was not only shown in *E. coli* spheroplasts, but additionally in *in vivo* experiments. However, functional complementation of *C. glutamicum* YggB in the *E. coli* double deletion strain MJF455 ( $\Delta mscL \Delta yggB$ ) was just shown for the  $\Delta 247$ -His mutant, resembling the exact length of the *E. coli* homolog. Such an effect was reported previously for the MscS channel homolog MSC1 from *Chlamydomonas* being only functionally expressed in *E. coli* cells upon N-terminal truncation down to the length of the *E. coli* homolog (Nakayama *et al.*, 2007). In contrast to the situation in *E. coli* spheroplasts and in *C. glutamicum*, expression of full length *yggB* did not complement the lethal phenotype of the *E. coli* mutant upon osmotic downshift. However, expression of the *yggB* gene was problematic in the high osmolality minimal medium required for the performed downshift experiments in contrast to *yggB* expression in rich medium (used for gene expression previous to preparation of giant spheroplasts). Consequently, it could not be discriminated whether the missing functional complementation was due to the lack of YggB full length protein or due to a non functional channel in *E. coli* under these conditions.

In order to verify the function of YggB as MS channel *in vivo*, further biochemical methods were used. Solute efflux by *C. glutamicum* as response to hypoosmotic shock was investigated as described previously (Nottebrock *et al.*, 2003). In the present work, however, some differences to previous results were observed. Efflux of glutamate upon osmotic downshift was clearly shown (Fig. 3.12), while previous work reported the efflux of only small amounts of the internal glutamate pool upon osmotic downshift (Ruffert *et al.*, 1997). But, involvement of YggB in this glutamate efflux could not be proven unequivocally. Taken together with the results obtained in patch clamp analysis, hypoosmotic solute efflux in *C. glutamicum* seems to be less specific as described before

(Ruffert *et al.*, 1997). Involvement of YggB in the efflux of glycine betaine was shown as reported previously (Nottebrock *et al.*, 2003). Additional evidence that YggB in fact mediates the efflux of betaine was provided by the elevated ability of the *yggB*-His overexpression strain to excrete betaine upon lowering the external osmolality. In contrast to the situation in *E. coli* (Levina *et al.*, 1999), double deletion of *mscL* and *yggB* is not lethal and betaine is still released upon osmotic downshift. These results indicate the existence of at least one more efflux channel in *C. glutamicum*, as previously suggested (Nottebrock *et al.*, 2003).

The results of this work furthermore provide strong evidence for an involvement of YggB not only in efflux of compatible solutes upon osmotic downshift but also in the cell's response upon salt stress, namely hyperosmotic conditions. Under hyperosmotic conditions cells accumulate compatible solutes to balance the osmotic gradient and maintain cell turgor (Wood, 1999). Accordingly, an exact adjustment of the internal solute concentration is required to provide cells with ideal conditions for growth and metabolism. To achieve such a balanced state different strategies are conceivable. (a) On the one hand the uptake carrier may be downregulated when the osmotic gradient across the membrane is balanced. At least a partial downregulation was shown for the activity of the betaine transporter BetP in *C. glutamicum* (Botzenhardt *et al.*, 2004). However, in order to adjust the internal solute concentration accurately the cell seems to require a type of dynamic control. (b) In general, secondary carrier systems switch from unidirectional uptake into an adapted state where an exchange of substrate occurs (Jung *et al.*, 2006). This mechanism does not change the internal solute concentration anymore and is therefore also not able to compensate slight variations of the concentration gradient across the plasma membrane. (c) Another model is the so-called 'pump and leak' system. This dynamic model achieves a fine-tuning of the internal solute pool by counterbalanced uptake and efflux mediated by two independent systems. Previous results already suggested the existence of a strictly regulated fine-tuning mechanism including uptake and efflux systems to balance the internal solute concentration accurately (Grammann *et al.*, 2002; Touzé *et al.*, 2001; Booth *et al.*, 2007). Grammann *et al.* (2002) proposed the existence of such an efflux system for ectoine in *Halomonas elongata*, since the deletion of the respective uptake system led to significant excretion of ectoine. Touzé *et al.* (2001) identified the protein BspA (a homolog of MscS channels), which was proposed to be required to maintain the internal glycine betaine pool during osmoadaptation in high-salt media containing this osmoprotectant. However, they

assumed BspA to be rather a regulator of a betaine efflux channel involved in controlling the intracellular level of betaine. While several uptake systems ('pump') for compatible solutes are known (Wood, 1999; Peter *et al.*, 1998; Morbach and Krämer, 2005a) the nature of efflux systems ('leak') likely to be involved in fine-tuning of the internal solute concentration was up to now unknown.

In this work evidence is provided for the first time that the MS channel YggB of *C. glutamicum* is the responsible efflux system involved in the fine-tuning mechanism of the internal betaine pool. In the case of *C. glutamicum* the preferred compatible solute betaine is accumulated by the uptake carrier BetP to compensate an osmotic gradient (Krämer and Morbach, 2004). Overexpression of *yggB*-His reduced the ability of the cells to accumulate betaine under hyperosmotic conditions resulting in a much lower steady-state betaine concentration compared to wild type cells (Fig. 3.15). Visualization of net betaine efflux during the steady state level of osmotic compensation revealed a strongly increased betaine efflux also upon moderate expression of *yggB* with and without His-tag (Fig. 3.16). Consequently, a small but significant portion of betaine efflux mediated by YggB was missing in the *yggB* deletion compared to the wild type. Residual betaine efflux in the  $\Delta yggB$  mutant can be explained by the exchange of equal amounts of betaine by the carrier BetP itself.

In addition to the switch from unidirectional uptake to an exchange of betaine molecules BetP was previously shown to become downregulated upon osmotic compensation (Botzenhardt *et al.*, 2004). This downregulation was verified for BetP activity in wild type cells under the conditions used here (Fig. 3.18). However, overexpression of *yggB* at moderate or *yggB*-His at highly elevated level reduced downregulation of BetP activity to different extents. Instead, BetP seemed to compensate the elevated outward flux of betaine via YggB by on-going betaine uptake which allows a comparable steady state concentration (at least in the strain expressing untagged *yggB* from a plasmid) as reached by wild type and the  $\Delta yggB$  mutant. The expected further decrease of BetP activity upon *yggB* deletion was probably too small to be detected in the kind of experiment used in the current study. Nevertheless, a tight regulation of betaine uptake and efflux activity represented by the uptake carrier BetP and the MS channel YggB was demonstrated.

The perfect cooperation of an active uptake carrier, like BetP, and a passive efflux channel, like YggB, allows precise fine-tuning of the internal betaine concentration in a very sensitive manner. Taken together, all three models (downregulation of the uptake

carrier, switch to a substrate exchanging state of the uptake carrier, and the pump and leak model, respectively) were shown to be involved in the osmotic adaptation of *C. glutamicum* (Fig. 4.1; the shown model was simplified since an involvement of LcoP and EctP cannot be completely excluded).

Further evidence supporting the pump and leak model was provided by the results obtained by patch clamp analysis. Under hypoosmotic conditions MS channels normally respond to drastic increases of membrane tension. Accordingly, the question arises if the membrane stretch caused by small fluctuations of the osmotic gradient during the steady state situation of betaine accumulation would be sufficient to activate the YggB channel. In order to answer this question the results of patch clamp analysis were used to calculate the concentration gradient required to open the channel. Based on the tension necessary to open the channel (40 - 100 mm Hg) the corresponding osmotic gradient can be calculated using the equation  $c = \rho gh/RT$ , where  $\rho$  is density of Hg (13.6 g/cm<sup>3</sup>),  $g$  (981 cm/s<sup>2</sup>), and  $h$  the height of Hg column (cm), leading to a value of 2.2 - 5.4 mOsm/l. For an alternative calculation the Van't Hoff's law  $\Delta\Pi = RT\Delta c$  was used to calculate the intracellular osmolarity change  $\Delta c$  (Osm) that would cause swelling of a bacterial cell, stretch the cell membrane and cause an increase in membrane tension (Martinac, 2007). The membrane tension  $\gamma$  in a uniformly curved spheroplast patch sufficient to activate MS channels can be estimated by using Laplace's law  $\gamma = pd/4$  (Hamill and Martinac, 2001), where  $d$  is the diameter of the patch. Assuming  $d = 1 \mu\text{m}$  the pressure sufficient to activate YggB channels in spheroplast patches of 40 - 100 mm Hg corresponds to a membrane tension of roughly  $\sim 1.5 - 3.5 \text{ mN/m}$ . An average volume of a bacterial cell of  $0.4 \mu\text{m}^3$  (Heldal *et al.*, 1994) and a diameter of about  $0.9 \mu\text{m}$  (approximates the diameter of the spheroplast patch) was assumed. Consequently, the magnitude of osmotic stress that would cause membrane tension of  $\sim 1.5 - 3.5 \text{ mN/m}$  corresponds to a change in osmolarity of  $\sim 2.5 - 5.5 \text{ mOsm/l}$  (Martinac, personal communication).

The results obtained by these two different calculations match perfectly and demonstrate that even small concentration differences of about 5 mM betaine across the membrane are sufficient to open the MS channel YggB. Variation of the internal betaine concentration to such a small extent is easily accomplished by an active BetP system, since BetP is able to change the internal betaine concentrations by several 100 mM within short time (Botzenhardt *et al.*, 2004; Morbach and Krämer, 2005b). Consequently, the functional interplay of betaine uptake (via BetP) and betaine efflux (via YggB) is required to adjust

the internal betaine concentration in an extremely sensitive manner to achieve a perfectly balanced osmotic gradient.

A further evidence for a functional connection between BetP and YggB was given by the effects caused by expression of truncated *yggB* derivatives. The decreased ability to accumulate certain amounts of betaine seems to be caused by a combination of two effects. One is the highly increased betaine efflux via truncated versions of YggB that cannot be compensated by BetP anymore. At least upon osmotic stress, including osmotic down- and upshift, truncations of the C-terminal domain of YggB seem to activate the channel resulting in free efflux of betaine. The resulting effect is most likely a reduced BetP activity caused by the decreased membrane potential in the relevant strains. This is consistent with the observation that continuous efflux of glycine betaine decreased the membrane potential which stayed low as long as the efflux of betaine continued (Ruffert *et al.*, 1997). The observed decrease in the electrical potential is probably due to a leak of charged molecules, presumably protons, released together with betaine through the efflux channel under conditions of channel opening. The decreased membrane potential, the driving force of the betaine uptake carrier BetP, together with a strongly increased betaine efflux largely abolishes betaine accumulation. Consequently, no osmotic compensation was possible in these mutants (especially  $\Delta 110$ -His and  $\Delta 247$ -His).

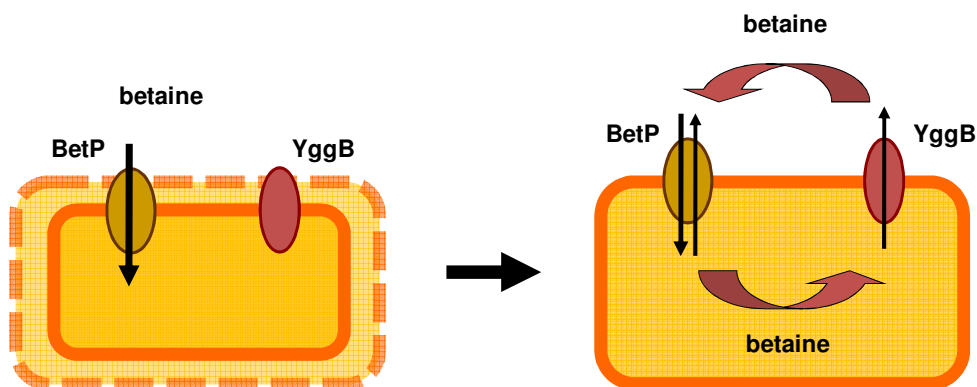


**Fig. 4.1: Pump and leak model.**

Increase in external osmolality leads to cell shrinkage. To maintain cell turgor compatible solutes, here e.g. betaine, are accumulated until the osmotic gradient is compensated. Fine-tuning of the steady state betaine concentration is ensured by a sensitively balanced uptake (pump) and efflux (leak) of betaine. This regulation is mediated in *C. glutamicum* by the active betaine uptake carrier BetP and the passive MS channel YggB. Shown is a simplified model as involvement of LcoP and EctP cannot be excluded.

In contrast to the disability of some YggB truncation mutants to handle severe osmotic stress conditions caused by osmotic down- and upshifts, the same strains were able to grow

under high salt conditions, although some strains had a delayed onset of growth and a slightly diminished growth rate directly correlated with the external salt concentration (Fig. 3.20). Interestingly, under these conditions other mutants than YggB  $\Delta$ 247-His, namely  $\Delta$ 110-His and YggB-His, were more severely impaired than under severe hyperosmotic conditions subsequent to an osmotic downshift. Consequently, the conditions of a severe osmotic downshift followed by an immediate upshift have to be treated separately from the conditions of growth in high osmolality medium that were also used for the glutamate excretion experiments (discussed later). Under the latter conditions the YggB  $\Delta$ 110-His mutant was shown to excrete glutamate specifically since no leakiness for any other substrate was observed (see section 3.5.5). Taken together, the function of YggB as MS channel upon hypoosmotic conditions and as possible system responsible for glutamate excretion should be accounted separately (especially regarding the specificity of the channel under these two different conditions). Also, the role of YggB's C-terminal domain might depend on the external conditions and the corresponding function of the protein under these conditions.

#### **4.4 Involvement of YggB in glutamate production**

Besides its function in the regulation of osmotic shifts, YggB of *C. glutamicum* was proposed to be involved in the export of glutamate. This assumption was based on the results obtained by Nakamura *et al.* (2007) in the strain *Brevibacterium lactofermentum* ATCC13869 that is closely related to *C. glutamicum* ATCC13032 used in this work. Deletion of about half of the C-terminal domain of YggB downstream Val419 upon spontaneous insertion of a transposon resulted in constitutive glutamate excretion without any further trigger. This deletion corresponds to the  $\Delta$ 110-His mutant used in this work. Similar to the published results a permanent glutamate production was shown for this mutant in the organism used in the current study. In contrast, deletion of *yggB* reduced glutamate production down to about 30 % upon all triggers used (Table 3.4), indicating a major contribution of YggB to glutamate production. However, at least one further protein is supposed to be involved in the export of glutamate responsible for the residual glutamate excretion (Nakamura *et al.*, 2007).

Glutamate excretion rates of all strains used in this work are summarized in table 7.3 in the supplement.

Complementation of the *yggB* deletion phenotype by plasmid-encoded expression of *yggB* led to a normal glutamate production behavior which requires one of the treatments inducing glutamate production. The addition of a 6xHis-tag to the C-terminal end of the protein greatly increased the level of membrane integrated YggB protein. The corresponding strain excreted glutamate constitutively without further induction. However, using this strain without induction of gene expression by IPTG, a normal glutamate excretion rate comparable to the complementation strain and no 'leakiness' for glutamate was observed. Consequently, we argue that continuous glutamate excretion of the YggB-His strain (expression of the plasmid-encoded *yggB*-His gene induced by 25  $\mu$ M IPTG) was caused by a dramatically increased protein level of YggB-His and not by the addition of the C-terminal His-tag interfering with the function of the C-terminal domain.

With respect to the C-terminal domain, truncated mutants of YggB had different effects on glutamate production. Consistent with the results concerning its function as MS channel the  $\Delta$ 132-His mutant mediated no glutamate excretion. Both results indicate that truncation of 132 AA results in a permanently inactive and therefore non-functional channel. While the  $\Delta$ 247-His mutant was strongly affected under osmotic stress conditions (osmotic down- and upshift), hardly able to accumulate betaine, the conditions used for glutamate production did not affect this mutant in a comparable way. Consequently, spontaneous glutamate excretion was negligible. However, for this mutant as for all other strains, the detected amount of excreted glutamate especially without treatment to induce glutamate production did probably not reflect the real extent of glutamate excretion. Previous publications indicate that competing glutamate uptake is active simultaneously (Krämer *et al.*, 1990a, b; Trötschel *et al.*, 2003) which would mask possible low level excretion of glutamate. The most significantly impaired  $\Delta$ 110-His mutant excreted glutamate continuously without induction. Surprisingly, this glutamate excretion seemed to be quite specific as no other molecules were found to be released under these conditions. On the contrary, under osmotic stress conditions the  $\Delta$ 110-His mutant seems to be transiently open allowing the unspecific release of solutes and ions, as indicated by the strongly decreased membrane potential. A possible explanation for the observed preferred glutamate excretion might be the high intracellular glutamate concentration of 100 - 150 mM (Gutmann *et al.*, 1992). However, this high internal glutamate pool does not explain the spontaneous but still specific excretion of glutamate by some mutants without induction compared to the more unspecific efflux upon osmotic downshift. Consequently, two different mechanisms or conformations of the YggB protein responsible for

mechanosensitive efflux on the one hand and glutamate excretion on the other might be considered.

A main focus of this work was the question if YggB is in fact the glutamate export system or whether it is a regulator of another so far unknown export carrier. Several physiological parameters, like change in osmolality and pH value, had an influence on glutamate production by *C. glutamicum*. As described previously (Lambert *et al.*, 1995) a shift in osmolality during on-going glutamate production changes the amount of excreted glutamate. Consistent with the function of a MS channel a shift towards lower osmolality (hypoosmotic conditions) resulted in increased glutamate production. However, the same effect was observed in the *yggB* deletion mutant (Fig. 3.23), indicating a sensor for osmotic alterations and a transport system different from YggB under these conditions. Since the presence of another MS channel (Nottebrock *et al.*, 2003) and also of another minor glutamate exporter (Nakamura *et al.*, 2007) was proposed, the existence of an additional protein responsible for both functions is conceivable.

All previously obtained results could not exclude that YggB may harbor the function of a regulator involved in activation of an unknown glutamate export system. The residual glutamate production in the *yggB* deletion mutant might be triggered by the 'real' glutamate exporter which is just less active in the absence of YggB. However, attempts to identify other glutamate export systems did not succeed. The *C. glutamicum* genes *Cgl0063*, *Cgl0590*, and *Cgl2211*, which were supposed to be candidates for alternative export systems, are not involved in glutamate production.

Interesting results to discriminate between the two possible functions of YggB in the export of glutamate were provided by the heterologous expression of different variants of *mscS* and of the *mscS/CtyggB* fusion, respectively. Already the presence of MscS in the *yggB* deletion strain triggered an increased glutamate excretion. Additional presence of the C-terminal domain of YggB fused to MscS further enhanced the ability of the cells to produce glutamate (Fig. 3.30). In this case the C-terminal domain of *C. glutamicum* YggB fused to *E. coli* MscS had a significant impact on glutamate excretion while its truncation had not such a strong effect in the native YggB protein. Consequently, the importance of the C-terminal domain seems to be somehow dependent of the nature of the core protein (N-terminal part including the channel domain). The partial complementation of the  $\Delta yggB$  phenotype by expression of the genes *mscS* (*E. coli*) and the fused gene *mscS/CtyggB* suggested that the produced glutamate actually passed through the pore formed by YggB,

or MscS in this case, since the N-terminal part of YggB and MscS are highly homologous and are therefore assumed to form a similar pore.

In patch clamp analysis it was shown that glutamate is able to pass the pore formed by YggB subunits. In order to elucidate if glutamate also passes through YggB under glutamate productive conditions the model system using heterologous expression of *mscS* and *mscS/CtyggB*, respectively, was further modified. For *E. coli* MscS several loss-of-function (LOF)-mutants resulting in an inactive channel were described (Nomura *et al.*, 2006; Miller *et al.*, 2003). These mutations abolish the ability of MscS to prevent cell lysis upon osmotic downshift. Furthermore, no channel activity could be detected in patch clamp analysis of the respective mutants.

Introduction of LOF-mutations into *mscS* as well as *mscS/CtyggB*, expressed in the *yggB* deletion strain, led to a complete loss of glutamate excretion triggered by the native gene products (Fig. 3.31). In *E. coli* the LOF-mutations A51N(TM1)/F68N(TM2) and I37N(TM1)/L86N(TM2) of MscS are located at the cytoplasmic and periplasmic ends of the transmembrane domains, respectively, and impair the MscS function almost entirely (Fig. 4.2). The localization of the LOF-mutations indicates that a similar degree of lipid-protein interaction at both ends of TM1 and TM2 is important for proper MscS function. Unbalanced interactions between the two ends of TM1 and TM2 with the membrane surrounding result in severe loss of function (Nomura *et al.*, 2006). Consequently, the disability of these mutants to mediate glutamate efflux in *C. glutamicum* might be due to an impaired protein-membrane interaction. The ability of MS channels to transduce increasing membrane tension into a conformational change allowing the efflux of solutes is supposed not to work properly in these mutants. Related to the glutamate excretion of *C. glutamicum* this result indicates that alterations in the membrane (tension) are directly correlated with the excretion of glutamate. An impaired sensing of these alterations might abolish glutamate excretion at least by MscS.

Presence of the MscS-His L109S gain-of-function (GOF) mutant in the *C. glutamicum*  $\Delta yggB$  strain led to permanent glutamate excretion. GOF-mutants in *E. coli* MscS cause severe problems for the cell since they open easily or even randomly. An *E. coli* mutant with a MscS L109S mutation was strongly impaired concerning growth, survival of an osmotic downshift, and susceptibility for different antibiotics (Miller *et al.*, 2003). Since highly active channels cause severe problems for the cell, the expression level of *mscS* L109S in *E. coli* was very low. Indeed in patch clamp analysis of MscS L109S in *E. coli* MscS-like channels were shown based on the conductance and pressure threshold

but in very low abundance (Miller *et al.*, 2003). Consistent with the results in *E. coli* the expression level of *mscS* L109S in the *C. glutamicum*  $\Delta$ *yggB* strain was also very low and resulted in a severe growth phenotype (Fig. 3.32), indicating that also in *C. glutamicum* the channel might be highly active. This high activity led to continuous excretion of glutamate without need of any of the common triggers used for the induction of glutamate production (Fig. 3.33). Leu109 is localized within the third transmembrane domain (residues 96 - 127) of MscS (Fig. 4.2), of which seven helices assemble the channel pore. A mutation within this pore region resulting in elevated channel activity strongly suggests that the efflux is mediated by the channel itself and not by another protein just regulated by the channel.

Taken together with the results obtained with the *E. coli mscS* LOF-mutants expressed in *C. glutamicum*, strong evidence is provided that glutamate excretion by *C. glutamicum* can be mediated by the heterologously expressed *E. coli mscS*. This indicates that also the *C. glutamicum* homolog YggB is able to mediate glutamate excretion and is not just a regulator of another glutamate export system.

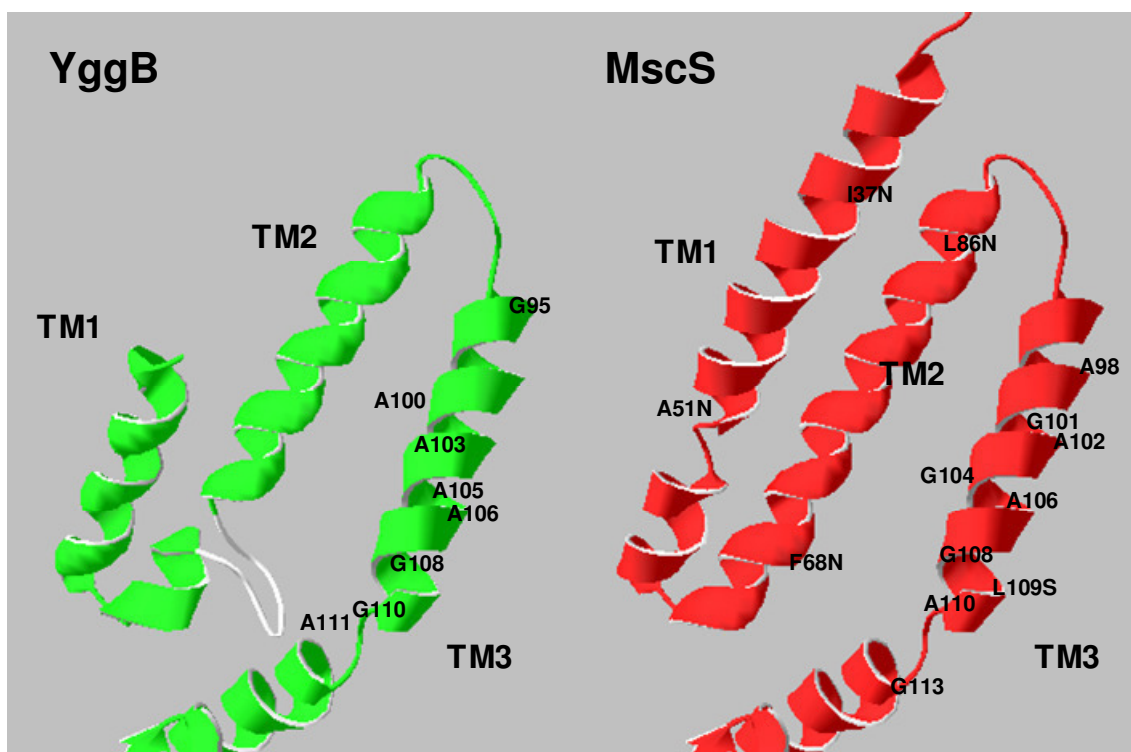


**Fig. 4.2: 3D model of *C. glutamicum* YggB compared to *E. coli* MscS.**

3 D structure of *C. glutamicum* YggB (N-terminal part of 286 AA) was modeled using Swiss Model (Arnold *et al.*, 2006; Bordoli *et al.*, 2009) based on the 3D crystal structure of *E. coli* MscS (Wang *et al.*, 2008). Shown is the N-terminal part of both proteins harboring three transmembrane (TM) domains (*E. coli* MscS: TM1 (AA 21 - 57), TM2 (AA 68 - 91), and TM3 (AA 96 - 127)). Positions of LOF- and GOF-mutations in MscS are indicated as well as (possibly) important glycine and alanine residues within the third TM of both proteins.

A pattern of glycine and alanine residues is conserved in the MscS-type family (Perozo and Rees, 2003). Four glycines Gly101, Gly104, Gly108 and Gly113 form interacting pairs with four alanines Ala98, Ala102, Ala106 and Ala110, proposed to be involved in gating of the channel (Fig. 4.2) (Edwards *et al.*, 2005). The predicted TM3 of *C. glutamicum* YggB (putative residues 92 - 109) also harbors several glycines (Gly95, Gly108, Gly110) and alanines (Ala100, Ala103, Ala105, Ala106, Ala111) that at least partly might be involved in a similar opening mechanism (Fig. 4.2). Although the YggB sequence does not harbor exactly the same sequence pattern of a putative gate as *E. coli* MscS, the presence of several glycine and alanine residues indicates the formation of a similar pore mediating efflux. The Swiss Model workspace models 3D protein structures using experimentally determined structures of related family members as template (Arnold *et al.*, 2006; Bordoli *et al.*, 2009). The 3D structure of *C. glutamicum* YggB was modeled based on the known structure of *E. coli* MscS (Wang *et al.*, 2008). The model shown in figure 4.2 reveals a highly similar structure of YggB compared to MscS. The structure of the TM3 of both proteins, forming the channel pore of the oligomere, displays especially high similarity. This similarity argues for the possibility of transferring the experimentally obtained data, using *E. coli* MscS, to *C. glutamicum* YggB.

The hypothesis of MscS and YggB assembling a similar pore is also consistent with the results obtained via electrophysiological analysis where YggB was characterized as a channel with similar properties as *E. coli* MscS, however, with unique features.

Taken together several arguments were provided to discriminate between YggB being the glutamate export system or a regulator. Comparison of the glutamate excretion by wild type and the *yggB* deletion strain under different conditions did not enable to discriminate between these two possible functions. However, several other results rather support the hypothesis of YggB being in fact the glutamate excretion system. In electrophysiological analysis YggB was proven to function as MS channel that allows the efflux of glutamate. Additionally, the YggB  $\Delta$ 110-His mutant showed a significantly changed betaine efflux and accumulation pattern under osmotic stress conditions (down- and upshift) and also distinct alteration of glutamate production indicating that these two functional effects are in fact caused by the same protein. The strongest arguments are provided by the results obtained with the LOF- and GOF-mutants of *E. coli mscS*. The effects of these mutants on the glutamate excretion mediated by the native MscS channel present in *C. glutamicum* (completely abolished or enhanced glutamate production,

respectively) strongly suggest that the MscS channel and accordingly also the structural homolog YggB mediates glutamate excretion.

#### **4.5 Function of YggB – current knowledge and future perspectives**

In the present work it was shown that the membrane protein YggB of *C. glutamicum* harbors three different functions: (a) YggB functions as MS channel involved in solute efflux of betaine and probably glutamate to prevent cell lysis upon osmotic downshift; (b) YggB is significantly involved in the fine-tuning of the steady state internal betaine concentration, accumulated under hyperosmotic conditions. Such an involvement of a MS channel in this mechanism was shown for the first time in this work, acting not just as an emergency valve but also in a very sensitive manner; (c) YggB is most likely also the excretion channel for glutamate under glutamate productive conditions. A possible connection of these three functions might be via the sensing properties of the MS channel which is able to detect changes of membrane tension. Glutamate production can be triggered by several treatments all changing the cell envelope. While addition of antibiotics or local anesthetics affects the cell wall directly, other treatments, such as biotin limitation, addition of Tween 60, or trehalose deficiency, alter the cell wall concerning its structure. These alterations might be detected by the MS channel YggB and transduced in some conformational change allowing glutamate excretion. A similar model was already proposed by Nakamura *et al.* (2007), however, this work provides further evidence supporting this hypothesis.

Glutamate excretion triggered by a passive channel is in contrast to the previous assumption that ATP or a related high-energy metabolite is involved in the activity of glutamate export in *C. glutamicum* (Gutmann *et al.*, 1992). A possible explanation for this discrepancy might be the regulation of ODHC activity by PknG via phosphorylation status of OdhI (Niebisch *et al.*, 2006, Schultz *et al.*, 2007). Both PknG (directly or indirectly) and YggB might be able to sense membrane alterations caused by different triggers of glutamate production, independently or even in a somehow connected way. While YggB is activated to trigger glutamate excretion, PknG (and Ppp) leads to a metabolic flux change towards glutamate production by downregulation of ODHC activity in an energy dependent manner. Consequently, glutamate overproduction would be the result of a combination of metabolic alteration towards efficient glutamate synthesis and the activation of a glutamate excretion system, possibly via cell wall alteration.

The elongated C-terminal domain of YggB is a unique feature of bacteria belonging to the family of *Corynebacteria*. As the involvement of YggB in the excretion of glutamate is a novel function possibly independent from its function as MS channel the C-terminal domain missing in most homologs of the MscS-type family was proposed to harbor an important function under glutamate productive conditions. However, truncations of different extent resulted in ambiguous effects on both functions of YggB, under osmotic stress (osmotic down- and upshift) on the one hand and in glutamate excretion on the other (Fig. 4.3).

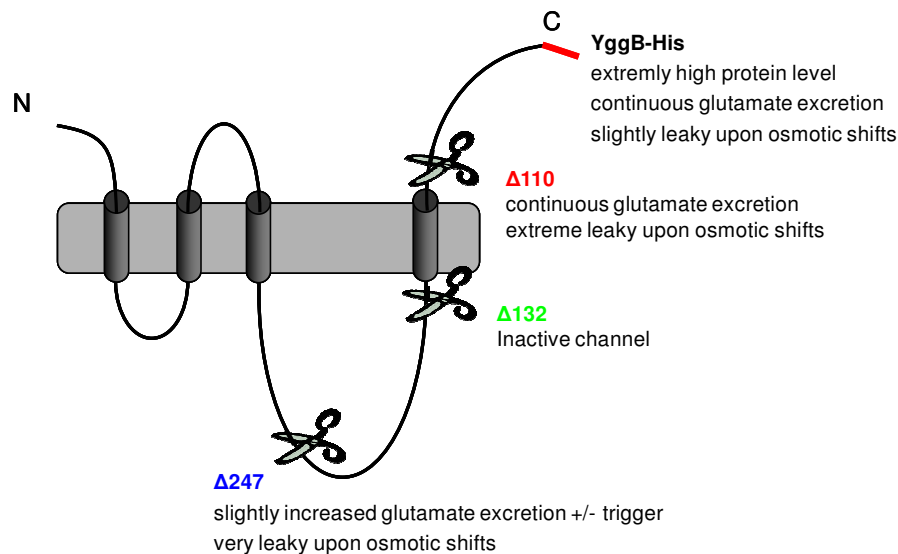


**Fig. 4.3: Phenotypes of mutants harboring different YggB derivatives.**

Shown are the different YggB truncations used in this work and their phenotypes upon osmotic challenges and in glutamate excretion.

Deletion of the last 110 AA resulted in a highly active channel for compatible solutes upon osmotic down- and upshift as well as for glutamate. However, additional deletion of the fourth transmembrane domain ( $\Delta 132$ ) completely abolished the function of the YggB channel. One possible hypothesis to explain these effects might be the interplay of the periplasmic C-terminal end and the fourth transmembrane domain to regulate channel function. These parts of the protein might be involved in the transition between active and inactive state of the channel,  $\Delta 110$  assembling a permanently active and  $\Delta 132$  a permanently inactive channel. Surprisingly, further truncation of 247 AA resulted again in a functional channel. However, this channel seems to open more easily upon osmotic down- and upshift, indicating the lack of the proposed regulatory function of the C-terminal domain. Switching between active and inactive state of the channel might be less

well regulated and therefore easier to achieve in the  $\Delta 247$  mutant. However, without any trigger (osmotic down- and upshift or induction of glutamate production) the YggB  $\Delta 247$  subunits may form a closed channel. In general the protein does not seem to be fixed in either an active or an inactive conformation.

Although unlikely, an additional effect of different protein levels has to be taken into account as explanation for the phenotypes of the YggB truncation mutants. Strong overexpression of *yggB*-His had a very pronounced effect on glutamate excretion which occurred permanently. Concerning its function upon osmotic up- and downshift it was more impervious than the truncated forms of YggB ( $\Delta 110$  and  $\Delta 247$ ). Thus, an elevated protein level has a much stronger impact on glutamate excretion than on the ability of the cells to cope with osmotic stress situations.

Taken together, the functions of YggB as MS channel upon osmotic challenge (hypo- as well as hyperosmotic stress) and as a glutamate excretion system, although mediated by the same channel protein, seem to be based on different activation mechanisms and have, at least partly, to be considered separately. In view of the present results the function of YggB as an excretion system for glutamate is assumed to be mediated through the same pore of the channel as solute efflux triggered by osmotic stress. However, dependent on the function as MS channel or glutamate excretion system, the channel might be either regulated differently, the pore opened in a different way, or maybe just to a different extent.

In order to gain comprehensive understanding of YggB's function in *C. glutamicum* further research is required in the future. The possible effect of the protein level was most obvious in the case of *yggB*-His overexpression. In order to completely exclude such an effect as reason for the phenotypes observed, gene expression of all *yggB* variants under the native promoter may be a proper tool. In order to further investigate physiological influences like the interesting effect of different pH values on glutamate production, constant pH conditions have to be guaranteed, e.g. by cultivation in a controlled fermenter. The ability of MS channels to sense external pH values was already shown for the MS channel of large conductance (MscL) of *E. coli*. Dependent on the pH the channel sensitivity to membrane tension is adjusted (Kloda *et al.*, 2006). Different effects of pH changes on glutamate excretion possibly sensed by YggB in the wild type may account to a better understanding of YggB's function in glutamate production by *C. glutamicum*.

Final confirmation that YggB is the glutamate excretion channel might be gained by an approved method to characterize transporters/carriers, like e.g. BetP, which includes protein purification followed by reconstitution into liposomes. This system guarantees strictly controlled conditions but requires that the protein is able to function independently in such an *in vitro* system. For YggB being a MS channel it might be a difficult task to simulate increasing membrane tension or the conditions of glutamate production in liposomes. Therefore, the patch clamp technique might be a better tool to further characterize YggB and also its truncated forms under controlled conditions. A possible regulatory role of the C-terminal domain could be revealed if the open probabilities of the different YggB truncations differ significantly in this type of analysis.

Since the mechanism leading to glutamate production is a very complex process, the interplay of additional proteins involved may be assumed. Therefore, the identification of possible interaction partners of YggB is a further aim in the future. Interaction with e.g. PknG directly or via another unknown linker protein is conceivable. Identification of these proteins by cross-linking or pull down methods might provide a better understanding of the complex network leading to export activation and glutamate production in *C. glutamicum*. Interaction with other proteins is also a possible function of the additional C-terminal domain of YggB. In order to clarify the role of this domain, detailed analysis, e.g. via further mutations, is necessary. Additionally, crystallization and X-ray structure analysis might provide more information about the conformation and related functions of the C-terminal domain.

## 5 Summary

In this work the membrane protein YggB of *Corynebacterium glutamicum* was investigated with respect to its function under general osmotic stress conditions on the one hand and in the production of glutamate on the other. YggB was previously described to belong to the MscS-type family functioning as MS channel in the bacterial hypoosmotic stress response (Nottebrock *et al.*, 2003). Recently, YggB was also connected to the glutamate export in *C. glutamicum* under glutamate productive conditions. Since *C. glutamicum* is used in the industrial production of amino acids, mainly glutamate, understanding of export mechanisms is of major interest. Deletion of *yggB* led to a drastic decrease in glutamate excretion while truncation of 110 AA, among other mutations, resulted in continuous glutamate excretion (Nakamura *et al.*, 2007). Computer prediction proposed a fourth transmembrane segment within the unique C-terminal domain only present in close relatives of *C. glutamicum*. In this work the predicted topology of YggB was confirmed. Using an alkaline phosphatase –  $\beta$  galactosidase reporter cassette fused to different YggB constructs the localization of the C-terminal domain in the periplasmic space could be shown. As an approved method to characterize channel proteins the patch clamp technique was used in this work. Patch clamp analysis of *E. coli* giant spheroplasts expressing *yggB* clearly revealed the presence of a pressure-sensitive channel similar to the *E. coli* homolog MscS. However, clear functional differences between YggB and MscS were observed. YggB shows a lower conductance, does not inactivate rapidly, and displays a slight preference for cations over anions. Additional physiological characterization of YggB showed its involvement in glycine betaine as well as glutamate efflux upon osmotic downshift. Surprisingly, also an involvement of YggB in the hyperosmotic stress response of *C. glutamicum* was revealed. Uptake kinetics and energetic of betaine accumulation during osmotic compensation and under steady state conditions were performed to investigate the effects of *yggB* deletion and presence of different YggB derivatives, respectively, under hyperosmotic conditions. Overexpression of *yggB* or *yggB*-His led to a strongly increased betaine efflux while *yggB* deletion led to a slightly but significantly reduced betaine efflux. In a so called ‘pump and leak’ model solute uptake (via the active transporter BetP) and efflux (via the passive channel YggB) are functionally balanced. For the first time this work provides evidence that MS channels are key players in this response to hyperosmotic conditions.

Furthermore, the proposed function of YggB in the excretion of glutamate was confirmed in this work. Additionally, several C-terminal truncations were investigated due to their effect on glutamate production. Obviously, the integrity of the C-terminal domain has a strong effect on the inducibility of glutamate production. Taken together with the results obtained for the different truncations under varying osmotic conditions the C-terminal domain is proposed to harbor some regulatory function, mediating the switch between active and inactive state of the channel. However, this hypothesis is still highly speculative and has to be investigated further. One of the main questions to answer in this work was if YggB harbors the function of a glutamate excretion system or whether it is a regulator of another so far unknown glutamate exporter. Several arguments were found in favor for either one or the other hypothesis. The strongest argument is provided by heterologous expression of *E. coli mscS* and *mscS/CtyggB*, respectively, leading to elevated glutamate excretion in the *C. glutamicum yggB* deletion strain. Introduction of loss-of-function- and gain-of-function-mutations in *mscS* completely abolished or elevated, respectively, glutamate production in the *yggB* deletion, indicating that glutamate excretion is directly mediated by the *E. coli* MscS channel pore highly homologous to YggB concerning its structure.

Taken together, this work provides strong evidence that glutamate excretion is triggered directly by the *C. glutamicum* MS channel YggB of the MscS-type family. Additionally, it was shown for the first time that YggB does not only act as emergency valve upon **hyposmotic** stress but also in a very sensitive manner in the fine-tuning mechanism of internal solute concentration under **hyperosmotic** conditions.

## 6 Literature

Abe S, Takayama K, and Kinoshita S (1967) Taxonomical studies on glutamic acid-producing bacteria. *J. Gen. Appl. Microbiol.* **13**:279-301.

Akitake B, Anishkin A, Sukharev S (2005) The "dashpot" mechanism of stretch-dependent gating in MscS. *J Gen Physiol.* **125**:143-54.

Arnold K, Bordoli L, Kopp J, Schwede T (2006) The SWISS-MODEL workspace: a web-based environment for protein structure homology modelling. *Bioinformatics.* **22**:195-201.

Asakura Y, Kimura E, Usada Y, Kawahara Y, Matsui K, Osumi T, Nakamatsu T (2007) Altered metabolic flux due to deletion of *odhA* causes L-glutamate overproduction in *Corynebacterium glutamicum*. *Appl Environ Microbiol.* **73**:1308-19.

Bass RB, Strop P, Barclay M, Rees DC (2002) Crystal structure of *Escherichia coli* MscS, a voltage-modulated and mechanosensitive channel. *Science.* **298**:1582-7.

Berrier C, Besnard M, Ajouz B, Columbe A, Ghazi A (1996) Multiple mechanosensitive ion channels from *Escherichia coli*, activated at different thresholds of applied pressure. *J Membr Biol.* **151**:175-87.

Blum M, Beier H, Gross HJ (1987) Improved silverstaining of plant proteins, RNA and DNA in polyacrylamid gels. *Electrophoresis.* **8**:93-99.

Bolen DW, Rose GD (2008) Structure and energetics of the hydrogen-bonded backbone in protein folding. *Annu Rev Biochem.* **77**:339-362.

Booth IR, Edwards MD, Black S, Schumann U, Miller S (2007) Mechanosensitive channels in bacteria: signs of closure? *Nat Rev Microbiol.* **5**:431-40.

Bordoli L, Kiefer F, Arnold K, Benkert P, Battey J, Schwede T (2009) Protein structure homology modeling using SWISS-MODEL workspace. *Nat Protoc.* **4**:1-13.

Botzenhardt J, Morbach S, Krämer R (2004) Activity regulation of the betaine transporter BetP of *Corynebacterium glutamicum* in response to osmotic compensation. *Biochim Biophys Acta*. **1667**:229-40.

Bradford MM (1976) A rapid and sensitive method for the quantitation of microgram quantities of protein utilizing the principle of protein-dye binding. *Anal. Biochem.* **72**:248-254.

Brickman E, Beckwith J (1975) Analysis of the regulation of *Escherichia coli* alkaline phosphatase synthesis using deletions and phi80 transducing phages. *J Mol Biol.* **96**:307-316.

Chang G, Spencer RH, Lee AT, Barclay MT, Rees DC (1998) Structure of the MscL homolog from *Mycobacterium tuberculosis*: a gated mechanosensitive ion channel. *Science*. **282**:2220-6.

De Angeli A, Monachello D, Ephritikhine G, Frachisse JM, Thomine S, Gambale F, Barbier-Brygoo H (2006) The nitrate/proton antiporter AtCLCa mediates nitrate accumulation in plant vacuoles. *Nature*. **442**:939-42.

Duperray F, Jezequel D, Ghazi A, Letellier L, Shechter E (1992) Excretion of glutamate from *Corynebacterium glutamicum* triggered by amine surfactants. *Biochim Biophys Acta.*, **1103**:250-8.

Ebbighausen H, Weil B, Krämer R (1991) Na(+)-dependent succinate uptake in *Corynebacterium glutamicum* *FEMS Microbiol Lett.* **61**:61-5.

Edwards MD, Li Y, Kim S, Miller S, Bartlett W, Black S, Dennison S, Isla I, Blount P, Bowie J, Booth IR (2005) Pivotal role of the glycine-rich TM3 helix in gating the MscS mechanosensitive channel. *Nature Struct. Mol. Biol.* **12**:113-9.

Eggeling L, and Sahm H (2001) The Cell Wall Barrier of in *Corynebacterium glutamicum* and Amino Acid Efflux. *J Biosci Bioeng.* **92**:201-213.

Eggeling L, Besra GS, Alderwick L (2008) Structure and synthesis of the cell wall. In: Burkovski A (ed) *Corynebacterium glutamicum* genomics and molecular biology. Caister Academic Press, Norfolk, pp 313-34.

Eikmanns BJ, Kleinertz E, Liebl W, Sahm H (1991) A family of *Corynebacterium glutamicum*/*Escherichia coli* shuttle vectors for cloning, controlled gene expression, and promoter probing. *Gene*. **102**:93-8.

Epstein W (1986) Osmoregulation by potassium transport in *Escherichia coli*. *FEMS Microbiol. Lett.* **39**:73-8.

Epstein W, and Kim BS (1971) Potassium transport loci in *Escherichia coli* K-12. *J. Bacteriol.* **108**:639-44.

Follmann M, Becker M, Ochrombel I, Ott V, Krämer R, Marin K (2009) Potassium transport in *Corynebacterium glutamicum* is facilitated by the putative channel protein CgIK, which is essential for pH homeostasis and growth at acidic pH. *J Bacteriol.* **191**:2944-52.

Gande R, Dover LG, Krumbach K, Besra GS, Sahm H, Oikawa T, Eggeling L (2007) The two carboxylases of *Corynebacterium glutamicum* essential for fatty acid and mycolic acid synthesis. *J Bacteriol.* **189**:5257-64.

Gebhardt H, Meniche X, Tropis M, Krämer R, Daffe M, Morbach S (2007) The key role of the mycolic acid content in the functionality of the cell wall permeability barrier in *Corynebacterineae*. *Microbiology.* **153**:1424-34.

Grammann K, Volke A, Kunte HJ (2002) New type of osmoregulated solute transporter identified in halophilic members of the bacteria domain: TRAP transporter TeaABC mediates uptake of ectoine and hydroxyectoine in *Halomonas elongata* DSM 2581(T). *J Bacteriol.* **184**:3078-85.

Grant SGN, Jessee J, Bloom FR, and Hanahan D (1990) Differential plasmid rescue from transgenic mouse DNAs in *Escherichia coli* methylation- restriction mutants. *Proc. Natl. Acad. Sci. USA* **87**:4645-49.

Gutmann M, Hoischen C, Krämer R (1992) Carrier-mediated glutamate secretion by *Corynebacterium glutamicum* under biotin limitation. *Biochim Biophys Acta*. **1112**:115-23.

Hamill OP, Marty A, Neher E, Sackmann B, and Sigworth FJ (1981) Improved patch clamp techniques for high-resolution current recording from cells and cell-free membrane patches. *Pflügers Arch*. **391**:85-100.

Hamill OP, and Martinac B (2001) Molecular basis of mechanotransduction in living cells. *Physiol. Rev.* **81**:685-740.

Hashimoto K, Kawasaki H, Akazawa K, Nakamura J, Asakura Y, Kudo T, Sakuradani E, Shimizu S, Nakamatsu T (2006) Changes in composition and content of mycolic acids in glutamate-overproducing *Corynebacterium glutamicum*. *Biosci Biotechnol Biochem*. **70**:22-30.

Heldal M, Norland S, Bratbak G, and Riemann B (1994) Determination of bacterial cell number and cell volume by means of flow cytometry, transmission electron microscopy, and epifluorescence microscopy. *J. Microbiol. Methods* **20**:255-63.

Hoischen C, Krämer R (1989) Evidence for an efflux carrier system involved in the secretion of glutamate by *Corynebacterium glutamicum*. *Arch Microbiol*. **151**:342-7.

Hoischen C, Krämer R (1990) Membrane Alteration Is Necessary but Not Sufficient for Effective Glutamate Secretion in *Corynebacterium glutamicum*. *J Bacteriol*. **172**:3409-16.

Ikeda M, Nakagawa S (2003) The *Corynebacterium glutamicum* genome: features and impacts on biotechnological processes. *Appl Microbiol Biotechnol*. **62**:99-109.

Jäger W, Peters-Wendisch PG, Kalinowski J, Pühler A (1996) A *Corynebacterium glutamicum* gene encoding a two-domain protein similar to biotin carboxylases and biotin-carboxyl-carrier proteins. *Arch Microbiol.* **166**:76-82.

Jakoby M, Krämer R, Burkovski A (1999) Nitrogen regulation in *Corynebacterium glutamicum*: isolation of genes involved and biochemical characterization of corresponding proteins. *FEMS Microbiol Lett.* **173**:303-10.

Jarlier V, Nikaido H (1990) Permeability barrier to hydrophilic solutes in *Mycobacterium chelonae*. *J Bacteriol.* **172**:1418-23.

Jarlier V, Nikaido H (1994) Mycobacterial cell wall: structure and role in natural resistance to antibiotics. *FEMS Microbiol Lett.* **123**:11-8.

Jung H, Pirch T, Hilger D (2006) Secondary transport of amino acids in prokaryotes. *J Membr Biol.* **213**:119-33.

Kalinowski J, Bathe B, Bartels D, Bischoff N, Bott M, Burkovski A, Dusch N, Eggeling L, Eikmanns BJ, Gaigalat L, Goesmann A, Hartmann M, Huthmacher K, Krämer R, Linke B, McHardy AC, Meyer F, Möckel B, Pfefferle W, Pühler A, Rey DA, Rückert C, Rupp O, Sahm H, Wendisch VF, Wiegräbe I, Tauch A (2003) The complete *Corynebacterium glutamicum* ATCC 13032 genome sequence and its impact on the production of L-aspartate-derived amino acids and vitamins. *J Biotechnol.* **104**:5-25.

Kataoka M, Hashimoto KI, Yoshida M, Nakamatsu T, Horinouchi S, Kawasaki H (2006) Gene expression of *Corynebacterium glutamicum* in response to the conditions inducing glutamate overproduction. *Lett Appl Microbiol.* **42**:471-6.

Kawahara Y, Takahashi-Fuke K, Shimizu E, Nakamatsu T, Nakamori S (1997) Relationship between the glutamate production and the activity of 2-oxoglutarate dehydrogenase in *Brevibacterium lactofermentum*. *Biosci Biotechnol Biochem.* **61**:1109-12.

Kennerknecht N, Sahm H, Yen MR, Patek M, Saier MH Jr, Eggeling L (2002) Export of L-isoleucine from *Corynebacterium glutamicum*: a two-geneencoded member of a new translocator family. *J. Bacteriol.* **184**:3947-56.

Kim J, Hirasawa T, Sato Y, Nagahisa K, Furusawa C, Shimizu H (2009) Effect of *odhA* overexpression and *odhA* antisense RNA expression on Tween-40-triggered glutamate production by *Corynebacterium glutamicum*. *Appl Microbiol Biotechnol.* **81**:1097-106.

Kimura E, Abe C, Kawahara Y, Nakamatsu T (1996) Molecular Cloning of a Novel Gene, *dtsR*, Which Rescues the Detergent Sensitivity of a Mutant Derived from *Brevibacterium lactofermentum*. *Biosci Biotechnol Biochem.* **60**:1565-70.

Kimura E, Abe C, Kawahara Y, Nakamatsu T, Tokuda H. (1997) A *dtsR* gene-disrupted mutant of *Brevibacterium lactofermentum* requires fatty acids for growth and efficiently produces L-glutamate in the presence of an excess of biotin. *Biochem Biophys Res Commun.* **234**:157-61.

Kimura E. (2002) Triggering mechanism of L-glutamate overproduction by DtsR1 in coryneform bacteria. *J Biosci Bioeng.* **94**:545-51.

Kimura E. (2005) L-Glutamate Production. Handbook of *Corynebacterium glutamicum*. S. 439-464 (Eggeling L und Bott M, Herausgeber), CRC Press, Boca Raton, USA

Kinoshita S, Udaka S, and Shimono M (1957) Studies on the amino acid fermentation. Production of L-glutamate by various microorganisms. *J. Gen. Appl. Microbiol.* **3**:193-205.

Kloda A, Ghazi A, Martinac B (2006) C-terminal charged cluster of MscL, RKKEE, functions as a pH sensor. *Biophys J.* **90**:1992-8.

Koch A (1983) The surface stress theory of microbial morphogenesis. *Adv. Microbiol. Physiol.* **24**:301-36.

Krämer R, Lambert C, Hoischen C, Ebbighausen H (1990a) Uptake of glutamate in *Corynebacterium glutamicum*. 1. Kinetic properties and regulation by internal pH and potassium. *Eur J Biochem.* **194**:929-35.

Krämer R, Lambert C (1990b) Uptake of glutamate in *Corynebacterium glutamicum*. 2. Evidence for a primary active transport system. *Eur J Biochem.* **194**:937-44.

Krämer R, Morbach S (2004) BetP of *Corynebacterium glutamicum*, a transporter with three different functions: betaine transport, osmosensing, and osmoregulation. *Biochim Biophys Acta.* **1658**:31–36.

Krämer R (2009) Osmosensing and osmosignaling in *Corynebacterium glutamicum*. *Amino Acids.* **37**:487-97.

Kung C (2005) A possible unifying principle for mechanosensation. *Nature.* **436**:647-54.

Laber B, Amrhein N (1987) Metabolism of 1-aminophosphinate generates acetylphosphinate, a potent inhibitor of pyruvate dehydrogenase. *Biochem J.* **247**:351-8.

Laemmli UK (1970) Cleavage of structural proteins during assembly of bacteriophage T4. *Nature.* **227**:680-685.

Lambert C, Erdmann A, Eikmanns M, Krämer R. (1995) Triggering Glutamate Excretion in *Corynebacterium glutamicum* by Modulating the membrane State with Local Anesthetics and Osmotic Gradients. *Appl Environ Microbiol.* **61**:4334-42.

Landfald B, and Strom AR (1986) Choline-glycine betaine pathway confers a high level of osmotic tolerance in *Escherichia coli*. *J. Bacteriol.* **165**:849-855.

Leuchtenberger W, Huthmacher K, Drauz K (2005) Biotechnological production of amino acids and derivatives: current status and prospects. *Appl Microbiol Biotechnol.* **69**:1-8.

Levina N, Tötemeyer S, Stokes NR, Louis P, Jones MA, Booth IR (1999) Protection of *Escherichia coli* cells against extreme turgor by activation of MscS and MscL mechanosensitive channels: identification of genes required for MscS activity. *EMBO J.* **18**:1730-7.

Martinac B, Buechner M, Delcour AH, Adler J, and Kung C (1987) Pressure-sensitive ion channel in *Escherichia coli*. *Proc. Natl. Acad. Sci. USA* **84**:2297–2301.

Martinac B (2004) Mechanosensitive ion channels: molecules of mechanotransduction. *J Cell Sci.* **117**:2449-60.

Martinac B (2007) 3.5 billion years of mechanosensory transduction: structure and function of mechanosensitive channels in prokaryotes. In: Current Topics in Membranes **58**:25-57 (O.P. Hamill, Ed.), Elsevier Inc., San Diego, CA.

Miller JH (1992) A short course in bacterial genetics. A laboratory manual and handbook for *Escherichia coli* and related bacteria, Cold spring Harbour Laboratory Press, New York.

Miller S, Bartlett W, Chandrasekaran S, Simpson S, Edwards M, Booth IR (2003) Domain organization of the MscS mechanosensitive channel of *Escherichia coli*. *EMBO J.* **22**:36-46.

Möker N, Brocker M, Schaffer S, Krämer R, Morbach S, Bott M (2004) Deletion of the genes encoding the MtrA–MtrB two-component system of *Corynebacterium glutamicum* has a strong influence on cell morphology, antibiotics susceptibility and expression of genes involved in osmoregulation. *Mol Microbiol.* **54**:420-438.

Morbach S, Krämer R (2002) Body shaping under water stress: osmosensing and osmoregulation of solute transport in bacteria. *Chembiochem.* **3**:384-97.

Morbach S, Krämer R (2005a) Osmoregulation in *Corynebacterium glutamicum*. In: Eggeling L, Bott M (eds) *Corynebacterium glutamicum*. CRC Press LLC, Boca Raton, pp 417–438

Morbach S, Krämer R (2005b) Structure and Function of the betaine uptake system BetP of *Corynebacterium glutamicum*: strategies to sense osmotic and chill stress. *J Mol Microbiol Biotechnol.* **10**:143-53.

Morbach S, Krämer R (2008) Environmental stress response of *Corynebacterium glutamicum*. In: Burkovski A (ed) *Corynebacterium glutamicum* genomics and molecular biology. Caister Academic Press, Norfolk, pp 313–34.

Morris CE (2002) How did cells get their size? *Anat Rec.* **268**:239-51.

Mullis KB, Faloona FA, Schar S, Saiki R, Horn G, and Ehrlich H (1986) Specific amplification of DNA *in vitro*: the polymerase chain reaction. *Cold Spring Harbor Symp. Quant. Biol.* **51**:263-273.

Nakamura J, Hirano S, Ito H, Wachi M (2007) Mutations of the *Corynebacterium glutamicum* NCgl1221 gene, encoding a mechanosensitive channel homolog, induce L-glutamic acid production. *Appl Environ Microbiol.* **73**:4491-8.

Nakayama Y, Fujiu K, Sokabe M, Yoshimura K (2007) Molecular and electrophysiological characterization of a mechanosensitive channel expressed in the chloroplasts of *Chlamydomonas*. *Proc Natl Acad Sci U S A.* **104**:5883-8.

Nampoothiri KM, Hoischen C, Bathe B, Möckel B, Pfefferle W, Krumbach K, Sahm H, Eggeling L (2002) Expression of genes of lipid synthesis and altered lipid composition modulates L-glutamate efflux of *Corynebacterium glutamicum*. *Appl Microbiol Biotechnol.* **58**:89-96.

Niebisch A, Kabus A, Schultz C, Weil B, Bott M (2006) Corynebacterial Protein Kinase G Controls 2-Oxoglutarate Dehydrogenase Activity via the Phosphorylation Status of the OdhI Protein. *J Biol Chem.* **281**:12300-7.

Nomura T, Sokabe M, Yoshimura K (2006) Lipid-protein interaction of the MscS mechanosensitive channel examined by scanning mutagenesis. *Biophys J.* **91**:2874-81.

Nottebrock D, Meyer U, Krämer R, Morbach S. (2003) Molecular and biochemical characterization of mechanosensitive channels in *Corynebacterium glutamicum*. *FEMS Microbiol Lett.* **218**:305-9.

Nunheimer TD, Birnbaum J, Ihnen ED, Demain AL (1970) Product inhibition of the fermentative formation of glutamic acid. *Appl Microbiol.* **20**:215-7.

Okada K, Moe PC, Blount P (2002) Functional design of bacterial mechanosensitive channels. Comparisons and contrasts illuminated by random mutagenesis. *J Biol Chem.* **277**:27682-8.

Ott V, Koch J, Späte K, Morbach S, Krämer R (2008) Regulatory properties and interaction of the C- and N-terminal domains of BetP, an osmoregulated betaine transporter from *Corynebacterium glutamicum*. *Biochemistry.* **47**:12208-18.

Perozo E, Rees DC (2003) Structure and mechanism in prokaryotic mechanosensitive channels. *Curr Opin Struct Biol.* **13**:432-42.

Peter H, Burkovski A, and Krämer R (1996) Isolation, characterization, and expression of the *Corynebacterium glutamicum betP* gene, encoding the transport system for the compatible solute glycine betaine. *J. Bacteriol.* **178**:5229–5234.

Peter H, Weil B, Burkovski A, Krämer R, Morbach S (1998) *Corynebacterium glutamicum* is equipped with four secondary carriers for compatible solutes: identification, sequencing, and characterization of the proline/ectoine uptake system, ProP, and the ectoine/proline/glycine betaine carrier, EctP. *J Bacteriol.* **180**:6005-12.

Pivetti CD, Yen MR, Miller S, Busch W, Tseng YH, Booth IR, Saier MH Jr. (2003) Two families of mechanosensitive channel proteins. *Microbiol Mol Biol Rev.* **67**:66-85.

Puech V, Chami M, Lemassu A, Lanéelle MA, Schiffler B, Gounon P, Bayan N, Benz R, Daffé M (2001) Structure of the cell envelope of corynebacteria: importance of the non-covalently bound lipids in the formation of the cell wall permeability barrier and fracture plane. *Microbiology.* **147**:1365-82.

Radmacher E, Stansen KC, Besra GS, Alderwick LJ, Maughan WN, Hollweg G, Sahn H, Wendisch VF, Eggeling L. (2005) Ethambutol, a cell wall inhibitor of *Mycobacterium tuberculosis*, elicits L-glutamate efflux of *Corynebacterium glutamicum*. *Microbiology*. **151**:1359-68.

Ressl S, Terwisscha van Scheltinga AC, Vonnrhein C, Ott V, Ziegler C (2009) Molecular basis of transport and regulation in the Na(+)/betaine symporter BetP. *Nature*. **458**:47-52.

Rottenberg H (1979) Non-equilibrium thermodynamics of energy conversion in bioenergetics. *Biochim Biophys Acta*. **549**:225-53.

Rübenhagen R, Morbach S, Krämer R (2001) The osmoreactive betaine carrier BetP from *Corynebacterium glutamicum* is a sensor for cytoplasmic K<sup>+</sup>. *EMBO J*. **20**:5412-20.

Ruffert S, Lambert C, Peter H, Wendisch VF, Krämer R. (1997) Efflux of compatible solutes in *Corynebacterium glutamicum* mediated by osmoregulated channel activity. *Eur J Biochem*. **247**:572-80

Ruffert S, Berrier C, Krämer R, Ghazi A. (1999) Identification of mechanosensitive ion channels in the cytoplasmic membrane of *Corynebacterium glutamicum*. *J Bacteriol*. **181**:1673-6.

Ruthe HJ, and Adler J (1985) Fusion of bacterial spheroplasts by electric fields. *Biochim. Biophys. Acta* **819**:105-13.

Sambrook J, Fritsch EF and Maniatis T (1989) Molecular cloning: A laboratory manual (2nd ed.). *Cold Spring Harbor Laboratory Press*, New York, USA.

Sano C (2009) History of glutamate production. *Am J Clin Nutr*. **90**:728S-732S.

Schäfer A, Tauch A, Jäger W, Kalinowski J, Thierbach G, Pühler A (1994) Small mobilizable multi-purpose cloning vectors derived from the *Escherichia coli* plasmids pK18 and pK19: selection of defined deletions in the chromosome of *Corynebacterium glutamicum*. *Gene*. **145**:69-73.

- Schiekel J (2005) Glutamate excretion and mycolyltransferases in *Corynebacterium glutamicum*. Diploma thesis, University of Cologne.
- Schultz C, Niebisch A, Gebel L, Bott M (2007) Glutamate production by *Corynebacterium glutamicum*: dependence on the oxoglutarate dehydrogenase inhibitor protein OdhI and protein kinase PknG. *Appl Microbiol Biotechnol.* **76**:691-700.
- Seidel M, Alderwick LJ, Sahm H, Besra GS, Eggeling L (2007) Topology and mutational analysis of the single Emb arabinofuranosyltransferase of *Corynebacterium glutamicum* as a model of Emb proteins of *Mycobacterium tuberculosis*. *Glycobiology.* **17**:210-9.
- Shiio I, Otsuka SI, Katsuya N (1962) Effect of biotin on the bacterial formation of glutamic acid. II. Metabolism of glucose. *J Biochem.* **52**:108-16.
- Shirai T, Nakato A, Izutani N, Nagahisa K, Shioya S, Kimura E, Kawarabayasi Y, Yamagishi A, Gojobori T, Shimizu H (2005) Comparative study of flux redistribution of metabolic pathway in glutamate production by two coryneformbacteria. *Metab. Eng.* **7**:59-69.
- Simic P, Sahm H, Eggeling L (2001) L-Threonine export: Use of peptides to identify a new translocator from *Corynebacterium glutamicum*. *J. Bacteriol.* **183**:5317-24.
- Slotboom DJ, Konings WN, Lolkema JS (2001) Glutamate transporters combine transporter- and channel-like features. *Trends Biochem Sci.* **26**:534-9.
- Sotomayor M, Vásquez V, Perozo E, Schulten K (2007) Ion conduction through MscS as determined by electrophysiology and simulation. *Biophys J.* **92**:886-902.
- Stackebrandt E, Rainey FA, and Ward-Rainey NL (1997) Proposal for a new hierarchic classification system, Actinobacteria nov. *Int. J. Syst. Bacteriol.* **47**:479-91.
- Sukharev S (2002) Purification of the small mechanosensitive channel of *Escherichia coli* (MscS): the subunit structure, conduction, and gating characteristics in liposomes. *Biophys J.* **83**:290-8.

Thompson JD, Higgins DG, Gibson TJ (1994) CLUSTAL W: improving the sensitivity of progressive multiple sequence alignment through sequence weighting, position-specific gap penalties and weight matrix choice. *Nucleic Acids Res.* **22**:4673-80.

Touzé T, Gouesbet G, Boiangiu C, Jebbar M, Bonnassie S, Blanco C (2001) Glycine betaine loses its osmoprotective activity in a bspA strain of *Erwinia chrysanthemi*. *Mol Microbiol.* **42**:87-99.

Tropis M, Meniche X, Wolf A, Gebhardt H, Strelkov S, Chami M, Schomburg D, Krämer R, Morbach S, Daffé M (2005) The crucial role of trehalose and structurally related oligosaccharides in the biosynthesis and transfer of mycolic acids in Corynebacterineae. *J Biol Chem.* **280**:26573-85.

Trötschel C, Kandirali S, Diaz-Achirica P, Meinhardt A, Morbach S, Krämer R, Burkovski A (2003) GltS, the sodium-coupled L-glutamate uptake system of *Corynebacterium glutamicum*: identification of the corresponding gene and impact on L-glutamate production. *Appl Microbiol Biotechnol.* **60**:738-42.

Trötschel C, Deutenberg D, Bathe B, Burkovski A, Krämer R (2005) Characterization of methionine export in *Corynebacterium glutamicum*. *J. Bacteriol.* **187**:3786-94.

Udaka S (1960) Screening method for microorganisms accumulating metabolites and its use in the isolation of *Micrococcus glutamicus*. *J Bacteriol.* **79**:754-5.

Usuda Y, Tujimoto N, Abe C, Asakura Y, Kimura E, Kawahara Y, Kurahashi, Matsui H (1996) Molecular cloning of the *Corynebacterium glutamicum* ('*Brevibacterium lactofermentum*' AJ12036) odhA gene encoding a novel type of 2-oxoglutarate dehydrogenase. *Microbiology.* **142**:3347-54.

Vrljić M, Eggeling L, Sahm H (1996) A new type of transporter with a new type of cellular function: L-lysine export from *Corynebacterium glutamicum*. *Mol. Microbiol.* **22**:815-26.

Wang W, Black SS, Edwards MD, Miller S, Morrison EL, Bartlett W, Dong C, Naismith JH, Booth JR (2008) The structure of an open form of an *E. coli* mechanosensitive channel at 3.45 Å resolution. *Science* **321**:1179-83.

Wood JM (1999) Osmosensing in bacteria: signals and membrane based sensors. *Microbiol. Mol. Biol. Rev.* **63**:230-262.

Yao W, Chu C, Deng X, Zhang Y, Liu M, Zheng P, Sun Z (2009) Display of alpha-amylase on the surface of *Corynebacterium glutamicum* cells by using NCgl1221 as the anchoring protein, and production of glutamate from starch. *Arch Microbiol.* [Epub ahead of print]

Yon J, Fried M (1989) Precise gene fusion by PCR. *Nucleic Acids Res.* 17:4895.

Yukawa H, Omumasaba CA, Nonaka H, Kós P, Okai N, Suzuki N, Suda M, Tsuge Y, Watanabe J, Ikeda Y, Vertès AA, Inui M (2007) Comparative analysis of the *Corynebacterium glutamicum* group and complete genome sequence of strain R. *Microbiology.* **153**:1042-58.

Ziegler C, Morbach S, Schiller D, Krämer R, Tziatzios C, Schubert D, Kühlbrandt W (2004) Projection structure and oligomeric state of the osmoregulated sodium/glycine betaine symporter BetP of *Corynebacterium glutamicum*. *J Mol Biol.* **337**:1137-47.

## 7 Supplement

Table 7.1: Oligonucleotides used for amplification and deletion of respective genes

Name	Sequence 5' – 3'	Reference
yggB_orf_sense	ATGATTTTAGGCGTACCCATTC	this work
yggB_orf_as	CTAAGGGGTGGACGTCGG	this work
DelyggB_HindIII_sense	GCGCGCAAGCTTCAATTGGCTTGCCGAACTC	Nina Möker
DelyggB_PstI_sense	GCGCGCTGCAGGAGCCAAGATTAGCGCTG	Nina Möker
DelyggB_PstI_as	CGCGCGCTGCAGGACGCTGATTACAGACGTG	Nina Möker
DelyggB_XbaI_as	CGCGCGTCTAGACCTGTGGAATGTCGTTAGG	Nina Möker
yggB-his_sense	CCCGGGCATATGATTTTAGGCGTACCCATTC	Nina Möker
yggB-his_as	CCCGGGAAGCTTAGGGGTGGACGTCGGCGCAAC	Nina Möker
yggB-delta110_as	CCCGGGAAGCTTTTCCACAGTCATGACCTTAAATAG	Nina Möker
yggB-delta132_as	CCCGGGAAGCTTGCGGACACGTCCGCCAAACG	Nina Möker
yggB-delta247_as	CCCGGGAAGCTTAGTGGTTGCGCTGCCGTATTC	Nina Möker
yggB_phoA-lacZ_fw (SbfI)	CAGCCTGCAGGATGATTTTAGGCGTACCCATTC	this work
yggB_phoA-lacZ_rv (ScaI)	CAGAGTACTAGGGGTGGACGTCGGCGC	this work
yggBd110_phoA-lacZ_rv (ScaI)	CAGAGTACTTGGTTCCACAGTCATGACC	this work
yggBd132_phoA-lacZ_rv (ScaI)	CAGAGTACTCATGCGGACACGTCCG	this work
yggBd247_phoA-lacZ_rv (ScaI)	CAGAGTACTTGTAGTGGTTGCGCTGCCG	this work
pQE-60 yggB_fw (NcoI)	CAGCCATGGTTTTAGGCGTACCCATTC	this work
pQE-60 yggB_rv (BamHI)	CAGGGATCCCTAAGGGGTGGACGTCGG	this work
pQE-60 yggB_d110_rv (BamHI)	CAGGGATCCCTATGGTTCCACAGTCATGAC	this work
pQE-60 yggB_d132_rv (BamHI)	CAGGGATCCCTACATGCGGACACGTCCGC	this work
pQE-60 yggB_d247_rv (BamHI)	CAGGGATCCCTAGTAGTGGTTGCGCTGCC	this work
MscS fw (BamHI)	CAGGGATCCATGGAAGATTTGAATGTTGTCG	this work
MscS rv (NotI)	CAGGCGGCCGCTTACGCAGCTTTGTCTTCTTTC	this work
MscS-His rv (NotI)	CAGGCGGCCCGCCGCAGCTTTGTCTTCTTTCAC	this work
MscS-Fusion rv	GTGTAAGGAATCAATGAGGGTTCCCGATGTCGCAGCT TTGTCTTCTTTCAC	this work

Supplement

YggB-Fusion fw	ACATCGGGAACCCTCATTGATTCCTTACAC	this work
YggB-Fusion rv (NotI)	CAGGCGGCCGCCTAAGGGGTGGACGTCGG	this work
YggB-Fusion-His rv (NotI)	CAGGCGGCCGCAGGGGTGGACGTCGGCG	this work
Cgl0590 Del_1 (EcoRI)	GGGGAATTCGCGTTTTGAGCATGCCGCAG	this work
Cgl0590 Del_2	CTTATAAATTTGGAGTGTGAAGGTTATTGCGTGGGGCC ACAAACAGCACCGC	this work
Cgl0590 Del_3	CACGCAATAACCTTCACACTCCAAATTTATAAGCCGGA ACGGATCTTGCCAAC	this work
Cgl0590 Del_4 (EcoRI)	GGGGAATTCCTTCGCCGGTGGGAAGCAC	this work
Cgl2211 Del_1 (EcoRI)	GGGGAATTCGCTGCAGGTGTTGTAGCTGC	this work
Cgl2211 Del_2	CTTATAAATTTGGAGTGTGAAGGTTATTGCGTGCAGTA CAGCGGCGACGCCG	this work
Cgl2211 Del_3	CACGCAATAACCTTCACACTCCAAATTTATAAGGTTAT GTGTCAGATGCCTCCC	this work
Cgl2211 Del_4 (EcoRI)	GGGGAATTCGTGCTGTGCCTGGGCACTG	this work
Cgl0590_fw (Sall)	CAGGTCGACGTGCTTGATTTCTTAGCTGCG	this work
Cgl0590_rv (EcoRI)	CAGGAATTCTTAGAGCAGCAAGAACAATATC	this work
Cgl0590-His_fw (NdeI)	CAGCATATGGTGCTTGATTTCTTAGCTGCG	this work
Cgl0590-His_rv (HindIII)	CAGAAGCTTGAGCAGCAAGAACAATATCTGC	this work
Cgl2211-His_fw (NdeI)	CAGCATATGGTGAGCTTCCTTGAGAAAATC	this work
Cgl2211-His_rv (HindIII)	CAGAAGCTTGATAAGTAGGAACAACAACG	this work

**Table 7.2: Oligonucleotides used for site-directed mutagenesis.**

Name	Sequence 5' – 3'	Reference
mscS I37N_s	CGGCACTCGCGACCATCATCGTTGG	this work
mscS I37N_as	CCAACGATGATGTTTCGCGAGTGCCG	this work
mscS A51N_s	GATGATTTCCAACAACGTGAATCGCCTG	this work
mscS A51N_as	CAGGCGATTCACGTTGTTGGAAATCATC	this work
mscS F68N_s	CTGTTGCTGATAATCTTTCTGCATTAG	this work
mscS F68N_as	CTAATGCAGAAAGATTATCAGCAACAG	this work
mscS L86N_s	CTAATCGCTGCAAACGGACGCGTGGGTG	this work
mscS L86N_as	CACCCACGCGTCCGTTTGCAGCGATTAG	this work
mscS V40D_s	CGATCATCATCGATGGTTTTGATTATCGCGC	this work

mscS V40D_as	GCGCGATAATCAAACCATCGATGATGATCG	this work
mscS A106V_s	GGTGCCGCAGGCTTAGTTGTTGGTCTGGCT	this work
mscS A106V_as	AGCCAGACCAACAACCTAAGCCTGCGGCACC	this work
mscS L109S_s	CTTAGCTGTTGGTAGCGCTTTGCAGGGGTC	this work
mscS L109S_as	GACCCCTGCAAAGCGCTACCAACAGCTAAG	this work

**Fig. 7.1 Sequence comparison of *C. glutamicum* YggB and *E. coli* MscS.**

Sequence alignment of *C. glutamicum* YggB and *E. coli* MscS was performed as described earlier (Thompson et al., 1994). The localization of the (predicted) transmembrane domains is marked in red. Positions where *C. glutamicum* YggB was truncated are indicated.

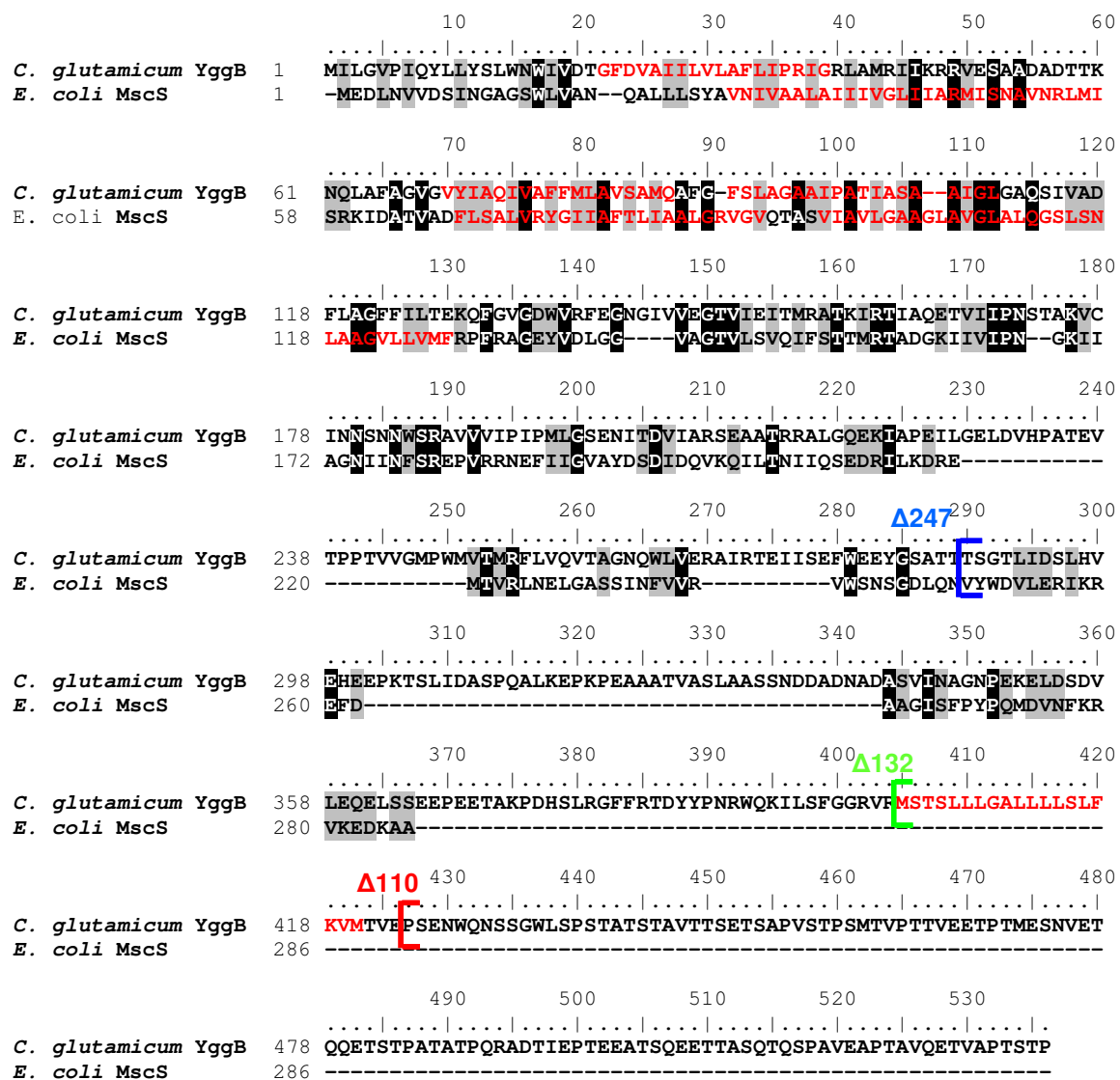


**Table 7.3: Glutamate excretion rates [ $\mu\text{mol}/(\text{min g dm})$ ] of *C. glutamicum* strains**

Glutamate excretion was induced by addition of 6 U/ml Penicillin G in the exponential growth phase. Plasmid-encoded gene expression was induced by addition of 25  $\mu\text{M}$  IPTG if not otherwise stated.

<b>Strain</b>	<b>Glutamate excretion rate [<math>\mu\text{mol}/(\text{min g dm})</math>]</b>	<b>Standard derivation</b>
wt	16.63	2.13
$\Delta yggB$	5.13	0.82
YggB	20.16	3.96
YggB-His	17.60	2.84
YggB-His (0 $\mu\text{M}$ IPTG)	19.12	3.25
$\Delta 110$ -His	13.86	3.74
$\Delta 132$ -His	4.69	0.30
$\Delta 247$ -His	21.11	4.54
MscS-His	9.85	0.73
MscS/CtYggB-His	13.95	0.79
MscS-His A51N F68N	5.78	1.70
MscS/CtYggB-His I37N L86N	4.77	1.61
MscS/CtYggB-His A51N F68N	4.74	1.20



## **Danksagung**

Ich möchte mich herzlich bei Herrn Prof. Dr. Reinhard Krämer für die Überlassung des interessanten Arbeitsthemas bedanken. Außerdem für die viele Zeit in Besprechungen und zwischendurch sowie für die Unterstützung mit vielen hilfreichen Tipps und Tricks.

Herrn Prof. Dr. Arnd Baumann danke ich für die freundliche Übernahme des Koreferates.

Außerdem möchte ich mich bei Dr. Susanne Morbach bedanken für die zwar kurze, aber ausgesprochen nette Betreuung zu Beginn meiner Arbeit.

Der gesamten Arbeitsgruppe, einschließlich aller Ehemaligen, für die entspannte und lustige Arbeitsatmosphäre und insgesamt eine tolle Zeit, mit diversen Sing Star, Wii oder einfach nur nett zusammen sitzen und ein Bierchen trinken Abenden. Besonders bedanken möchte ich mich noch bei Ute und Eva, für ihre Hilfsbereitschaft und ihr Wissen über den Aufenthaltsort (fast) aller Chemikalien, Geräte und uralter Stämme. Vielen Dank an die ‚rechte‘ Seite (die Osmogruppe löst sich ja langsam auf), besonders Nina (die mich ja sozusagen eingearbeitet hat), Sascha (meinem Urlaubsmann), Philipp (was soll ich sagen), Alex (‚I wanna dance with somebody‘) und natürlich Tina, meine Laborpartnerin und Bastelqueen.

Vielen Dank an Susanne und Marc für das Korrekturlesen dieser Arbeit.

Bei Prof. Dr. Boris Martinac und seinem gesamten Labor für die erfolgreiche Kooperation und die tolle Zeit, die ich bei ihm an der University of Queensland in Brisbane verbringen durfte. Außerdem danke ich Dr. Christine Ziegler und Katrin Rohde für die nette und hoffentlich weiterhin erfolgreiche Zusammenarbeit.

Ganz großer Dank geht an meine Familie, an alle meine Freunde und die Menschen, die mir wichtig sind und mein Leben neben der Arbeit bereichern.

## **Erklärung**

Ich versichere, dass ich die von mir vorgelegte Dissertation selbständig angefertigt, die benutzten Quellen und Hilfsmittel vollständig angegeben und die Stellen der Arbeit - einschließlich Tabellen, Karten und Abbildungen -, die anderen Werken im Wortlaut oder dem Sinn nach entnommen sind, in jedem Einzelfall als Entlehnung kenntlich gemacht habe; dass diese Dissertation noch keiner anderen Fakultät oder Universität zur Prüfung vorgelegen hat; dass sie - abgesehen von unten angegebenen Teilpublikationen – noch nicht veröffentlicht worden ist sowie, dass ich eine solche Veröffentlichung vor Abschluss des Promotionsverfahrens nicht vornehmen werde. Die Bestimmungen dieser Promotionsordnung sind mir bekannt. Die von mir vorgelegte Dissertation ist von Prof. Dr. R. Krämer am Institut für Biochemie der Mathematisch-Naturwissenschaftlichen Fakultät der Universität zu Köln betreut worden.

Ich versichere, dass ich alle Angaben wahrheitsgemäß nach bestem Wissen und Gewissen gemacht habe und verpflichte mich, jedmögliche, die obigen Angaben betreffende Veränderung dem Dekanat unverzüglich mitzuteilen.

Datum: Köln, September 2009

Unterschrift: